A Dissertation for the Degree of Doctor of Philosophy in Pharmacy

Part A. Asymmetric Total Synthesis of (–)-Penibruguieramine A Using Memory of Chirality and Dynamic Kinetic Resolution.

Part B. Biphasic CuAAC Reaction Using a Phase Transfer Agent.

Part A. 분자 비대칭성 기억 현상과 동적 속도론적 분할 현상을 이용한 **(−)-penibruguieramien A**의 비대칭 전합성.

Part B. 상 전이 촉진제를 이용한 **2**상 **CuAAC** 반응.

February 2016

Graduate School of Pharmacy
Seoul National University
Pharmaceutical chemistry Major

Jae Hyun Kim

Abstract

Part A. Asymmetric Total Synthesis of (–)-Penibruguieramine A Using Memory of Chirality and Dynamic Kinetic Resolution.

(–)-Penibruguieramine A is a novel marine pyrrolizidine alkaloid, which was recently identified by Guo from the endophytic fungus Penicillium sp. GD6 associated with Chinese mangroves. This natural product has an unprecedented 1-hydroxyl-2-methyl pyrrolizidin-3-one skeleton.

We have achieved the first total synthesis of this marine alkaloid using the principles of ‘memory of chirality (MOC)’ and ‘dynamic kinetic resolution (DKR)’ for the asymmetric synthesis from proline as the only chiral source. MOC and DKR are attractive strategies for asymmetric synthesis. However, although there have been reports of DKR being utilized, there are only few reports of MOC being applied in total synthesis of natural products. Moreover, the combination of these two concepts has not been previously reported for asymmetric synthesis.

Our synthesis follows the proposed biosynthetic pathway and features an asymmetric construction of stereocenters with essentially complete diastereo- and enantioselectivity in the absence of external chiral sources. Noteworthy is the excellent level of memory of chirality in a protic solvent environment. To understand this, we performed some experiments and provided a mechanistic rationale

Key word: Aldol reaction, Biomimetic synthesis, Dynamic kinetic resolution, Memory of chirality, Total synthesis

Student Number: 2012-31107

Abstract

Part B. Biphasic CuAAC Reaction Using a Phase Transfer Agent.

A phase transfer agent assisted biphasic Cu(I) catalyzed azide-alkyne 1,3-dipolar cycloaddition (CuAAC) reaction system was developed. A biphasic reaction media consisting of water and an organic solvent ensures a dissolution of reagents and substrates. Tris(triazolylmethyl)amine ligands with an appropriate hydrophilic-lipophilic balance are able to extract copper from the aqueous phase to the organic phase, accelerating the CuAAC reaction rate. The present system is widely applicable to substrates with various functionalities, including a free amino group and especially to lipophilic substrates.

Key word: Click chemistry, Ligand effect, Phase transfer agent, Solvent effect, Synthetic method

Student Number: 2012-31107

Table of Contents

Part A. Asymmetric Total Synthesis of (–)-Penibruguieramine A Using Memory of Chirality and Dynamic Kinetic Resolution.

I. Introduction ---------- **1**

II. Results and Discussion ---------- **3**

III. Conclusions ---------- **13**

IV. Experimental ---------- **14**

V. References ---------- **49**

VI. Acknowledgements ---------- **53**

Part B. Biphasic CuAAC Reaction Using a Phase Transfer Agent.

I. Introduction ---------- **54**

II. Results and Discussion ---------- **58**

III. Conclusions ---------- **67**

IV. Experimental ---------- **68**

V. References ---------- **81**

VI. Acknowledgements ---------- **86**

Appendix I ---------- **87**

Appendix II ---------- **102**

Abstract in Korean ---------- **125**

Part A.

Asymmetric Total Synthesis of (–)-Penibruguieramine A Using Memory of Chirality and Dynamic Kinetic Resolution.

I. Introduction

(–)-Penibruguieramine A (**1**, Scheme 1) is a novel marine pyrrolizidine alkaloid, which was recently identified by Guo and co-workers from the endophytic fungus *Penicillium* sp. GD6 associated with Chinese mangroves.[1] The relative configuration of **1** was established by rotating-frame Overhauser effect spectroscopy (ROESY) analysis, and its absolute configuration was determined by comparison of the electronic circular dichroism (ECD) spectra with the calculated ECD data. This natural product has an unprecedented 1-hydroxyl-2-methyl pyrrolizidin-3-one skeleton bearing an alkenyl chain at the C-1 position and a hydroxymethyl group at the C-8 position.

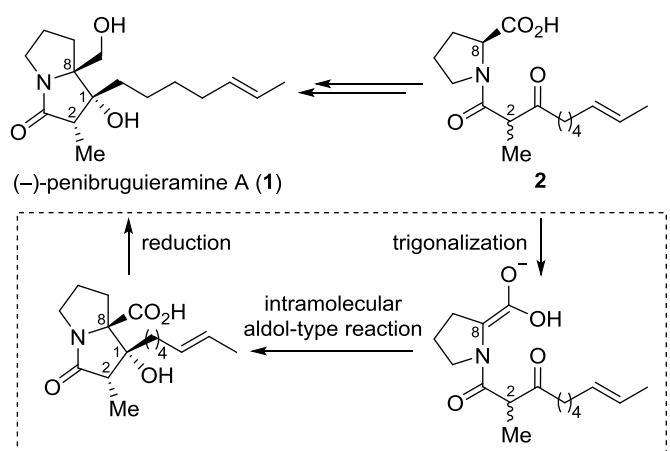

Scheme 1. Structure of (–)-penibruguieramine A (**1**) and its proposed biosynthetic pathway.

A biosynthetic pathway has been proposed,[1] as shown in Scheme 1, in which the bicyclic ring system is generated by an intramolecular aldol-type reaction of proline-pentaketide amide **2**.[2] In this process, the chiral center of the proline moiety in **2** might be destroyed by trigonalization and regenerated along with the adjacent stereocenters. Enzymes are most likely involved in this biosynthesis because most chiral natural products are synthesized in nature via enzyme-mediated catalysis.

We envisioned that the asymmetric synthesis of penibruguieramine A (**1**) could be achieved from the ester derivatives of **2** without the aid of external chiral influences if the principles of 'memory of chirality' (MOC) and 'dynamic kinetic resolution' (DKR) were applied to the aldol reaction step.[3–5] MOC and DKR are attractive strategies for asymmetric synthesis. Although there have been reports on the use of DKR, only few studies on the application of MOC to the total synthesis of natural products have been reported.[6,7] In addition, the combination of these two concepts has not been previously reported for asymmetric synthesis.[8] In this communication, we report the use of MOC and DKR for the first total synthesis of (–)-penibruguieramine A (**1**) from L-proline. Our synthesis follows the biosynthetic pathway proposed for **1** and features the asymmetric construction of stereocenters with essentially complete diastereo- and enantioselectivity in the absence of external chiral sources.[9]

II. Results and Discussion

As outlined in Scheme 2, we envisioned that the intramolecular aldol reaction of proline ester **3** would afford bicyclic compound **4** with the correct absolute and relative configuration required to proceed to penibruguieramine A (**1**). The chiral center of the proline moiety could direct the stereochemical course of the aldol reaction and could be preserved in the reaction product. For the success of this MOC reaction, axially chiral enolate **5** (with an arbitrary enolate geometry) should be formed selectively over *ent*-**5** via favored conformer **3-I**. In addition, chiral enolate **5** must have a sufficiently large energy barrier against racemization.[3] We anticipated the successful outcome of this reaction after considering the study reported by Stoodley et al. demonstrating the use of MOC in an aldol reaction of simpler proline derivatives.[10] In that report, although the diastereoselectivity and yield were low, a certain degree of configuration retention was obtained at the chiral center of the proline moiety.

The stereochemistry at the C-2 position of aldol product **4** can be introduced prior to the aldol reaction step. However, the C-2 stereocenter of **3** would not be retained over the course of the reaction due to facile enolization. We envisioned that if the DKR process occurred at the C-2 position during the aldol reaction and the reaction proceeded via conformationally favored intermediate **5**, then the C-2 stereocenter

would not require installation. Based on this assumption, the aldol substrate employed in this total synthesis was prepared as a diastereomeric mixture at the C-2 position.

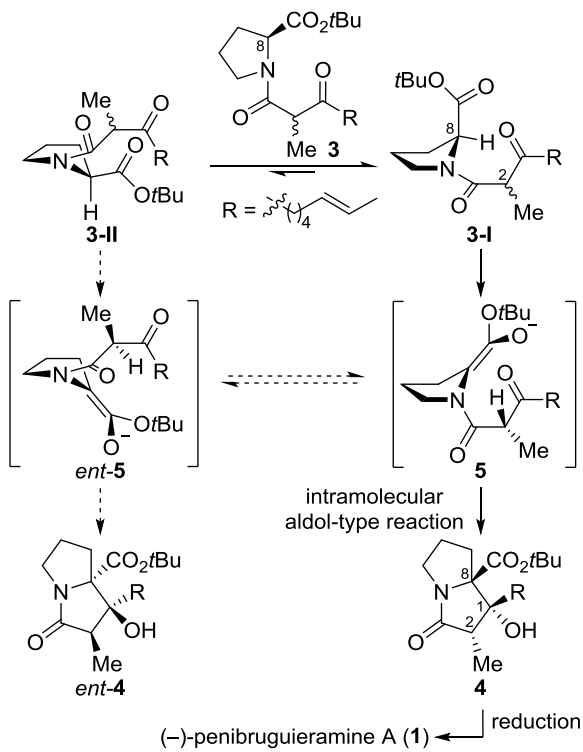

Scheme 2. Synthetic strategies for the total synthesis of (–)-penibruguieramine A (**1**).

Our total synthesis started from known bromide **6**,[11] which was readily prepared from commercial alcohol **7** (Scheme 3). The alkylation of the dianion of ethyl 2-methyl-acetoacetate (**8**) with bromide **6** afforded the racemate of ketoester **9**.[12] Subsequent hydrolysis with KOH in aqueous MeOH afforded -ketoacid **10**, which was coupled with L-proline *tert*-butyl ester (**11**) to yield aldol substrate **3** as

a diastereomeric mixture at the C-2 position in an overall good yield. The diastereomeric ratio of **3** was 1.4:1 implying that epimerization at C-2 occurred during the coupling reaction process (vide infra).

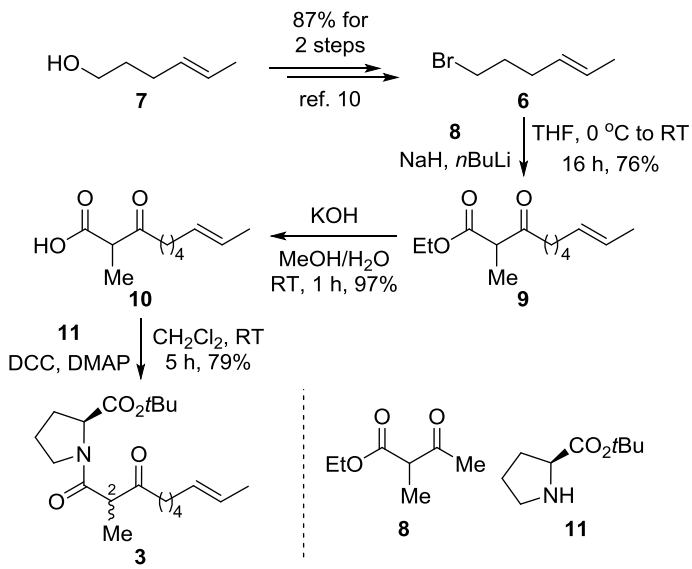

Scheme 3. Synthesis of proline-pentaketide amide **3**. DCC=*N*,*N'*-dicyclohexylcarbodiimide, DMAP=4-(*N*,*N*-dimethylamino)pyridine, THF= tetrahydrofuran.

With substrate **3** in hand, we investigated the envisioned intramolecular aldol reaction. In addition to the desired aldol reaction (path a, Table 1), **3** can undergo other competitive side reactions, including the Dieckmann condensation (path b) and the retro-Claisen reaction (path c). The bulky *tert*-butyl ester group of **3** was expected to be appropriate to avoid the side reaction via path b.[13] Various bases and

conditions were screened to obtain the desired product. The typical results are listed in Table 1.

Table 1. Reaction conditions for the intramolecular aldol reaction of **3**.[a]

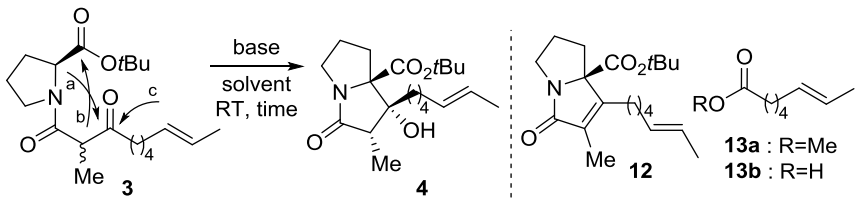

Entry	Base (equiv)	Solvent	Time (h)	Yield of **4**[b] (%)
1	NaOEt (5)	EtOH	9	77[c]
2	LiOEt (5)	EtOH	9	72
3	KOEt (5)	EtOH	6	66
4	NaOMe (5)	MeOH	24	30
5	NaO*i*Pr (5)	*i*PrOH	3	49
6	NaO*t*Bu (5)	*t*BuOH	16	0[d]
7	TBAOH·30H_2O (5)	THF	12	61

[a] Reactions were run with **3** (105 mg, 0.3 mmol) at a substrate concentration of 0.1 M. [b] Isolated yield. [c] **12** was also obtained in 10% yield. [d] Complex mixture. TBAOH=tetra-*n*-butylammonium hydroxide.

When substrate **3** was treated with NaOEt in EtOH, the reaction proceeded with satisfactory results to afford the desired aldol product **4** as a single diastereomer in 77% yield after 9 h (entry 1). The only notable side product present in the reaction

mixture was the aldol dehydration product **12**. Other alkali metal ethoxides, such as LiOE and KOEt, also yielded the desired **4** without significant loss of yield (entries 2 and 3). However, when **3** was treated with NaOMe (entry 4), the reaction suffered from low yield due to the retro-Claisen cleavage to provide **13a** (21%) via path c and transesterification (8%). Other sodium alkoxides having bulky organic substituents, such as NaO*i*Pr and NaO*t*Bu, were also inappropriate for the aldol reaction and suffered from low yield and decomposition (entries 5 and 6). Sterically hindered organic bases, including 1,8-diazabicyclo[5.4.0]undec-7-ene (DBU), failed to yield the desired product in an aprotic solvent (see the Experimental for details). Alkali metal hydroxides produced only a negligible amount of product, with most of the starting material remaining along with a small amount of **13b** formed via hydrolytic retro-Claisen cleavage (path c). On the other hand, the quaternary ammonium hydroxide base in THF gave the product **4** in moderate yield (entry 7). These results indicated that the nature of the base, with bulkiness in particular, was important in determining the outcome of the reaction.

Regardless of the nature of the base, the intramolecular aldol reaction of **3** resulted in a single diastereomer (**4**). The other possible isomers were not detected in the crude mixture. The relative stereochemistry of **4**, which was determined by 2D NMR analysis, was identical to that of penibruguieramine A. The absolute and relative stereochemistry of **4** was later confirmed by X-ray crystallography

(Scheme 4).[14] With this excellent stereochemical outcome in hand, the total synthesis of **1** was completed by reducing the sterically hindered *tert*-butyl ester group in **4** to the corresponding alcohol via two steps.[15] The NMR and mass spectral data of the resulting **1** were identical to those of the natural product. The synthetic sample exhibited a negative optical rotation [$[\alpha]^{22}_{D}$ –21.3 (*c* 0.05, $CHCl_3$)], which is consistent with that of the natural compound [$[\alpha]^{22}_{D}$ –22 (*c* 0.05, $CHCl_3$)].[1] This result indicates that the absolute configuration proposed for the natural compound was correct.

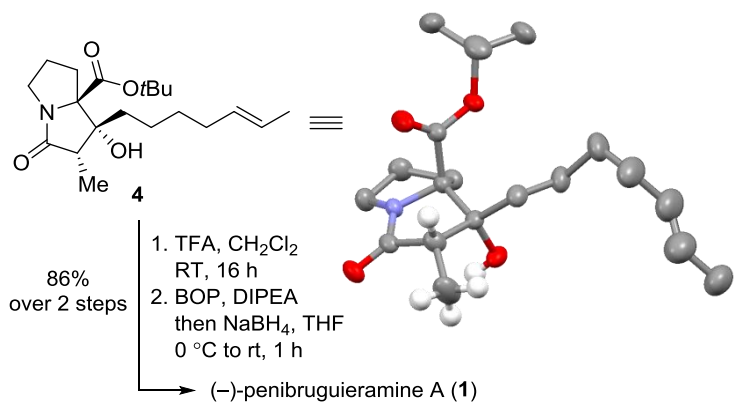

Scheme 4. Crystal structure of **4**[14] and completion of the synthesis of (–)-penibruguieramine A (**1**). BOP=benzotriazolyloxy-tris(dimethylamino) phosphonium hexafluorophosphate, DIPEA=*N*,*N*-diisopropylethylamine, TFA=trifluoroacetic acid.

The enantiomeric purity of **1** was greater than 99% (see the Experimental for details). These results confirmed that MOC was exerted during the intramolecular aldol reaction of **3**. The virtually complete retention of chirality obtained in the

polar protic solvent is remarkable considering the prior observations in which the competitive protonation of the enolate decreased the enantioselectivities of the MOC reactions in protic solvents.[16]

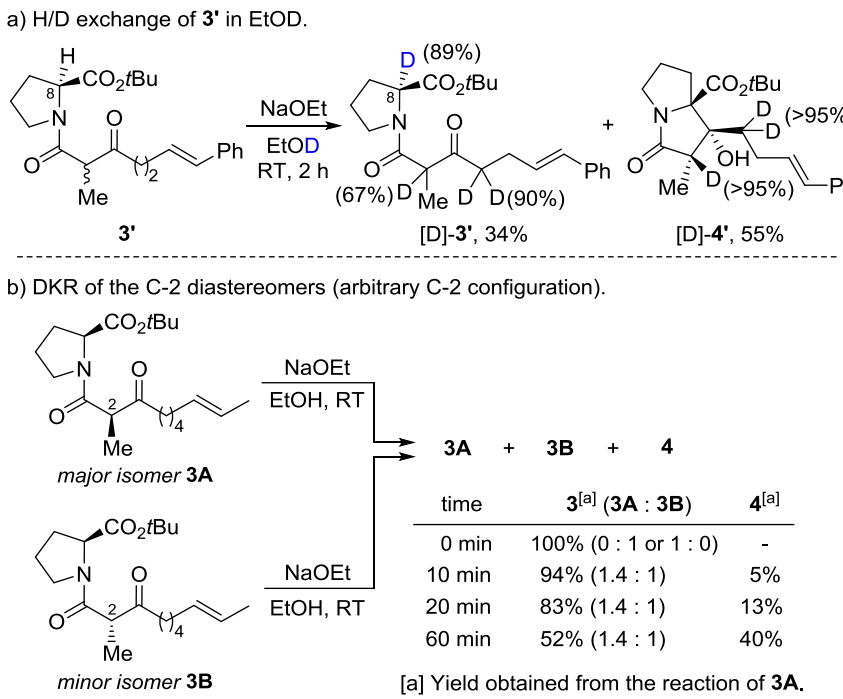

Scheme 5. Exploratory studies to determine the mechanism of the aldol reaction.

To understand our excellent stereochemical outcome, we performed additional experiments with model substrate **3′** (Scheme 5a), which consists of a UV-absorbing chromophore that allows for facile reaction analysis. When we analyzed the remaining aldol substrate in the incomplete reaction mixture, it was found that the proline stereocenter was not racemized (see the Experimental for details). In

addition, the hydrogen at the proline stereocenter was gradually replaced with deuterium when the aldol reaction was conducted in EtOD (Scheme 5a; see the Experimental for details). These observations suggested that the unreacted ester enolate intermediate was protonated with complete retention of configuration to regenerate the aldol substrate, which may result in excellent MOC in a protic solvent environment. A major factor for this MOC during deprotonation/protonation may be the torsional strain that develops when the axially chiral enolate, such as **5**, is protonated from the *si*-face, leading to the C-8 epimer of **3**.

When the two separated C-2 diastereomers of **3** were independently subjected to the optimized aldol reaction conditions, each reaction yielded the same results and afforded **4** in good yield. The monitoring of each reaction by NMR indicated the rapid epimerization at the C-2 position and the gradual formation of aldol product **4** as the only diastereomer (Scheme 5b; see the Experimental for details). The diastereomeric ratios of the two isomers from the two reactions were 1.4:1 after 10 min, and the ratio remained constant. The ratio was the same prior to the separation, and may reflect the thermodynamic stability of the isomers. Based on these observations, we are confident that DKR occurred during the reaction.

Because **4** was the only aldol product that appeared from the beginning of the reaction and because other diastereomers were not detected during the reaction, **4**

can be regarded as the kinetic product. Our computational study indicated that the obtained aldol product **4** is the most stable among all of the possible diastereomers (see the Experimental for details). Therefore, the aldol product **4** is not only the kinetic product but also the thermodynamically favored product.

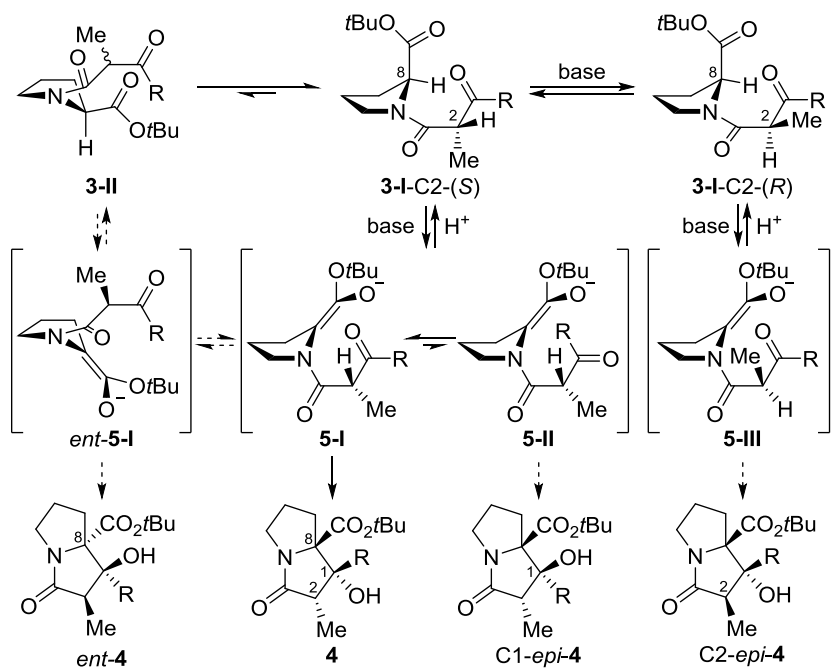

Scheme 6. Proposed mechanism for the aldol reaction.

Based on these results and earlier reports, an aldol reaction mechanism of **3** was proposed, as shown in Scheme 6. The presence of an acidic proton at the C-2 stereocenter of substrate **3** allows for easy epimerization under basic conditions. The conformer **3-I** is energetically more favored than **3-II** due to minimized 1,3-allylic strain,[10,17] and the deprotonation reaction at the proline α position on

conformer **3-I** generates an axially chiral enolate **5**. This transient enolate can be converted back to **3** by protonation with complete configuration retention at the C-8 position. Upon formation of **5**, the C2-(*S*) isomer undergoes an intramolecular aldol reaction via conformer **5-I** to yield aldol product **4**. The reaction via conformer **5-II** would be less favorable due to steric repulsion between the alkyl chain and the proline moiety. The aldol reaction of the C2-(*R*) isomer via conformer **5-III** would not be favored because the methyl group hinders enolate addition to the carbonyl group. However, based on the DKR principle, this unfavorable C-2 epimer could participate in the reaction via epimerization.[18] The excellent stereochemical outcome of the reaction may result from these kinetic factors as well as the thermodynamic preference of aldol product **4**.

III. Conclusion

In summary, using a biomimetic approach, the first total synthesis of (–)-penibruguieramine A (**1**) was achieved. The principles of 'memory of chirality' and 'dynamic kinetic resolution' were employed for the asymmetric synthesis using proline as the only chiral source. All three stereocenters were established in an intramolecular aldol reaction of proline-pentaketide amide **3** with complete diastereo- and enantioselectivity without the aid of an external chiral influence. The excellent MOC in the protic solvent environment may be associated with the return of the unreacted chiral enolate intermediate to the starting material by protonation with complete retention of configuration. The excellent diastereoselectivity is most likely related to the kinetic and thermodynamic preferences for the desired aldol product. Our synthesis is the first reported example of the combined use of MOC and DKR for the asymmetric construction of stereocenters.

IV. Experimental

IV-1. General.

All of the chemicals were of reagent grade and were used as received. All of the reactions were performed under an inert atmosphere consisting of dry nitrogen using distilled dry solvents. The reactions were monitored by thin layer chromatography (TLC) analysis using silica gel 60 F-254 TLC plates. Flash column chromatography was performed on silica gel (230-400 mesh). The melting points were measured using a Buchi B-540 melting point apparatus without correction. The optical rotations were measured using sodium light (D line 589.3 nm) at 22 ℃. ^{1}H NMR (400 or 500 MHz) and ^{13}C NMR (100 or 125 MHz) spectra were recorded in δ units relative to the non-deuterated solvent as the internal reference. The IR spectra were recorded on a Fourier Transform Infrared spectrometer. High-resolution mass spectra (HRMS) were recorded using fast atom bombardment (FAB). HPLC was performed on an Agilent 1200 series instrument with a diode array detector (DAD) and CHIRALCEL OD-H column (0.46 × 25 cm, 5 μm).

IV-2. Experimental procedure and spectroscopic data analysis

IV-2-1. Synthesis of (–)-penibruguieramine A (1)

Ethyl (*E*)-2-methyl-3-oxodec-8-enoate (9)

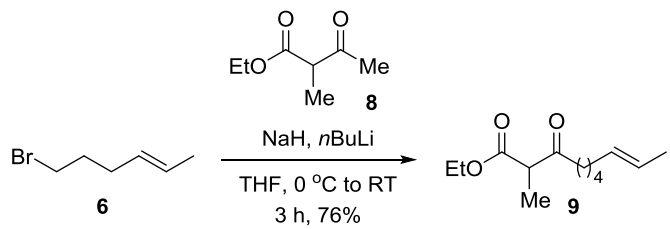

To a suspension of NaH (60% oil dispersion, 7.20 g, 180 mmol) in THF (400 mL) was slowly added ethyl 2-methylacetoacetate (**8**, 17.0 mL, 120 mmol) at 0 ℃. After 30 min, *n*BuLi (2.5 M in hexane, 52.8 mL, 132 mmol) was added slowly at 0 ℃. The mixture was stirred for an additional 30 min prior to dropwise addition of (*E*)-6-bromohex-2-ene (**6**, 6.52 g, 40.0 mmol). After 3 h of stirring at room temperature, the reaction was quenched by the slow addition of a saturated NH_4Cl aqueous solution at 0 ℃. Then, the mixture was extracted twice with ether. The combined organic layers were washed with brine, dried over $MgSO_4$, and concentrated in vacuo. The residue was purified by flash chromatography on silica gel (hexane/EtOAc, 15:1) to yield **9** (6.88 g, 76%) as a light yellow liquid: ^{1}H NMR (400 MHz, $CDCl_3$) δ 5.34–5.25 (m, 2H), 4.08 (q, J = 7.1 Hz, 2H), 3.41 (q, J = 7.1 Hz, 1H), 2.52–2.35 (m, 2H), 1.90–1.85 (m, 2H), 1.53 (d, J = 4.2 Hz, 3H),

1.51–1.45 (m, 2H), 1.27–1.23 (m, 2H), 1.22 (d, J = 7.2 Hz, 3H), 1.17 (t, J = 7.1 Hz, 3H); ^{13}C NMR (100 MHz, $CDCl_3$) δ 205.6, 170.4, 130.7, 124.9, 61.0, 52.6, 40.1, 32.1, 28.7, 22.8, 17.6, 13.9, 12.5; IR (neat, cm^{-1}) υ_{max} 2985, 2938, 2860, 1741, 1714, 1453, 1375, 1238, 1189, 966, 859; HRMS (FAB): calcd. for $C_{13}H_{23}O_3$ $[M+H]^+$ 227.1647, found 227.1656.

(*E*)-2-Methyl-3-oxodec-8-enoic acid (10)

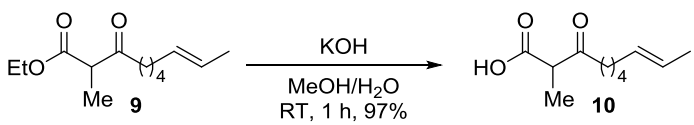

To a solution of **9** (4.52 g, 20.0 mmol) in MeOH (100 mL) was added 10% KOH aqueous solution (100 mL) at 0 ℃, and the resulting mixture was stirred at room temperature for 1 h. The reaction mixture was acidified with a 10% HCl aqueous solution and then extracted twice with EtOAc. The combined organic layers were dried over $MgSO_4$ and concentrated in vacuo to afford **10** (3.85 g, 97%) as a colorless oil, which was used in the subsequent step without further purification: ^{1}H NMR (400 MHz, $CDCl_3$) δ 11.6 (brs, 1H), 5.38–5.28 (m, 2H), 3.52 (q, J = 7.1 Hz, 1H), 2.62–2.44 (m, 2H), 1.93–1.89 (m, 2H), 1.56 (d, J = 4.7 Hz, 3H), 1.53–1.49 (m, 2H), 1.32–1.24 (m, 2H), 1.29 (d, J = 7.2 Hz, 3H); ^{13}C NMR (100 MHz, $CDCl_3$) δ 205.7, 176.2, 130.7, 125.0, 52.3, 41.3, 32.1, 28.7, 22.8, 17.6, 12.5; IR (neat, cm^{-1}) υ_{max} 3022, 2935, 2858, 1707, 1455, 1411, 1235, 966; HRMS (FAB):

calcd. for $C_{11}H_{19}O_3$ $[M+H]^+$ 199.1334, found 199.1333.

***tert*-Butyl ((*E*)-2-methyl-3-oxodec-8-enoyl)-L-prolinate (3)**

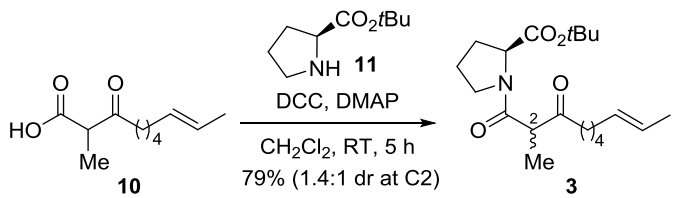

To a solution of **10** (2.50 g, 12.6 mmol) and L-proline *tert*-butyl ester (**11**, 2.56 g, 12.6 mmol) in CH_2Cl_2 (100 mL) was added DCC (2.87 g, 13.9 mmol) and DMAP (122 mg, 1.0 mmol) at 0 ℃. The reaction mixture was stirred at room temperature for 5 h and then filtered through a Celite pad. The filtrate was washed with a saturated NH_4Cl aqueous solution, dried over $MgSO_4$ and concentrated in vacuo. The residue was purified by flash chromatography on silica gel (hexane/EtOAc, 3:1) to yield a 1.4:1 mixture of **3A** and **3B** (3.50 g, 79%) as a colorless oil. Small amounts of **3A** and **3B** were carefully isolated from the mixture via chromatography on silica gel (hexane/EtOAc, 4:1) for spectroscopic analysis.

3A (major isomer): $[\alpha]^{22}_D$ –24.3 (*c* 0.5, $CHCl_3$); ^{1}H NMR (400 MHz, C_5D_5N, two rotamers in a 5:1 ratio) δ 5.40–5.34 (m, 2H), 4.82 (dd, *J* = 8.1 Hz, 2.8 Hz, 1/6H), 4.56 (dd, *J* = 8.5 Hz, 4.1 Hz, 5/6H), 3.78 (q, *J* = 6.9 Hz, 1H), 3.74–3.69 (m, 1H), 3.67–3.60 (m, 1/6H), 3.55–3.49 (m, 5/6H), 2.86 (td, *J* = 17.7 Hz, 7.4 Hz, 1H), 2.67 (td, *J* = 17.7 Hz, 7.1 Hz, 1H), 2.11–2.02 (m, 1H), 1.99–1.94 (m, 2H), 1.93–1.86 (m,

2H), 1.81–1.73 (m, 1H), 1.72–1.65 (m, 2H), 1.56–1.52 (m, 3H), 1.47 and 1.43 (each s, total 9H in a 5:1 ratio), 1.42 (d, J = 7.0 Hz, 3H), 1.38–1.27 (m, 2H); ^{13}C NMR (100 MHz, C_5D_5N; rotamer 1/ rotamer 2) δ 206.6/206.3, 172.0/171.7, 169.8/169.5, 131.6/131.5, 125.1/125.0, 82.1/81.0, 60.8/60.2, 53.0/52.6, 47.8/47.1, 40.1/40.0, 32.6/31.6, 29.4, 29.3/29.1, 27.9/27.8, 25.0, 23.4/22.8, 18.0, 13.7/13.1; IR (neat, cm^{-1}) υ_{max} 2979, 2935, 2882, 1729, 1643, 1417, 1367, 1151, 966; HRMS (FAB): calcd. for $C_{20}H_{34}NO_4$ $[M+H]^+$ 352.2488, found 352.2486.

3B (minor isomer): $[\alpha]^{22}_D$ –88.6 (*c* 0.5, $CHCl_3$); ^{1}H NMR (400 MHz, C_5D_5N, two rotamers in a 4:1 ratio) δ 5.30–5.23 (m, 2H), 4.58 (dd, J = 8.1 Hz, 2.5 Hz, 1/5H), 4.54 (dd, J = 8.5 Hz, 3.7 Hz, 4/5H), 3.75 (q, J = 7.0 Hz, 4/5H), 3.69–3.66 (m, 1/5H), 3.60–3.51 (m, 2H), 2.81 (td, J = 17.4 Hz, 7.5 Hz, 1/5H), 2.65–2.56 (m, 1H), 2.48 (td, J = 17.4 Hz, 7.2 Hz, 4/5H), 2.08–1.96 (m, 1H), 1.91–1.80 (m, 4H), 1.77–1.71 (m, 1H), 1.65–1.51 (m, 2H), 1.49–1.48 (m, 3H), 1.42 and 1.37 (each s, total 9H in a 1:4 ratio), 1.39 (d, J = 7.0 Hz, 3H), 1.28–1.19 (m, 2H); ^{13}C NMR (100 MHz, C_5D_5N; rotamer 1/ rotamer 2) δ 206.5/206.0, 172.0/171.6, 170.5/169.8, 131.54/131.48, 125.1/125.0, 82.2/80.8, 60.7/60.3, 52.6/52.4, 47.6/46.9, 40.6/40.5, 32.7/32.6, 31.6/29.5, 29.3/29.2, 27.93/27.85, 25.0/23.6, 23.5/22.6, 18.0, 13.8/13.0; IR (neat, cm^{-1}) υ_{max} 2979, 2935, 2882, 1726, 1643, 1417, 1368, 1151, 966; HRMS (FAB): calcd. for $C_{20}H_{34}NO_4$ $[M+H]^+$ 352.2488, found 352.2492.

Representative procedure for the intramolecular aldol reaction of 3 and characterization of compounds.

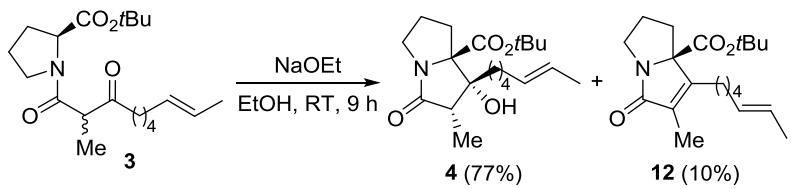

To a solution of **3** (105 mg, 0.3 mmol) in EtOH (3 mL) was added NaOEt (102 mg, 1.5 mmol), and the mixture was stirred for 9 h at room temperature. The reaction was quenched by the addition of a saturated NH_4Cl aqueous solution and extracted twice with EtOAc. The combined organic layers were dried over $MgSO_4$ and concentrated in vacuo. The residue was purified by flash chromatography on silica gel (hexane/EtOAc, 2:1) to afford **4** (81.6 mg, 77%) as a white crystalline solid and **12** (10.0 mg, 10%) as a colorless oil.

***tert*-Butyl (1*R*,2*S*,7a*R*)-1-((*E*)-hept-5-en-1-yl)-1-hydroxy-2-methyl-3-oxotetrahydro-1*H*-pyrrolizine-7a(5*H*)-carboxylate (4)** : white crystalline solid; m.p. 104–105 ℃; $[\alpha]^{22}_{D}$ –64.0 (*c* 0.5, $CHCl_3$); ^{1}H NMR (400 MHz, $CDCl_3$) δ 5.34–5.32 (m, 2H), 3.44 (td, *J* = 11.0 Hz, 7.6 Hz, 1H), 2.93 (ddd, *J* = 11.2 Hz, 8.0 Hz, 3.9 Hz, 1H), 2.83 (q, *J* = 7.2 Hz, 1H), 2.51 (brs, 1H), 2.18–2.08 (m, 2H), 1.97–1.86 (m, 3H), 1.84–1.79 (m, 1H), 1.59–1.52 (m, 5H), 1.46–1.37 (m, 2H), 1.40 (s, 9H), 1.30–1.22 (m, 2H), 1.00 (d, *J* = 7.3 Hz, 3H); ^{1}H NMR (400 MHz, C_5D_5N) δ 6.71 (s, 1H), 5.51–5.40 (m, 2H), 3.60 (td, *J* = 10.9 Hz, 7.5 Hz, 1H), 3.24 (q, *J* = 7.2 Hz, 1H), 3.06 (ddd, *J* = 11.3 Hz, 7.6 Hz, 4.4 Hz, 1H), 2.59 (td, *J* = 12.6 Hz, 8.8 Hz, 1H),

2.41 (ddd, *J* = 12.4 Hz, 7.4 Hz, 4.7 Hz, 1H), 2.09–2.04 (m, 2H), 1.96–1.78 (m, 5H), 1.75–1.68 (m, 1H), 1.59 (d, *J* = 4.9 Hz, 3H), 1.50 (s, 9H), 1.47–1.34 (m, 2H), 1.44 (d, *J* = 7.2 Hz, 3H); ^{13}C NMR (100 MHz, $CDCl_3$) δ 175.0, 171.5, 131.0, 124.8, 82.1, 81.3, 80.4, 49.3, 40.9, 35.6, 32.4, 30.1, 27.73, 27.69, 26.0, 22.8, 17.7, 7.2; IR (neat, cm^{-1}) υ_{max} 3315, 2980, 2920, 2883, 1718, 1676, 1442, 1367, 1223, 1153, 1104, 965, 847, 760; HRMS (FAB): calcd. for $C_{20}H_{34}NO_4$ $[M+H]^+$ 352.2488, found 352.2481.

***tert*-Butyl (*R*,*E*)-7-(hept-5-en-1-yl)-6-methyl-5-oxo-2,3-dihydro-1*H*-pyrrolizine-7a(5*H*)-carboxylate (12)** : colorless oil; $[\alpha]^{22}_D$ +85.9 (*c* 0.5, $CHCl_3$); ^{1}H NMR (400 MHz, $CDCl_3$) δ 5.39–5.28 (m, 2H), 3.46 (td, *J* = 11.0 Hz, 8.7 Hz, 1H), 3.19 (ddd, *J* = 11.3 Hz, 8.9 Hz, 2.6 Hz, 1H), 2.46 (dd, *J* = 12.1 Hz, 6.5 Hz, 1H), 2.40–2.32 (m, 1H), 2.25–2.06 (m, 3H), 1.93–1.89 (m, 2H), 1.71 (s, 3H), 1.57 (d, *J* = 4.8 Hz, 3H), 1.54–1.47 (m, 1H), 1.38 (s, 9H), 1.35–1.20 (m, 4H); ^{13}C NMR (100 MHz, $CDCl_3$) δ 176.1, 169.5, 154.6, 130.7, 130.1, 125.1, 82.2, 79.2, 41.4, 33.1, 32.1, 29.5, 28.4, 27.7, 27.1, 26.9, 17.7, 9.0; IR (neat, cm^{-1}) υ_{max} 2976, 2933, 2860, 1726, 1695, 1367, 1293, 1152, 1106, 966, 843, 763; HRMS (FAB): calcd. for $C_{20}H_{32}NO_3$ $[M+H]^+$ 334.2382, found 334.2385.

Table S1. Additional conditions tested to optimize the intramolecular aldol reaction of **3** (see Table 1 in the main text).[a]

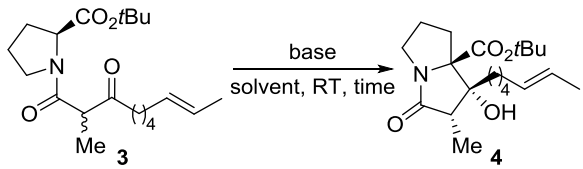

Entry	Base (equiv)	Solvent	Time (h)	Yield[b] (%)
1	KO*t*Bu (5)	*t*BuOH	3	0[c]
2	KO*t*Bu (5)	THF	3	0[c]
3	DBU (5)	THF	16	0[d]
4	DTBPy (5)	THF	16	0[d]
5	KOH (5)	H_2O/THF (3/1)	72	<2[e]
6	CsOH (5)	H_2O/THF (3/1)	72	<2[e]

[a] Reactions were run with **3** (105 mg, 0.3 mmol) at a substrate concentration of 0.1 M. [b] Determined by ^{1}H NMR analysis. [c] Complex mixture. [d] **3** was recovered. [e] **3** was recovered in ca. 80% yield. DBU =1,8-diazabicyclo[5.4.0]undec-7-ene. DTBPy=2,6-di-*tert*-butylpyridine.

(–)-Penibrugueiramine A (1)

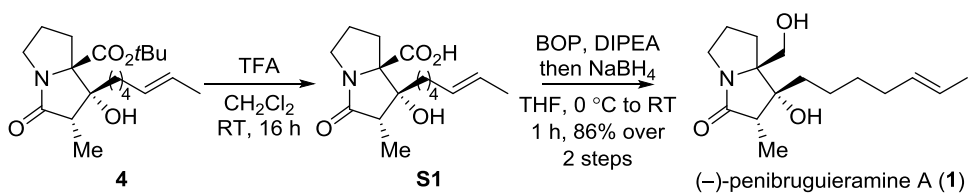

To a solution of **4** (52.7 mg, 0.15 mmol) in CH_2Cl_2 (1.0 mL) was added trifluoroacetic acid (TFA) (0.5 mL) at 0 ℃, and the mixture was stirred for 16 h at room temperature. The reaction mixture was concentrated in vacuo to afford crude **S1** as a white solid, which was used in the subsequent step without further

purification: m.p. 206 ℃ (dec.); $[\alpha]^{22}_{D}$ –70.7 (*c* 0.5, MeOH); ^{1}H NMR (400 MHz, CD_3OD) δ 5.46–5.35 (m, 2H), 3.44 (td, *J* = 10.9 Hz, 7.8 Hz, 1H), 3.02 (ddd, *J* = 11.2 Hz, 8.4 Hz, 3.4 Hz, 1H), 2.94 (q, *J* = 7.2 Hz, 1H), 2.26–2.22 (m, 2H), 2.09–2.02 (m, 1H), 1.99–1.90 (m, 3H), 1.73–1.66 (m, 1H), 1.62 (d, *J* = 3.2 Hz, 3H), 1.57–1.45 (m, 3H), 1.34–1.29 (m, 2H), 1.04 (d, *J* = 7.2 Hz, 3H); ^{13}C NMR (100 MHz, CD_3OD) δ 178.6, 176.4, 133.2, 126.4, 83.3, 82.7, 51.7, 42.8, 37.6, 34.2, 32.1, 29.3, 27.7, 24.9, 18.9, 8.6; IR (neat, cm^{-1}) υ_{max} 3415, 2943, 2894, 2853, 2479, 1693, 1633, 1451, 1257, 1222, 1096, 983, 959, 710; HRMS (FAB): calcd. for $C_{16}H_{26}NO_4$ $[M+H]^+$ 296.1862, found 296.1863.

To a solution of crude **S1** in THF (2.0 mL) was added benzotriazol-1-yloxytris(dimethylamino)phosphonium hexafluorophosphate (BOP, 75.0 mg, 0.17 mmol) and diisopropylethyl amine (32.0 μL, 0.23 mmol) at room temperature. The resulting solution was stirred for 10 min, and then $NaBH_4$ (17.0 mg, 0.45 mmol) was added in portions at 0 ℃. After 1 h of stirring at room temperature, the reaction was quenched by the addition of a saturated NH_4Cl aqueous solution and was extracted four times with EtOAc. The combined organic layers were dried over $MgSO_4$ and concentrated in vacuo. The residue was purified by flash chromatography on silica gel (CH_2Cl_2/MeOH, 20:1) to yield **1** (36.1 mg, 86%) as a white solid: m.p. 173–174 ℃; $[\alpha]^{22}_{D}$ –21.3 (*c* 0.05, $CHCl_3$); ^{1}H NMR (500 MHz, $CDCl_3$) δ 5.44–5.35 (m, 2H), 3.77 (ddd, *J* = 11.5 Hz, 8.1 Hz, 3.6 Hz, 1H), 3.69 (d, *J*

= 11.8 Hz, 1H), 3.52 (d, *J* = 11.9 Hz, 1H), 2.96 (q, *J* = 7.1 Hz, 1H), 2.93–2.90 (m, 1H), 2.25 (ddd, *J* = 13.2 Hz, 9.0 Hz, 4.5 Hz, 1H) 2.15 (brs, 1H, OH), 2.02–1.96 (m, 2H), 1.95–1.90 (m, 1H), 1.88–1.81 (m, 1H), 1.71 (ddd, *J* = 14.3 Hz, 12.4 Hz, 4.1 Hz, 1H), 1.63 (d, *J* = 4.9 Hz, 3H), 1.59 (dd, *J* = 14.5 Hz, 4.5 Hz, 1H), 1.56–1.50 (m, 1H), 1.45 (td, *J* = 13.0 Hz, 8.0 Hz, 1H), 1.41 (s, 1H, OH), 1.39–1.33 (m, 2H), 1.28–1.21 (m, 1H), 1.05 (d, *J* = 7.3 Hz, 3H); ^{13}C NMR (125 MHz, $CDCl_3$) δ 177.2, 131.0, 125.2, 81.5, 75.8, 65.8, 49.1, 42.7, 34.2, 32.3, 30.0, 27.2, 26.5, 23.2, 17.9, 7.1; IR (neat, cm^{-1}) υ_{max} 3366, 3201, 2932, 2868, 1677, 1452, 1055, 969, 721; HRMS (FAB): calcd. for $C_{16}H_{28}NO_3$ $[M+H]^+$ 282.2069, found 282.2078.

Data comparison between natural and synthetic (–)-penibrugueiramine A.

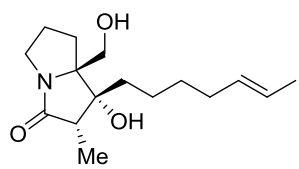

(–)-penibruguieramine A

$[\alpha]^{22}_D$ -21.3 (*c* 0.05, $CHCl_3$)

lit. $[\alpha]^{22}_D$ -22 (*c* 0.05, $CHCl_3$)

^{1}H NMR (500 MHz, $CDCl_3$)		**^{13}C NMR (125 MHz, $CDCl_3$)**	
Natural[1]	**Synthetic**	**Natural**[1]	**Synthetic**
5.41 (m, 2H)	5.44–5.35 (m, 2H)	177.4	177.2
3.78 (m, 1H)	3.77 (ddd, *J* = 11.5 Hz, 8.1 Hz, 3.6 Hz, 1H)	130.9	131.0
3.71 (d, *J* = 11.9 Hz, 1H)	3.69 (d, *J* = 11.8 Hz, 1H)	125.2	125.2
3.54 (d, *J* = 11.9 Hz, 1H)	3.52 (d, *J* = 11.9 Hz, 1H)	81.6	81.5

2.98 (q, *J* = 7.2 Hz, 1H)	2.96 (q, *J* = 7.1 Hz, 1H)	75.8	75.8
2.94 (m, 1H)	2.93–2.90 (m, 1H)	65.8	65.8
2.228 (ddd, *J* = 13.5 Hz, 11.0 Hz, 6.3 Hz, 1H)	2.25 (ddd, *J* = 13.2 Hz, 9.0 Hz, 4.5 Hz, 1H)	49.1	49.1
	2.15 (brs, 1H, OH)	42.8	42.7
2.00 (m, 2H)	2.02–1.96 (m, 2H)	34.2	34.2
1.95 (m, 1H)	1.95–1.90 (m, 1H)	32.3	32.3
1.86 (ddd, *J* = 12.2 Hz, 12.9 Hz, 6.3 Hz, 1H)	1.88–1.81 (m, 1H)	30.0	30.0
1.72 (m, 1H)	1.71 (ddd, *J* = 14.3 Hz, 12.4 Hz, 4.1 Hz, 1H)	27.2	27.2
1.65 (d, *J* = 4.9 Hz, 3H)	1.63 (d, *J* = 4.9 Hz, 3H)	26.5	26.5
1.61 (dd, *J* = 14.5 Hz, 4.5 Hz, 1H)	1.59 (dd, *J* = 14.5 Hz, 4.5 Hz, 1H)	23.2	23.2
1.54 (m, 1H)	1.56–1.50 (m, 1H)	17.9	17.9
1.47 (m, 1H)	1.45 (td, *J* = 13.0 Hz, 8.0 Hz, 1H)	7.1	7.1
	1.41 (s, 1H, OH)		
1.38 (m, 1H)	1.39–1.33 (m, 2H)		
1.26 (m, 1H)			
1.24 (m, 1H)	1.28–1.21 (m, 1H)		
1.06 (d, *J* = 7.2 Hz, 3H)	1.05 (d, *J* = 7.3 Hz, 3H)		

Determination of the enantiomeric excess of 1

a. Via the ^{1}H NMR spectra of its Mosher ester derivatives

Scheme S1. Preparation of Mosher esters of **1**.

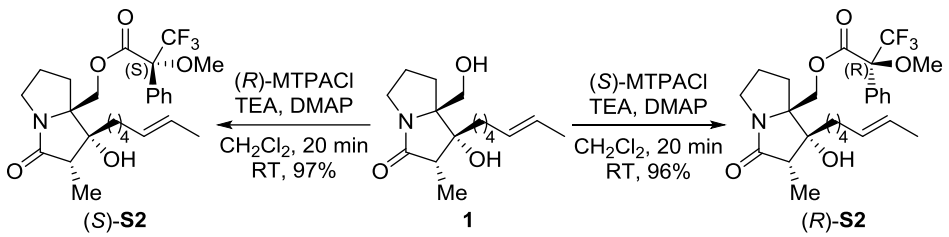

To a solution of **1** (10.0 mg, 0.036 mmol) in CH_2Cl_2 (0.5 mL) was added trimethylamine (30.0 μL, 0.22 mmol) and a catalytic amount of DMAP at 0 ℃. (*R*)-α-Methoxy-α-(trifluoromethyl)phenylacetyl chloride (16.1 μL, 0.086 mmol) was added, and the reaction mixture was stirred for 20 min at room temperature. The reaction was quenched by the addition of a saturated NH_4Cl aqueous solution and extracted twice with CH_2Cl_2. The combined organic layers were dried over $MgSO_4$ and concentrated in vacuo. The residue was purified by flash chromatography on silica gel (hexane/EtOAc, 1:1) to yield (*S*)-**S2** (17.3 mg, 97%) as a colorless oil: ^{1}H NMR (400 MHz, $CDCl_3$) δ 7.48–7.38 (m, 5H), 5.43–5.31 (m, 2H), 4.25 (d, J = 11.7 Hz, 1H), 4.15 (d, J = 11.7 Hz, 1H), 3.70 (ddd, J = 11.6 Hz, 8.0 Hz, 3.7 Hz, 1H), 3.49 (s, 3H), 2.77 (td, J = 11.3 Hz, 8.0 Hz, 1H), 2.54 (q, J = 7.1 Hz, 1H), 2.31 (ddd, J = 13.4 Hz, 9.0 Hz, 4.7 Hz, 1H), 1.96–1.84 (m, 3H), 1.82–1.77 (m, 1H), 1.64 (d, J = 5.1 Hz, 3H), 1.57 (brs, 1H), 1.46–1.29 (m, 3H), 1.27–1.20 (m, 3H), 1.16–1.09 (m, 1H), 0.92 (d, J = 7. 2 Hz, 3H).

(*R*)-**S2** was prepared according to the procedure described above for (*S*)-**S2** using (*S*)-α-methoxy-α-(trifluoromethyl)phenylacetyl chloride (16.1 μL, 0.086 mmol)

instead of (*R*)-α-methoxy-α-(trifluoromethyl)phenylacetyl chloride to yield (*R*)-**S2** (17.1 mg, 96%) as a colorless oil: ^{1}H NMR (400 MHz, $CDCl_3$) δ 7.47–7.39 (m, 5H), 5.44–5.33 (m, 2H), 4.33 (d, *J* = 11.4 Hz, 1H), 4.19 (d, *J* = 11.4 Hz, 1H), 3.68 (ddd, *J* = 11.5 Hz, 7.1 Hz, 4.4 Hz, 1H), 3.47 (s, 3H), 2.72 (td, *J* = 11.2 Hz, 8.1 Hz, 1H), 2.56 (q, *J* = 7.1 Hz, 1H), 2.28 (ddd, *J* = 13.2 Hz, 8.0 Hz, 5.4 Hz, 1H), 1.97–1.94 (m, 2H), 1.77–1.68 (m, 2H), 1.64 (d, *J* = 5.1 Hz, 3H), 1.50–1.44 (m, 2H), 1.42–1.36 (m, 1H), 1.33–1.18 (m, 5H), 0.98 (d, *J* = 7. 2 Hz, 3H).

Scheme S2. Preparation of the (*S*)-Mosher ester of *rac*-**1**.

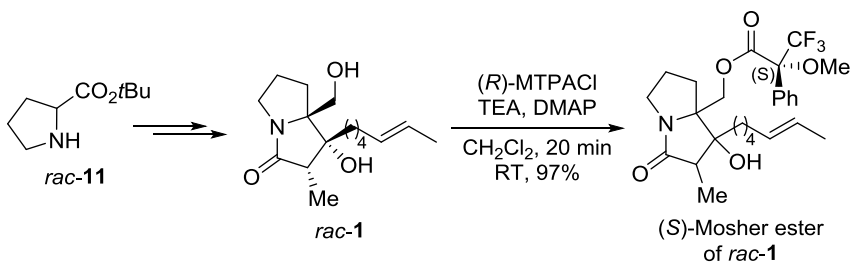

Rac-**1** was prepared according to the procedure described above for **1** using *rac*-**11** instead of **11**. *Rac*-**1** (10 mg, 0.036 mmol) was subjected to Mosher ester formation with (*R*)-α-methoxy-α-(trifluoromethyl)phenylacetyl chloride (16.1 μL, 0.086 mmol) according to the procedure described above for (*S*)-**S2** to yield the (*S*)-Mosher ester of *rac*-**1** (17.3 mg, 97%) as a colorless oil.

The ^{1}H NMR spectra of the crude products of (*S*)-**S2** and (*R*)-**S2** were obtained and compared with the ^{1}H NMR spectrum of the (*S*)-Mosher ester of *rac*-**1**. Based on these spectra, the enantiomeric purity of **1** was determined as > 99%.

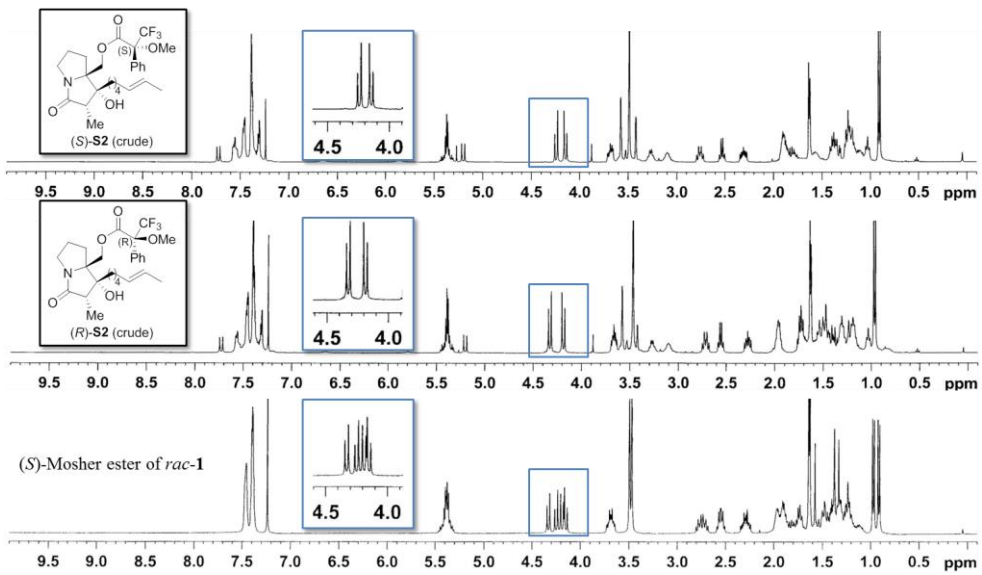

Figure S1. Comparison of the ^{1}H NMR spectra of crude (*S*)-**S2**, (*R*)-**S2** and the (*S*)-Mosher ester of *rac*-**1** (400 MHz, $CDCl_3$).

b. Via separation using chiral HPLC

Scheme S3. Preparation of the **S3**.

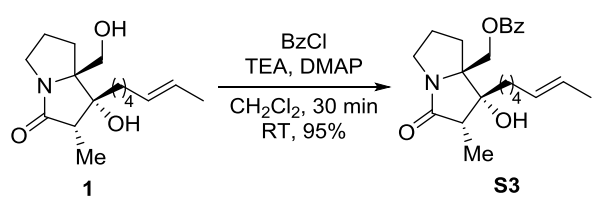

To a solution of **1** (5.00 mg, 0.018 mmol) in CH_2Cl_2 (0.5 mL) was added trimethylamine (10.0 μL, 0.072 mmol) and a catalytic amount of DMAP at 0 °C. Benzoyl chloride (4.18 μL, 0.036 mmol) was added, and the reaction mixture was stirred for 30 min at room temperature. The reaction mixture was concentrated in

vacuo The residue was purified by flash chromatography on silica gel (hexane/EtOAc, 1:2) to yield **S3** (6.50 mg, 95%) as a colorless oil: ^{1}H NMR (400 MHz, $CDCl_3$) δ 7.95 (d, J = 7.4 Hz, 2H), 7.57 (t, J = 7.5 Hz, 1H), 7.44 (t, J = 7.7 Hz, 2H), 5.41–5.33 (m, 2H), 4.38 (d, J = 11.7 Hz, 1H), 4.32 (d, J = 11.7 Hz, 1H), 3.79 (ddd, J = 11.6 Hz, 8.2 Hz, 3.7 Hz, 1H), 3.03 (td, J = 11.1 Hz, 8.2 Hz, 1H), 2.92 (q, J = 7.2 Hz, 1H), 2.40 (ddd, J = 13.4 Hz, 9.1 Hz, 4.7 Hz, 1H), 2.07–2.02 (m, 1H), 1.96–1.88 (m, 3H), 1.71–1.64 (m, 3H), 1.62–1.51 (m, 4H), 1.37–1.28 (m, 3H), 1.10 (d, J = 7. 3 Hz, 3H).

Scheme S4. Preparation of the *rac*-**S3**.

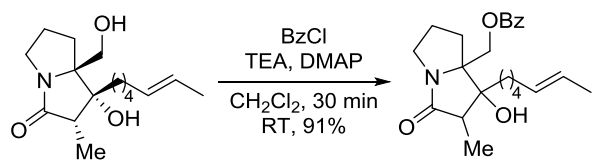

rac-**1** *rac*-**S3**

Rac-**1** (5.00 mg, 0.018 mmol) was subjected to benzoate formation with benzoyl chloride (4.18 μL, 0.036 mmol) according to the procedure described above for **S3** to yield *rac*-**S3** (6.20 mg, 91%) as a colorless oil.

The enantiomeric purity of **S3** was analyzed by chiral HPLC. The chiral HPLC chromatogram of **S3** was compared with that of *rac*-**S3.** Based on this comparison, the enantiomeric purity of **S3** was determined to be 99%.

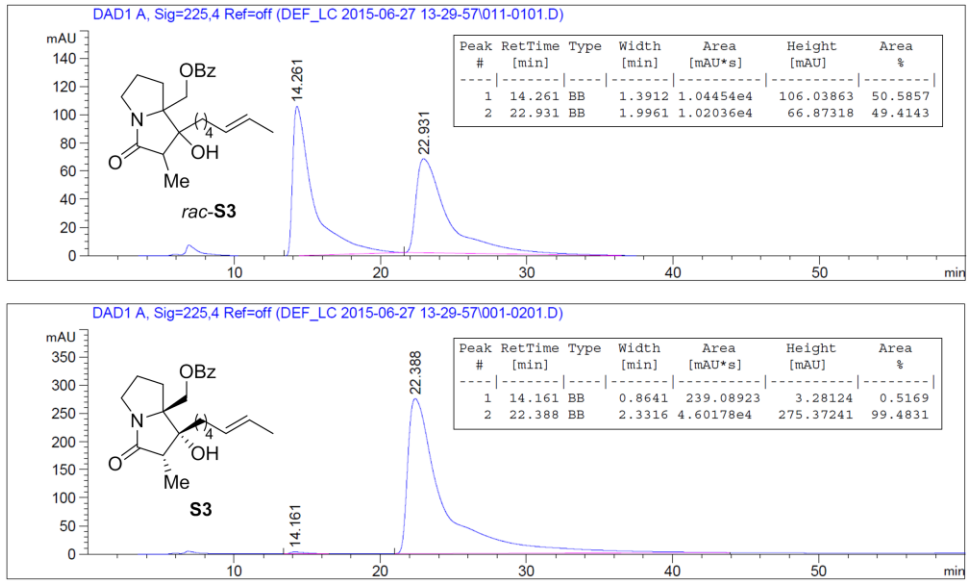

Figure S2. Chiral HPLC chromatograms of **S3** and *rac*-**S3**.

HPLC conditions: CHIRALCEL OD-H (0.46 × 25 cm, 5 μm), hexane/2-propanol = 90:10, flow rate = 0.5 mL/min, λ = 225.4 nm. The retention times are shown in Figure S2.

IV-2-2. Exploratory studies to determine the mechanism of the aldol reaction.

To understand our 'memory of chirality' (MOC) results, we employed a model substrate **3′**, which contained a UV-absorbing chromophore. **3′** was prepared according to the procedure described for **3** using cinnamyl bromide (**S4**) instead of

6.

Scheme S5. Preparation of **3′**

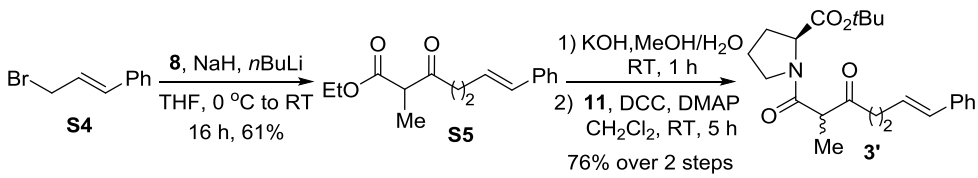

To a suspension of NaH (60% oil dispersion, 480 mg, 12.0 mmol) in THF (40 mL) was slowly added ethyl 2-methylacetoacetate (**8**, 1.13 mL, 8.0 mmol) at 0 ℃. After 30 min, *n*BuLi (2.5 M in hexane, 3.5 mL, 8.8 mmol) was added slowly at 0 ℃. The mixture was stirred for an additional 30 min prior to dropwise addition of cinnamyl bromide (**S4**, 1.58 g, 8.0 mmol) in THF (10 mL). After 30 min of stirring at room temperature, the reaction was quenched by the slow addition of a saturated NH_4Cl aqueous solution at 0 ℃. Then, the mixture was extracted twice with ether. The combined organic layers were washed with brine, dried over $MgSO_4$, and concentrated in vacuo. The residue was purified by flash chromatography on silica gel (hexane/EtOAc, 15:1) to afford **S5** (1.27 g, 61%) as a light yellow liquid.

To a solution of **S5** (1.27 g, 4.9 mmol) in MeOH (50 mL) was added 10% KOH aqueous solution (50 mL) at 0 ℃, and the resulting mixture was stirred at room temperature for 1 h. The reaction mixture was acidified with a 10% HCl aqueous solution and then extracted twice with EtOAc. The combined organic layers were dried over $MgSO_4$ and concentrated in vacuo to yield the crude acid as a colorless oil, which was used in the subsequent step without further purification.

To a solution of this crude acid and L-proline *tert*-butyl ester (**11**, 840 mg, 4.9 mmol) in CH_2Cl_2 (50 mL) was added DCC (1.01 g, 4.9 mmol) and DMAP (47.6 mg, 0.39 mmol) at 0 ℃. The reaction mixture was stirred at room temperature for 5 h and then filtered through a Celite pad. The filtrate was washed with a saturated NH_4Cl aqueous solution, dried over $MgSO_4$ and concentrated in vacuo. The residue was purified by flash chromatography on silica gel (hexane/EtOAc, 3:1) to yield a 1.3:1 diastereomeric mixture of **3′** (1.44 g, 76% in 2 steps) as a light yellow oil. A small amount of **3′A** and **3′B** was carefully isolated from the mixture by chromatography on silica gel (hexane/EtOAc, 4:1) for spectroscopic analysis.

3′A (major isomer): $[\alpha]^{22}_{D}$ –15.4 (*c* 0.3, $CHCl_3$); ^{1}H NMR (400 MHz, C_5D_5N, two rotamers in a 4:1 ratio) δ 7.44–7.18 (m, 5H), 6.54–6.33 (m, 2H), 4.84 (dd, *J* = 7.9 Hz, 2.8 Hz, 1/5H), 4.57 (dd, *J* = 8.5 Hz, 4.0 Hz, 4/5H), 3.81 (q, *J* = 6.8 Hz, 1H), 3.73–3.67 (m, 1H), 3.64–3.59 (m, 1/5H), 3.50 (td, *J* = 9.7 Hz, 6.7 Hz, 4/5H), 3.06 (td, *J* = 17.8 Hz, 7.3 Hz, 1H), 2.91–2.83 (m, 1H), 2.62–2.49 (m, 2H), 2.08–2.00 (m, 1H), 1.94–1.84 (m, 2H), 1.77–1.69 (m, 1H), 1.44 and 1.42 (each s, total 9H in a 4:1 ratio), 1.42 (d, *J* = 6.6 Hz, 3H); ^{13}C NMR (100 MHz, C_5D_5N; rotamer 1/ rotamer 2) δ 205.9/205.5, 171.7, 169.7/169.4. 138.2/138.1, 131.0/130.9, 129.9/129.7, 128.9, 127.4/127.3, 126.5, 82.1/81.1, 60.8/60.3, 53.1/52.7, 47.8/47.1, 40.3/39.8, 31.5/29.5, 27.8/27.7, 27.3/27.2, 25.0/22.7, 13.1/13.0; IR (neat, cm^{-1}) υ_{max} 2979, 2934, 3880, 1727, 1641, 1419, 1367, 1149, 966, 743, 694; HRMS (FAB): calcd. for $C_{23}H_{32}NO_4$

$[M+H]^+$ 386.2331, found 386.2327.

3′B (minor isomer): $[\alpha]^{22}_D$ –56.9 (*c* 0.5, $CHCl_3$); ^1H NMR (400 MHz, C_5D_5N, two rotamers in a 4:1 ratio) δ 7.40–7.16 (m, 5H), 6.46–6.24 (m, 2H), 4.67 (dd, *J* = 7.8 Hz, 2.8 Hz, 1/5H), 4.61 (dd, *J* = 8.5 Hz, 3.6 Hz, 4/5H), 3.85 (q, *J* = 7.0 Hz, 4/5H), 3.80–3.74 (m, 2/5H), 3.70 (q, *J* = 6.9 Hz, 1/5H), 3.65–3.57 (m, 8/5H), 3.16–3.02 (m, 1/5H), 2.93–2.83 (m, 1H), 2.78–2.70 (m, 4/5H), 2.63–2.52 (m, 2H), 2.17–1.99 (m, 1H), 1.94–1.85 (m, 2H), 1.80–1.67 (m, 1H), 1.47 (d, *J* = 7.7 Hz, 3H), 1.46 and 1.43 (each s, total 9H in a 1:4 ratio); ^{13}C NMR (100 MHz, C_5D_5N; rotamer 1/ rotamer 2) δ 205.9/205.4, 172.1/171.6, 170.5/169.7, 138.1, 131.0/130.8, 130.0/129.8, 128.91/128.89, 127.4/127.3, 126.5, 82.3/80.8, 60.7/60.3, 52.7/52.6, 47.7/46.9, 40.3/40.2, 31.6/29.5, 27.9/27.8, 27.5/27.4, 25.0/22.6, 13.9/13.0; IR (neat, cm^{-1}) υ_{max} 2980, 2932, 1722, 1639, 1420, 1367, 1150, 966, 735, 694; HRMS (FAB): calcd. for $C_{23}H_{32}NO_4$ $[M+H]^+$ 386.2331, found 386.2325.

IV-2-2-1. Chiral HPLC chromatograms of 3′

Using **3′**, we analyzed the remaining aldol substrate of the incomplete reaction mixture (NaOEt/EtOH, RT, after 0.5, 1 and 2 h) by chiral HPLC. The chromatograms were compared with the chromatogram obtained from an analogue of **3′**, which was prepared from *rac*-**11**. As shown in Figure S3, only two peaks were identified, which correspond to the two C-2 diastereomers of **3′**, and no peaks

due to the racemization at the proline stereocenter were observed. The proline stereocenter was not racemized under the optimized aldol reaction conditions.

HPLC conditions : CHIRALCEL OD-H (0.46 × 25 cm, 5 μm), hexane/2-propanol = 90:10, flow rate = 0.7 mL/min, λ = 254 nm. The retention times are shown in Figure S3.

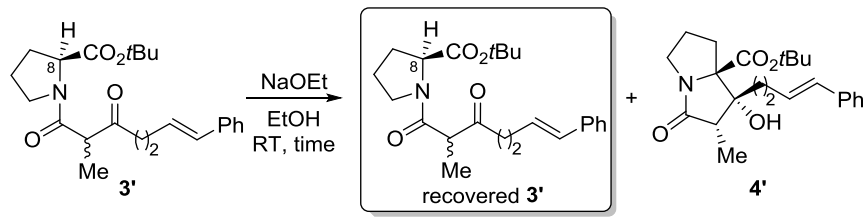

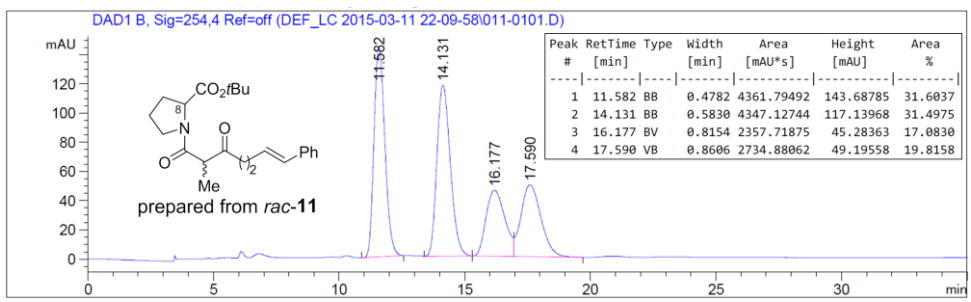

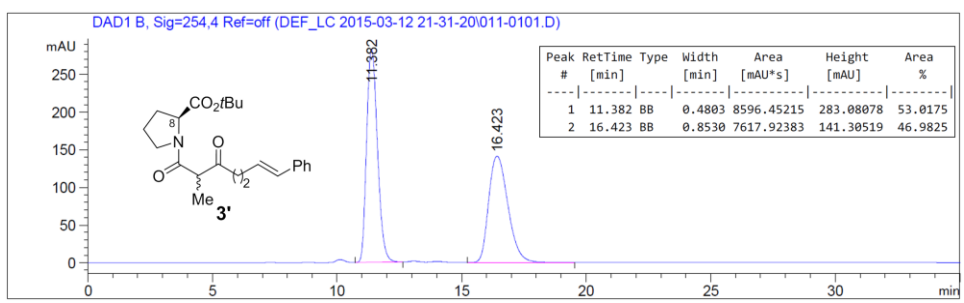

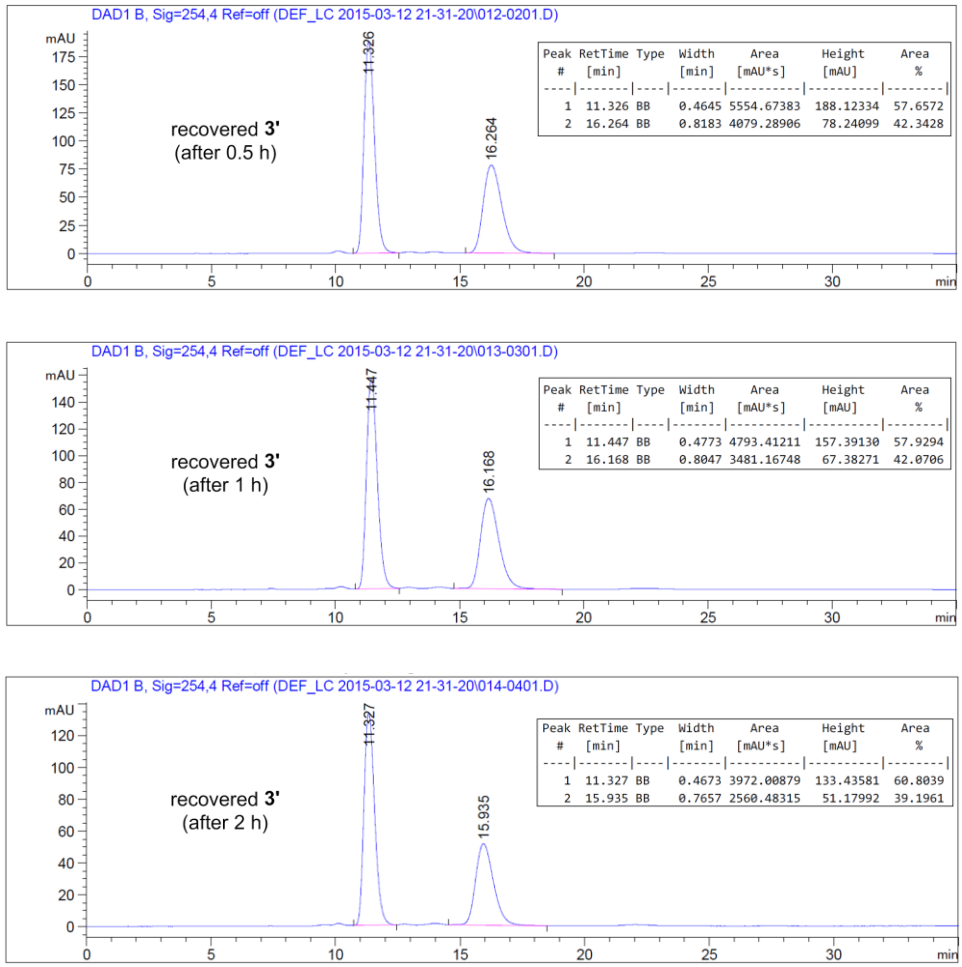

Figure S3. Chiral HPLC chromatograms of **3′** after the corresponding reaction times under the optimized aldol reaction conditions.

4′: m.p. 159–160 ℃; $[\alpha]^{22}_{D}$ –93.8 (*c* 0.5, $CHCl_3$); ^{1}H NMR (400 MHz, $CDCl_3$) δ 7.30–7.24 (m, 4H), 7.18–7.15 (m, 1H), 6.40 (d, *J* = 15.8 Hz, 1H), 6.21–6.14 (m, 1H), 3.51 (td, *J* = 10.8 Hz, 7.7 Hz, 1H), 3.01 (ddd, *J* = 11.7 Hz, 7.8 Hz, 4.1 Hz, 1H), 2.92 (q, *J* = 7.1 Hz, 1H), 2.67 (s, 1H), 2.44 (q, *J* = 7.4 Hz, 2H), 2.30–2.18 (m, 2H),

2.03–1.98 (m, 1H), 1.91–1.80 (m, 2H), 1.71–1.63 (m, 1H), 1.46 (s, 9H), 1.09 (d, *J* = 7.2 Hz, 3H); ^{13}C NMR (100 MHz, $CDCl_3$) δ 174.8, 171.5, 137.4, 130.2, 129.9, 128.4, 126.9, 125.8, 82.4, 81.3, 80.4, 49.5, 41.0, 35.1, 27.9, 27.8, 26.9, 26.1, 7.2; IR (neat, cm^{-1}) υ_{max} 3283, 2976, 2954, 2881, 1717, 1678, 1443, 1152, 1103, 959, 847, 757; HRMS (FAB): calcd. for $C_{23}H_{32}NO_4$ $[M+H]^+$ 386.2331, found 386.2327.

IV-2-2-2. Deuterium exchange experiment

We conducted the intramolecular aldol reaction of **3′** in EtOD and analyzed the remaining **3′** ([D]-**3′**) in the incomplete reaction mixture (NaOEt/EtOD, RT, after 0.5, 1 and 2 h) by ^{1}H NMR. The hydrogen at the α-carbon of the proline moiety of **3′** was gradually exchanged with deuterium over the course of the reaction. This result suggested that the aldol reaction of the transient enolate is not faster than the deuteration; otherwise, the deuterium would not be incorporated into the substrate.

Note: Deuteration at the other two α-positions of the ketone of **3′** also occurred, which was more rapid than the deuteration at the α-carbon of proline. After 0.5 h, deuterium incorporation was observed at the C-2 and C-1′ positions at approximately 70% and 90%, respectively. The partial deuterium/hydrogen exchange during the work-up appears to be responsible for the incomplete deuteration at these positions. Significant levels of deuteration (>95% D) were also observed at the C-2 and C-1′ positions of [D]-**4′**.

Table S2. H/D exchange of **3′** in EtOD.[a]

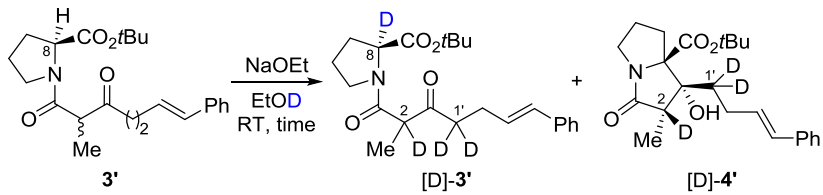

Entry	Time (h)	% D at C-8 of [D]-**3′**[b]	yield[c] (%)	
			[D]-**3′**	[D]-**4′**
1	0.5	27	79	15
2	1	79	49	44
3	2	89	34	55

[a] Reactions were run with **3′** (77 mg, 0.2 mmol) and NaOEt (68 mg, 1.0 mmol) in EtOD (2 mL). [b] Determined by ^{1}H NMR. [c] Isolated yield.

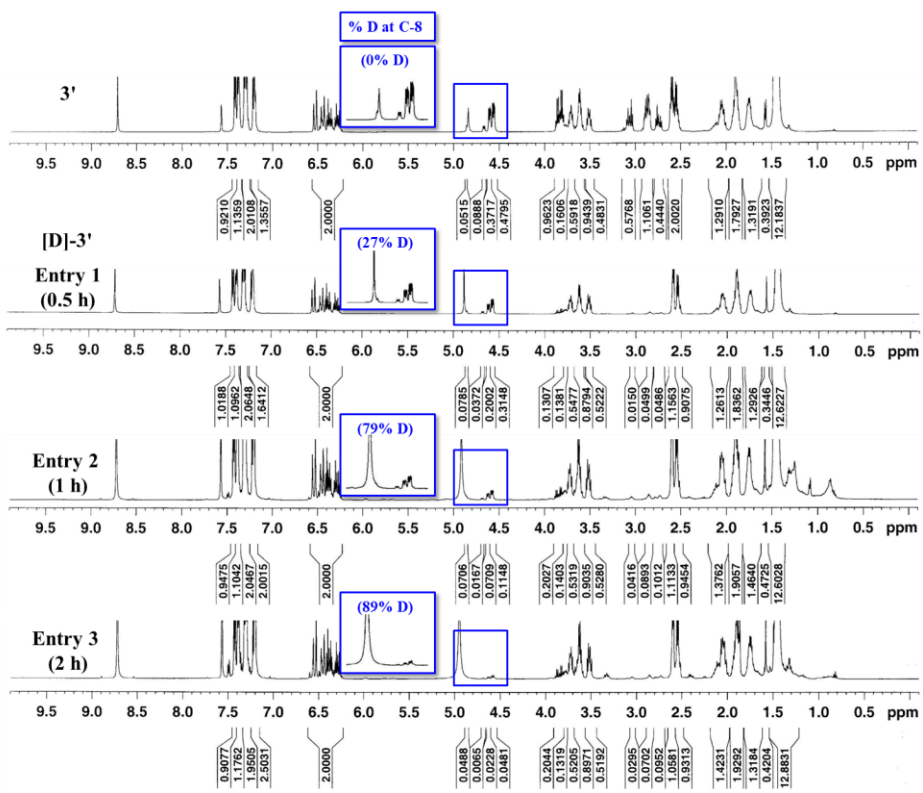

Figure S4. ^{1}H NMR spectra of **3′** and [D]-**3′** after the corresponding reaction times in EtOD (500 MHz, C_5D_5N).

Overall, the chiral HPLC analysis and deuterium exchange experiment suggested that the unreacted enolate intermediate was protonated with complete retention of configuration to regenerate aldol substrate **3**. This result may explain the excellent MOC in the protic solvent environment.

IV-2-2-3. DKR of the C-2 diastereomers of 3.

To verify that the reaction proceeded via DKR, the C-2 diastereomers of **3** were separated by careful column chromatography from the 1.4:1 mixture. The major isomer was assigned as **3A**, and the minor isomer was assigned as **3B**. The monitoring of each reaction by NMR indicated the rapid epimerization at the C-2 position and the gradual formation of aldol product **4** as the only diastereomer. The diastereomeric ratio of the two isomers was 1.4:1 after 10 min, which remained constant. This ratio was the same prior to the separation, which may reflect the thermodynamic stability of the isomers. The rationale for these observations could be that one of the C-2 epimers of substrate **3** may be kinetically preferred in the intramolecular aldol reaction, and the other isomer undergoes facile epimerization to the favored isomer to reach thermodynamic equilibrium.

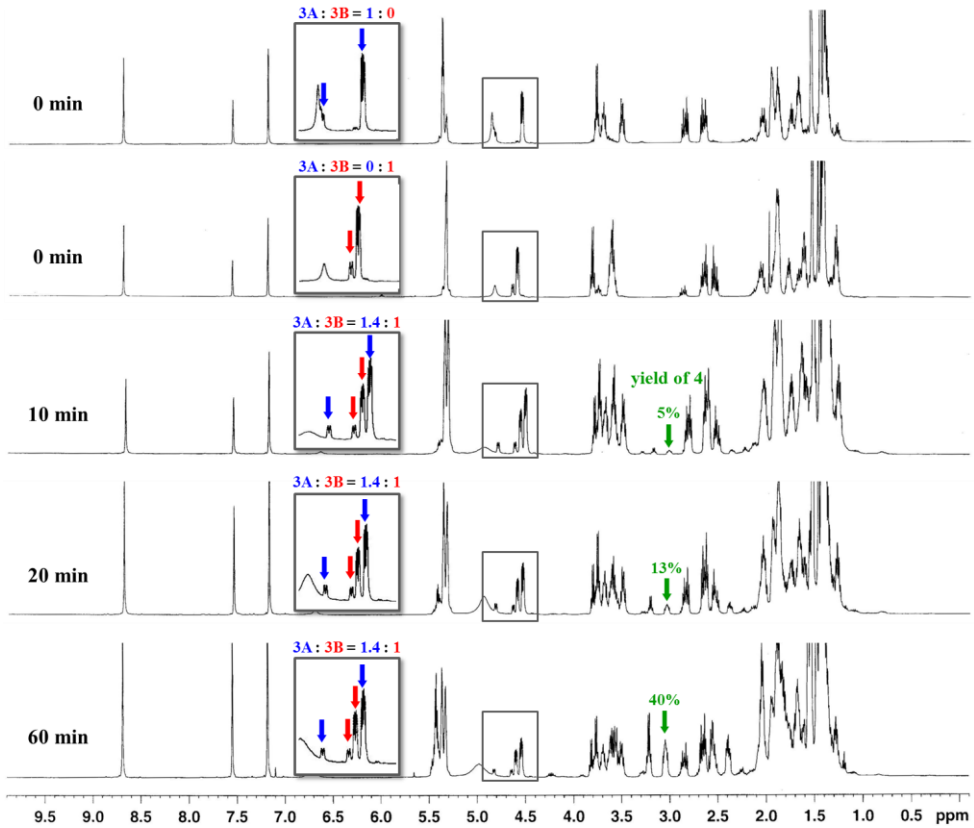

Figure S5. ^{1}H NMR spectra of the crude reaction mixture after the corresponding reaction times (500 MHz, C_5D_5N, see Scheme 5b in the main text).

IV-3. X-ray Crystallographic data for 4.

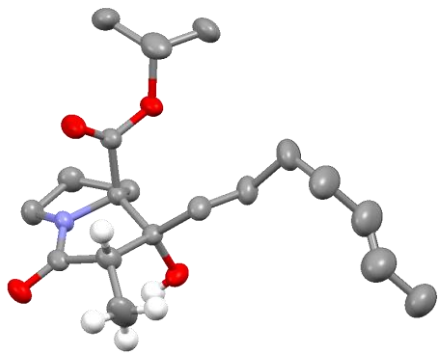

Figure S6. X-ray crystallographic structure of **4**.

CCDC 1062803 (**4**) contains the supplementary crystallographic data for this paper. These data can be obtained free of charge from the Cambridge Crystallographic Data Centre via www.ccdc.cam.ac.uk/data_request/cif.

Table S3. Crystal data and structure refinement for **4**.

Identification code	**4**	
Empirical formula	$C_{20}H_{33}NO_4$	
Formula weight	351.47	
Temperature	223(2) K	
Wavelength	1.54178 Å	
Crystal system	Orthorhombic	
Space group	P2(1)2(1)2(1)	
Unit cell dimensions	a = 6.1810(6) Å	α = 90°.
	b = 16.5751(15) Å	β = 90°.
	c = 19.3701(18) Å	γ = 90°.
Volume	1984.5(3) $Å^3$	
Z	4	

Density (calculated)	1.176 Mg/m^3
Absorption coefficient	0.647 mm^{-1}
F(000)	768
Crystal size	0.24 × 0.19 × 0.12 mm^3
Theta range for data collection	3.51 to 72.21°.
Index ranges	-7<=h<=7, -20<=k<=20, -23<=l<=23
Reflections collected	36253
Independent reflections	3759 [R(int) = 0.0388]
Completeness to theta = 72.21°	96.50%
Absorption correction	Semi-empirical from equivalents
Max. and min. transmission	0.9264 and 0.8602
Refinement method	Full-matrix least-squares on F^2
Data / restraints / parameters	3759 / 0 / 232
Goodness-of-fit on F^2	1.177
Final R indices [I>2sigma(I)]	R1 = 0.0487, wR2 = 0.1373
R indices (all data)	R1 = 0.0513, wR2 = 0.1426
Absolute structure parameter	0.1(3)
Largest diff. peak and hole	0.500 and -0.295 $e.Å^{-3}$

IV-3. Computational study

General procedure for molecular energy calculations

Computational energy minimization was performed on **4** and its diastereomers using the DMol3 program in Material Studio 8.0 (Accelrys software, Inc., San Diego, CA). A generalized gradient approximation (GGA) for the Perdew, Burke and Ernzerhof (PBE) exchange-correlation function was applied with double-numerical plus d-functions polarization (DNP), as implemented in DMol3.

Geometry optimization and energy minimization of the compounds

The compounds were calculated to compare their energy levels using the method described above. This computational energy minimization demonstrated that **4** is thermodynamically more stable than the other compounds. The energy differences are 1.88–6.48 kcal/mol.

Table S4. Molecular energies of **4** and its diastereomers.

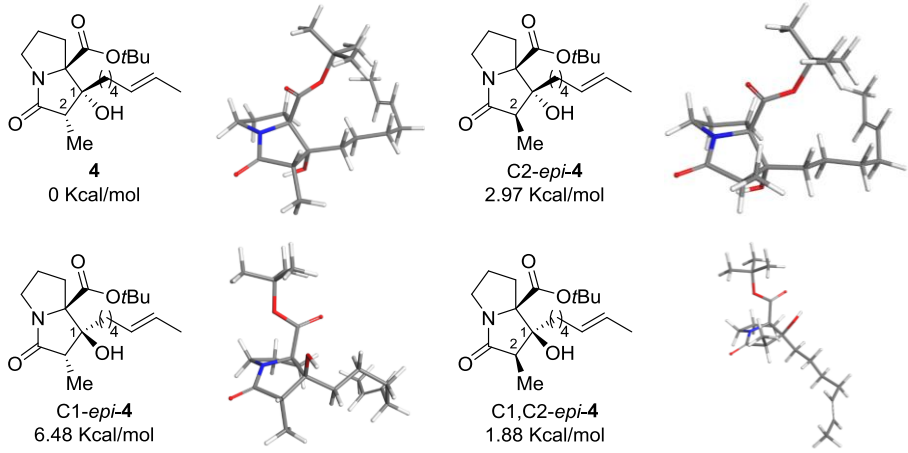

compound	Hartree (Ha)[a]	kcal/mol	Relative energy (kcal/mol)
4	–1136.672533	–713272.6886	0
C2-*epi*-**4**	–1136.667796	–713269.7164	2.972260981
C1-*epi*-**4**	–1136.662203	–713266.2068	6.481795503
C1,C2-*epi*-**4**	–1136.669529	–713270.8041	1.884536203

[a]1Ha = 627.509391 kcal/mol.

Calculation input

All calculations are performed under following conditions.

Task parameters

Calculate	optimize
Opt_energy_convergence	1.0000e–005
Opt_gradient_convergence	2.0000e–003 A
Opt_displacement_convergence	5.0000e–003 A
Opt_max_displacement	0.3000 A
Initial_hessian	improved
Symmetry	off

Electronic parameters

Spin_polarization	restricted
Charge	0
Basis	dnp
Pseudopotential	none
Functional	pbe
Aux_density	octupole
Integration_grid	fine
Occupation	fermi
Cutoff_Global	3.7000 angstrom
Scf_density_convergence	1.0000e–006
Scf_charge_mixing	2.0000e–001
Scf_diis	6 pulay

Print options

Print	eigval_last_it

Calculated properties

Frequency_analysis on

Calculation output

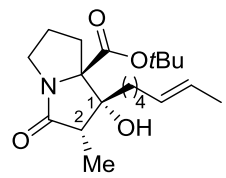

4

Atom	X	Y	Z	Atom	X	Y	Z
C	10.48937	-27.6646	5.523028	H	11.82351	-32.8406	5.731369
C	11.42256	-28.4138	4.523993	H	10.55091	-31.1873	7.587394
C	10.75227	-29.8608	4.543686	H	9.606884	-31.9081	6.253856
N	10.29471	-29.9446	5.927957	H	11.04137	-25.566	5.357421
C	10.2004	-28.7433	6.580044	H	12.01484	-26.4801	6.532626
C	11.70045	-31.0881	4.38809	H	10.34222	-26.0434	6.926888
C	11.75179	-31.7461	5.788336	H	12.68351	-28.764	5.992017
C	10.47159	-31.2686	6.495947	H	11.80373	-26.6574	3.389549
O	9.977788	-28.5798	7.7771	H	10.56687	-27.6964	2.686911
C	11.00706	-26.3621	6.113764	H	12.42509	-29.3477	2.04594
O	12.75204	-28.5049	5.055413	H	13.59701	-28.1989	2.695513
C	9.525911	-29.9531	3.600221	H	12.70432	-26.4606	1.04872
C	11.55303	-27.7085	3.174879	H	11.66081	-27.7009	0.357796
C	12.60693	-28.2774	2.221611	H	14.736	-27.8358	0.478273
C	12.62323	-27.5473	0.876676	H	13.79398	-27.3103	-0.92169
C	13.77836	-27.9831	-0.04714	H	12.80306	-29.6424	-1.13942
C	13.67748	-29.403	-0.52	H	15.42275	-30.1415	0.375631
C	14.54888	-30.3827	-0.24187	H	15.30665	-32.0809	-1.33664

C	14.44166	-31.7984	-0.71502	H	13.53016	-31.959	-1.30862
O	8.375895	-29.8268	3.982781	H	14.42433	-32.5028	0.132272
O	9.914059	-30.2264	2.334166	H	7.358319	-31.8278	0.722969
C	8.901939	-30.4222	1.247503	H	7.373354	-31.4052	2.455382
C	8.005121	-31.6114	1.585042	H	8.612608	-32.5058	1.783443
C	8.112632	-29.1315	1.036668	H	8.794088	-28.2924	0.840508
C	9.777506	-30.7314	0.036603	H	7.492537	-28.8968	1.908813
H	9.533634	-27.4804	5.003471	H	7.457735	-29.2473	0.161341
H	12.6922	-30.7642	4.051331	H	10.46076	-29.8985	-0.17188
H	11.30082	-31.7825	3.639095	H	9.145709	-30.8978	-0.84631
H	12.62819	-31.3848	6.345869	H	10.37818	-31.6347	0.210934

Total energy = –1136.672533 Ha

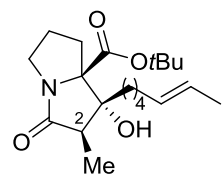

C2-*epi*-**4**

Atom	**X**	**Y**	**Z**	**Atom**	**X**	**Y**	**Z**
C	14.04103	-28.2543	5.369442	H	18.62697	-30.2153	3.510406
C	14.55166	-28.0651	3.914233	H	17.45993	-30.3284	6.038573
C	15.34074	-29.4346	3.639567	H	16.97209	-31.5154	4.796226
N	15.72554	-29.8256	4.988413	H	16.07801	-27.1098	4.71503
C	15.04646	-29.2184	6.010116	H	12.947	-26.7883	3.378129
C	16.69402	-29.354	2.869418	H	12.74807	-28.4407	2.793111
C	17.77777	-29.6593	3.930278	H	14.52314	-28.0095	1.038869
C	17.03948	-30.4412	5.031878	H	14.73193	-26.377	1.681898
O	15.25035	-29.3814	7.210907	H	12.28847	-25.9075	1.188452
H	14.11802	-27.2869	5.88754	H	12.1562	-27.4937	0.433312
O	15.51887	-26.9915	3.92683	H	14.08639	-25.2718	-0.47444

C	14.45265	-30.5678	3.050068	H	12.49088	-25.5705	-1.17203
C	13.48345	-27.6313	2.911012	H	13.25544	-27.8423	-1.99572
C	13.99811	-27.184	1.539107	H	15.88743	-26.29	-1.72874
C	12.86538	-26.674	0.644113	H	16.18216	-27.5834	-3.94056
C	13.35113	-26.0649	-0.68591	H	15.02855	-28.8074	-3.35629
C	13.93948	-27.0607	-1.64057	H	16.62208	-28.6168	-2.58034
C	15.20421	-27.0707	-2.08391	H	11.44022	-32.1123	0.78841
C	15.77999	-28.0707	-3.03763	H	11.56952	-30.4771	1.469551
O	14.0651	-31.5216	3.703507	H	12.00379	-31.898	2.465762
O	14.24133	-30.3829	1.729155	H	14.53034	-30.6711	-0.82425
C	13.4652	-31.3869	0.93134	H	13.02304	-29.795	-0.47793
C	12.0344	-31.4724	1.456715	H	12.95693	-31.4368	-1.16861
C	13.49724	-30.7839	-0.47015	H	15.23229	-32.613	0.648463
C	14.18501	-32.7345	0.95835	H	13.6992	-33.4142	0.244451
C	12.61139	-28.7852	5.548204	H	14.15567	-33.1885	1.954267
H	16.82004	-28.3637	2.418026	H	12.4648	-29.7458	5.036711
H	16.71154	-30.0975	2.06285	H	11.86821	-28.0664	5.175415
H	18.17043	-28.7225	4.353058	H	12.42467	-28.9459	6.618819

Total energy = -1136.667796 Ha

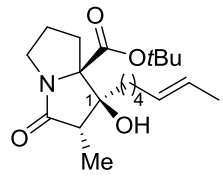

C1-*epi*-**4**

Atom	X	Y	Z	Atom	X	Y	Z
C	15.05361	-35.6805	0.078805	H	9.983213	-35.6524	0.797866
C	14.24143	-37.0117	0.006988	H	11.933	-33.4046	0.450032
C	12.73057	-36.539	-0.02863	H	10.9439	-34.2228	-0.78416
N	12.81179	-35.1142	-0.33568	H	15.38615	-37.8782	-1.33511

C	14.0694	-34.5739	-0.29934	H	14.44519	-37.552	2.090078
C	11.93112	-36.5117	1.303309	H	15.71674	-38.146	1.044759
C	10.97044	-35.3093	1.139262	H	14.05487	-39.7931	0.029369
C	11.61613	-34.3847	0.069065	H	12.87953	-39.3045	1.226813
O	14.33188	-33.3784	-0.41074	H	15.64943	-40.4879	1.8629
H	15.84631	-35.7266	-0.68377	H	14.13165	-41.3839	1.854509
O	14.45603	-37.5969	-1.29917	H	14.83219	-39.0805	3.778678
C	11.90514	-37.3522	-1.05787	H	14.85826	-40.8039	4.141358
C	14.61976	-38.0144	1.108219	H	12.31999	-40.9009	3.755721
C	13.95942	-39.3932	1.048753	H	12.85109	-37.9976	4.601084
C	14.56535	-40.3888	2.045536	H	10.70048	-38.6022	5.885702
C	14.34628	-40.0382	3.533245	H	10.32408	-39.8241	4.646242
C	12.89884	-39.9828	3.924269	H	10.28713	-38.0885	4.249869
C	12.27104	-38.915	4.436845	H	8.691225	-37.9314	-3.46357
C	10.82498	-38.8623	4.822108	H	8.841541	-36.8135	-2.08956
O	11.64009	-38.5298	-0.89055	H	9.473411	-38.4823	-1.95898
O	11.51939	-36.585	-2.09377	H	11.45912	-35.5786	-4.47194
C	10.68047	-37.1513	-3.19283	H	9.983895	-35.1273	-3.58046
C	9.342512	-37.6284	-2.63173	H	9.876487	-36.2313	-4.97608
C	10.48951	-35.9459	-4.11071	H	12.42299	-37.8949	-4.248
C	11.44598	-38.2628	-3.90634	H	10.87052	-38.5862	-4.7851
C	15.69592	-35.2924	1.418745	H	11.60187	-39.1241	-3.24876
H	12.62958	-36.3298	2.130932	H	14.95092	-35.2165	2.224067
H	11.41313	-37.4568	1.502925	H	16.46399	-36.0142	1.728322
H	10.81752	-34.7848	2.091274	H	16.16606	-34.3068	1.307728

Total energy = –1136.662203 Ha

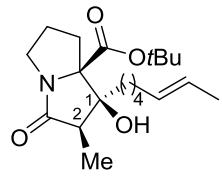

C1,C2-*epi*-**4**

Atom	X	Y	Z	Atom	X	Y	Z
C	9.474507	-38.1832	-0.51487	H	9.860445	-33.0972	0.456619
C	9.645243	-37.6055	0.920853	H	10.88191	-34.716	-1.88441
C	9.470247	-36.0126	0.719444	H	9.292989	-33.962	-1.64594
N	9.574493	-35.8524	-0.72381	H	8.587065	-37.5813	2.567575
C	9.625475	-36.9993	-1.46444	H	11.21564	-37.3484	2.394603
C	10.54693	-35.0203	1.226918	H	11.80708	-37.6554	0.757347
C	10.55417	-33.8986	0.163442	H	10.96271	-40.0626	0.989059
C	10.07771	-34.5534	-1.15304	H	10.48532	-39.6927	2.641974
O	9.810907	-37.0515	-2.67885	H	13.34442	-39.5343	1.511873
C	8.166803	-38.9356	-0.78126	H	12.89647	-39.0497	3.150323
O	8.620582	-38.1348	1.763929	H	13.85498	-41.2751	3.242667
C	8.107405	-35.5912	1.305887	H	12.13983	-41.3697	3.65546
C	11.03569	-37.9518	1.488514	H	11.64002	-42.3503	1.359816
C	11.20926	-39.4291	1.856031	H	14.63447	-42.9093	1.69542
C	12.63262	-39.7379	2.328918	H	12.40235	-44.1186	-0.11269
C	12.84104	-41.1846	2.822127	H	13.74864	-45.0581	0.58172
C	12.65139	-42.2337	1.765759	H	14.07486	-43.8455	-0.65823
C	13.6238	-43.0206	1.284416	H	4.083303	-36.03	1.645691
C	13.44739	-44.0603	0.222368	H	5.611208	-36.25	2.540387
O	7.955272	-35.4785	2.51884	H	5.317258	-37.1558	1.031086
O	7.182906	-35.3793	0.362697	H	6.194471	-32.9317	0.846336
C	5.763655	-35.055	0.721553	H	6.206832	-33.7706	2.425689
C	5.165131	-36.1954	1.541386	H	4.663418	-33.427	1.602721

C	5.713193	-33.7135	1.449435	H	5.584004	-34.1875	-1.26176
C	5.099895	-34.9588	-0.64932	H	4.040473	-34.6969	-0.52842
H	10.30964	-38.8619	-0.74122	H	5.166546	-35.917	-1.18116
H	11.52269	-35.5199	1.240991	H	8.085878	-39.8199	-0.13702
H	10.33384	-34.6557	2.238058	H	8.149549	-39.2511	-1.8331
H	11.5469	-33.4418	0.061512	H	7.293395	-38.2981	-0.59221

Total energy = -1136.669529 Ha

V. References

(1) Z.-F. Zhou, T. Kurtán, X.-H. Yang, A. Mándi, M.-Y. Geng, B.-P. Ye, O. Taglialatela-Scafati, Y.-W. Guo, *Org. Lett*. **2014**, *16*, 1390–1393.

(2) The stereochemistry of the C-8 of **2** was depicted as (*R*) in Ref 1.

(3) For reviews on asymmetric synthesis via MOC, see: a) T. Kawabata, K. Fuji, *Top. Stereochem.* **2003**, *23*, 175–205; b) H. Zhao, D. C. Hsu, P. R. Carlier, *Synthesis* **2005**, 1–16; c) D. Campolo, S. Gastaldi, C. Roussel, M. P. Bertrand, M. Nechab, *Chem. Soc. Rev.* **2013**, *42*, 8434–8466.

(4) For recent reports related to the MOC, see: a) S. A. Antolak, Z.-K. Yao, G. M. Richoux, C. Slebodnick, P. R. Carlier, *Org. Lett.* **2014**, *16*, 5204–5207; b) B. Viswambharan, D. Gori, R. Guillot, C. Kouklovsky, V. Alezra, *Org. Lett.* **2014**, *16*, 788–791; c) K. Tomohara, T. Yoshimura, R. Hyakutake, P. Yang, T. Kawabata, *J. Am. Chem. Soc.* **2013**, *135*, 13294–13297; d) F. Foschi, A. Tagliabue, V. Mihali, T. Pilati, I. Pecnikaj, M. Penso, *Org. Lett*. **2013**, *15*, 3686–3689; e) M. K. Ghorai, K. Ghosh, A. K. Yadav, Y. Nanaji, S. Halder, M. Sayyad, *J. Org. Chem.* **2013**, *78*, 2311–2326; f) S. Mondal, M. Nechab, N. Vanthuyne, M. P. Bertrand, *Chem. Commun.* **2012**, *48*, 2549–2551; g) P. MacLellan, J. Clayden, *Chem. Commun.* **2011**, *47*, 3395–3397.

(5) For recent reviews on DKR, see: a) H. Pellissier, *Tetrahedron* **2011**, *67*, 3769–

3802; b) J. Steinreiber, K. Faber, H. Griengl, *Chem. Eur. J.* **2008**, *14*, 8060–8072; c) B. Mártin-Matute, J.-E. Bäckvall, *Curr. Opin. Chem. Biol.* **2007**, *11*, 226–232.

(6) For selected reports on total syntheses using DKR, see: a) C. Liu, J.-H. Xie, Y.-L. Li, J.-Q. Chen, Q.-L. Zhou, *Angew. Chem., Int. Ed.* **2013**, *52*, 593–596; *Angew. Chem.* **2013**, *125*, 621–624; b) Y. Li, Z.-X. Chen, Q. Xiao, Q.-D. Ye, T.-W. Sun, F.-K. Meng, W.-W. Ren, L. You, L.-M. Xu, Y.-F. Wang, J.-H. Chen, Z. Yang, *Chem. Asian J.* **2012**, *7*, 2334–2340; c) S. G. Pardeshi, D. E. Ward, *J. Org. Chem.* **2008**, *73*, 1071–1076; d) M. P. Rainka, J. E. Milne, S. L. Buchwald, *Angew. Chem., Int. Ed.* **2005**, *44*, 6177–6180; *Angew. Chem.* **2005**, *117*, 6333–6336.

(7) To the best of our knowledge, only one total synthesis of a natural product using MOC has been reported. See: T. Yoshimura, T. Kinoshita, H. Yoshioka, T. Kawabata, *Org. Lett.* **2013**, *15*, 864–867.

(8) There is a report utilizing the concept of DKR to explain the high enantioselectivity observed in the MOC reaction. See: M. Branca, S. Pena, R. Guillot, D. Gori, V. Alezra, C. Kouklovsky, *J. Am. Chem. Soc.* **2009**, *131*, 10711–10718.

(9) For selected reports on the total synthesis using biomimetic aldol type cyclization, see: a) C. Qi, T. Qin, D. Suzuki, J. A. Porco, Jr., *J. Am. Chem. Soc.*

2014, *136*, 3374–3377; b) H. Nguyen, G. Ma, T. Gladysheva, T. Fremgen, D. Romo, *J. Org. Chem.* **2011**, *76*, 2–12; c) E. M. O'Brien, B. J. Morgan, M. C. Kozlowski, *Angew. Chem. Int. Ed*. **2008**, *47*, 6877–6880; *Angew. Chem*. **2008**, *120*, 6983–6986; d) G. Ma, H. Nguyen, D. Romo, *Org. Lett.* **2007**, *9*, 2143–2146.

(10) A. G. Brewster, J. Jayatissa, M. B. Mitchell, A. Schofield, R. J. Stoodley, *Tetrahedron Lett.* **2002**, *43*, 3919–3922.

(11) D. L. J. Clive, S. Hisaindee, *J. Org. Chem.* **2000**, *65*, 4923–4929.

(12) L. Weiler, *J. Am. Chem. Soc*. **1970**, *92*, 6702–6704.

(13) A. G. Brewster, C. S. Frampton, J. Jayatissa, M. B. Mitchell, R. J. Stoodley, S. Vohra, *Chem. Commun.* **1998**, 299–300.

(14) See the Experimental for further details. CCDC 1062803 (**4**) contains the supplementary crystallographic data for this paper. These data can be obtained free of charge from the Cambridge Crystallographic Data Centre at www.ccdc.cam.ac.uk/data_request/cif.

(15) R. P. McGeary, *Tetrahedron Lett.* **1998**, *39*, 3319–3322.

(16) T. Yoshimura, M. Takuwa, K. Tomohara, M. Uyama, K. Hayashi, P. Yang, R. Hyakutake, T. Sasamori, N. Tokitoh, T. Kawabata, *Chem. Eur. J.* **2012**, *18*, 15330–15336.

(17) R. W. Hoffmann, *Chem. Rev.* **1989**, *89*, 1841–1860.

(18) a) T. T. Ling, V. R. Macherla, R. R. Manam, K. A. McArthur, B. C. M. Potts, *Org. Lett.* **2007**, *9*, 2289–2292; b) M. D. Andrews, A. G. Brewster, M. G. Moloney, *Synlett* **1996**, 612–614.

(19) a) B. Delley, *J. Chem. Phys.* **1990**, *92*, 508–517. b) B. Delley, *J. Chem. Phys.* **2000**, *113*, 7756–7764.

(20) J. P. Perdew, K. Burke, M. Ernzerhof, *Phys. Rev. Lett.* **1996**, *77*, 3865–3868.

VI. Acknowledgements

Reproduced from *Angew. Chem. Int. Ed.* **2015**, *54*, 10875–10878 with permission from the John Wiley and Sons.

Part B.

Biphasic CuAAC Reaction Using a Phase Transfer Agent.

I. Introduction

While the traditional thermal azide-alkyne 1,3-dipolar cycloaddition reaction requires prolonged heating at elevated temperatures and results in mixtures of both 1,4- and 1,5-substituted triazole regioisomers,[1] the Cu(I) catalyzed version (CuAAC) provides only the 1,4-regioisomer under relatively mild conditions.[2] Since its discovery, CuAAC has emerged as the archetypical example of "click chemistry",[3] and has found widespread application in many areas such as drug discovery, material science, and bioconjugation.[4] This broad application was made possible in part by the advent of new reaction conditions that are more efficient and adaptable than the original CuAAC conditions.[5]

The original CuAAC conditions suggested by Sharpless use an *in situ* generated Cu(I) catalyst derived from the reaction of $CuSO_4 \cdot 5H_2O$ and sodium ascorbate, and a mixture of water and *t*-BuOH.[2a] The general issues in the development of new CuAAC conditions are generating the effective Cu(I) catalyst and maintaining high levels of the catalytically active Cu(I) during the reaction. As a consequence, a wide range of Cu(I) sources have been introduced, and various Cu ligands were developed to prevent the formation of unreactive polynuclear Cu(I) acetylides and increase the thermodynamic stability of Cu(I).[5b,6,7] Alternatively, a variety of immobilized copper catalysts have been devised for heterogeneous or soluble

polymer catalyst systems.[8]

Another important issue has been the different solubility preferences of the Cu(I) catalyst and substrates.[9] As one may notice, most of the copper salts have limited solubility in organic solvents[10] while the substrates of interest in organic synthesis generally have a high organic solubility. To solve this problem, the use of organic-soluble Cu(I) complexes has been suggested such as $(PPh_3)_3 \cdot CuBr$, $(EtO)_3P \cdot CuI$,[11a] bis-triazolylidene dicopper(I) complexes[11b] and $C_3H_7COOCu(PPh_3)_2$.[11c] Although these ligand chelated Cu(I) reagents exhibited better organic solubility and high reactivity, they possess some drawbacks. For example, phosphine based Cu(I) complexes have the intrinsic risk of the Staudinger reduction of azide.[5c] In some cases, these catalysts require harsh reaction conditions, such as elevated temperatures. In addition, the lengthy and complex procedures for catalysts preparation reduce the wide application of such catalysts.

Another way of solving the problem derived from the different solubility preferences is the careful choice of solvent systems.[5a] Most commonly, the reaction is performed in a mixture of water and water-miscible organic solvent, which facilitates solvation of hydrophobic substrates while still retaining the advantages of water. Organic solvents of intermediate polarity, such as THF, acetone, pyridine, CH_3CN, and DMSO, are often employed when partially organic soluble CuI or organic-soluble Cu complexes are used as a source of Cu(I). The two-phase solvent

system composed of water and organic solvent was also reported to be effective to produce the triazole products with or without a ligand.[12] Although many solvent systems are available, finding the optimum solvent is still a case-to-case basis because there is no obvious correlation between which solvent is used and performance of the reaction.

Given our interest in developing reliable, general reaction conditions for CuAAC in organic synthesis, we sought to explore the possibility of applying the concept of phase transfer catalysis (PTC) as a solution for the different solubility preferences. PTC is an efficient and widely used method for promoting reactions between reaction partners that are present in two immiscible phases.[13] However, the concept of PTC has rarely been applied to CuAAC reactions,[14] and its potential use has not been sufficiently explored. One of the few investigations employing this concept is the utilization of α-cyclodextrin in water medium.[14a] Although this reaction system quickly provides the product by making a host-guest complex within the hydrophobic cyclodextrin cavity, there are some substrate limitations due to the capacity allowances of cyclodextrins.[15] Polyethylene glycol 400 (PEG-400) has been employed as a phase transferring agent in a one-pot multi-component CuAAC reaction in water medium.[14b,c] In this case, a large excess of PEG-400 was used as like a co-solvent.

Unlike the previous phase transfer CuAAC reactions in which substrates are

delivered to the water medium, we employed an aqueous/organic two-phase solvent system and planned to transfer copper from the aqueous phase to the organic phase where the reaction occurs. We envisioned that the aqueous biphasic reaction system would be advantageous for a broad range of substrates and would be highly generalizable if the biphasic CuAAC reactions could be facilitated by a phase transfer agent. Herein, we report our studies on this subject and describe new CuAAC reaction conditions which are highly efficient, especially when a lipophilic substrate is involved.

II. Results and Discussion

Our working hypothesis for the phase transfer agent assisted CuAAC reaction is shown in Figure 1. The *in situ* generated Cu(I) catalyst produced by the reaction of Cu(II) and sodium ascorbate in aqueous phase would be ferried into the organic phase by a phase transfer agent as a complex form.[16] Similarly to other organic-soluble Cu(I) complexes, the relocated Cu(I) species would promote the CuAAC reactions in the organic phase. During the reaction process, Cu(I) can be inadvertently oxidized to Cu(II). In aqueous phase in which sodium ascorbate is dissolved, these oxidized Cu(II) species can revert back to the catalytically active Cu(I) species,[17] which are able to reenter the cycle with the help of the phase transfer agent.

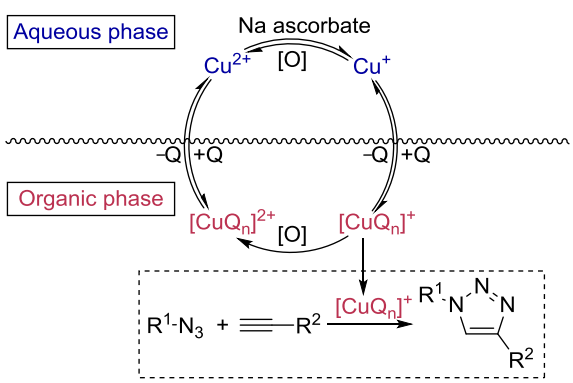

Figure 1. Schematic representation of phase transfer agent assisted CuAAC reaction.

In this phase transfer system, the phase transfer agents should be able to

encapsulate Cu(I) in the aqueous phase or at the interface to deliver it to the organic phase. In addition, it is advantageous if they are able to be coordinated with Cu(I) during the reaction to enhance the rate of reaction and to protect the Cu(I) from oxidation.

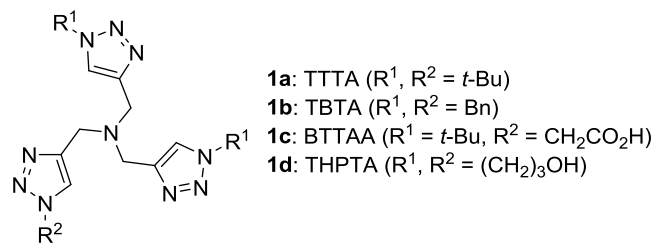

Figure 2. Structures of tris(triazolylmethyl)amine ligands (**1a**–**1d**).

To identify phase transfer agents that fulfill the above conditions, we surveyed several types of ligands which have been devised to promote the Cu(I) catalyzed triazole formation. This effort resulted in the selection of tris(triazolylmethyl)amine ligands that are easily available and consist of several variants with different physicochemical properties.[7a,18] Four typical tris(triazolylmethyl)amine ligands (**1a**–**1d**, Figure 2) with different functional groups and log P values were chosen for the first step of the development. Benzyl azide (**2a**) and phenyl acetylene (**3a**) were chosen as a CuAAC reaction partners, and water soluble $CuSO_4 \cdot 5H_2O$ (0.5 mol%) and sodium ascorbate (1.5 mol%) were used to generate the Cu(I) *in situ*. A mixture of CH_2Cl_2/H_2O (1:1) was employed as a biphasic solvent system (Table 1).

Table 1. Effects of tris(triazolylmethyl)amine ligands on the CuAAC reaction.[a]

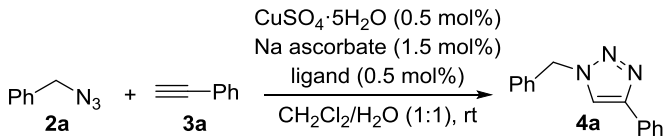

Entry	Ligand	Time (min)	Yield [b] (%)
1	none	240	20
2	**1a**	20	100
3	**1b**	40	100
4	**1c**	240	47
5	**1d**	240	3

[a] Reaction conditions: **2a** (0.50 mmol), **3a** (0.55 mmol), $CuSO_4 \cdot 5H_2O$ (0.5 mol%), Na ascorbate (1.5 mol%), and ligand (0.5 mol%) in CH_2Cl_2/H_2O (1:1) (1 mL) at rt. [b] Determined by ^1H NMR analysis using 1,1,2,2-tetrachloroethane as an internal standard.

When the reaction was performed without a ligand for 240 min (entry 1), most of the starting materials remained intact and the desired product was obtained in poor yield (20%). However, in the presence of TTTA (**1a**), the reaction was completed within 20 min with the formation of product in nearly quantitative yield (entry 2). TBTA (**1b**) increased the reaction rate such that the reaction was completed within 40 min (entry 3).[19] BTTAA (**1c**) was far less effective in accelerating the reaction (entry 4). The most hydrophilic ligand THPTA (**1d**) significantly retarded the reaction, resulting in only 3% product yield even after 240 min (entry 5).

Table 2. Effects of tris(triazolylmethyl)amine ligands on the Cu content in the CH_2Cl_2

layer.[a]

Entry	Ligand	Clog P[b]	Cu content (ppb)[c]
1	none	-	78
2	**1a**	1.1	70330
3	**1b**	2.7	39475
4	**1c**	–0.37	125
5	**1d**	–3.7	128

[a] Conditions: $CuSO_4 \cdot 5H_2O$ (0.0025 mmol), Na ascorbate (0.0075 mmol), and ligand (0.0025 mmol) in CH_2Cl_2/H_2O (1:1) (1 mL) at rt for 30 min. [b] Clog P values were calculated using ChemBioDraw Ultra 13.0. [c] Determined by ICP-MS analysis.

To verify whether the observed reaction rates were related to the phase transfer activity of tris(triazolylmethyl)amine ligands, we used ICP-MS analysis to measure the copper content in the organic layer of the substrate-blank biphasic reaction system. As shown in Table 2, the copper content in the organic layer was very low (78 ppb) without any ligand (entry 1). In the presence of TTTA (**1a**, Clog P = 1.1), the copper content was increased approximately 900 times (entry 2). TBTA (**1b**, Clog P = 2.7) also resulted in an increase of copper content by approximately 500 times (entry 3). The more hydrophilic ligands **1c** and **1d** did not cause a significant increase in the copper content (entries 4 and 5). This result indicated that the tris(triazolylmethyl)amine ligands with appropriate hydrophilic-lipophilic balances are able to extract copper from the aqueous phase to the organic phase, thereby accelerating the rate of the CuAAC reaction.

To understand the mechanism of copper transfer, we measured the partition ratio

of TTTA (**1a**) between CH_2Cl_2 and H_2O by ^1H NMR analysis. To our surprise, although the calculated log P value for **1a** is 1.1, only a negligible amount of **1a** was resided in the aqueous layer while the overwhelming majority of **1a** was detected in the CH_2Cl_2 layer. This result suggested that the complexation between **1a** and Cu(I) might occur mostly at or near the interface between CH_2Cl_2 and H_2O, and then this complex would move to the organic phase to promote the CuAAC reactions.[13c,20]

Table 3. Effects of solvent systems on the CuAAC reaction.[a]

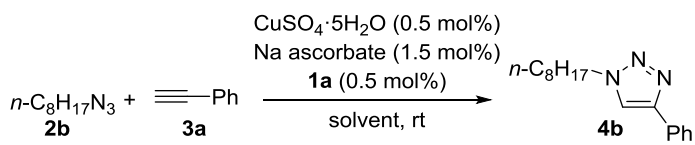

Entry	Solvent	Time (min)	Yield (%)[b]
1	$CHCl_3/H_2O$ (1:1)	25	100
2	toluene/H_2O (1:1)	50	97
3	CH_2Cl_2/H_2O (1:1)	15	100
4	*t*-BuOH/H_2O (2:1)	360	99
5	H_2O	360	78
6	CH_2Cl_2	360	<1

[a] Reaction conditions: **2b** (0.50 mmol), **3a** (0.55 mmol), $CuSO_4 \cdot 5H_2O$ (0.5 mol%), Na ascorbate (1.5 mol%), and **1a** (0.5 mol%) in solvent (1 mL) at rt. [b] Determined by ^1H NMR analysis using 1,1,2,2-tetrachloroethane as an internal standard.

Toluene and $CHCl_3$ can also be used as the organic phase of the biphasic system (Table 3). The CuAAC reaction between the highly lipophilic alkyl azide **2b** and

phenyl acetylene (**3a**) in biphasic $CHCl_3/H_2O$ medium was completed in 25 min in the presence of **1a** (entry 1), and the reaction in toluene/H_2O was completed in 50 min (entry 2). Although the reaction in these solvent systems was slower than reactions performed in the CH_2Cl_2/H_2O solvent system (entry 3), the necessary reaction time was still short and the yield was very high. The corresponding reaction in the monophasic *t*-BuOH/H_2O solvent system was much less efficient and reached full conversion in 360 min (entry 4). When water was used as the only solvent, full conversion was not reached even after 360 min primarily because of the limited solubility of substrates (entry 5). The reaction in only CH_2Cl_2 solvent provided a trace amount of the product in 360 min because of the limited solubility of $CuSO_4 \cdot 5H_2O$ and sodium ascorbate (entry 6).

The scope of applicability of the phase transfer agent assisted CuAAC reaction was explored with 0.5 mol% of TTTA (**1a**) in a biphasic CH_2Cl_2/H_2O medium containing $CuSO_4 \cdot 5H_2O$ and ascorbate (0.5 and 1.5 mol%, respectively; conditions A). First, we applied various types of azides to the reaction system. As shown in Table 4, the azide structure has no significant effect on the reaction rates. All of the reactions proceeded efficiently and were completed in less than 15 min, with excellent isolated yields (entries 1–5). However, the effects of alkyne structures on the reaction rates were significant. Alkynes with an ester group or a phenyl group proceeded efficiently, resulting in the corresponding triazole products within 20

Table 4. CuAAC reaction with various alkynes and azides using phase transfer agent.[a]

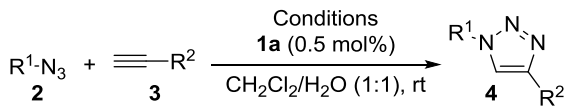

Entry	R^1	R^2	Conditions[b]	Time (min)	**4**	Yield (%)[c]
1	cyclohexyl (**2c**)	Ph (**3a**)	A	15	**4c**	97
2	$C_2H_5OCOCH_2$ (**2d**)	Ph (**3a**)	A	5	**4d**	98
3	*p*-$NO_2C_6H_4CH_2$ (**2e**)	Ph (**3a**)	A	10	**4e**	96
4	*p*-$BrC_6H_4CH_2$ (**2f**)	Ph (**3a**)	A	15	**4f**	96
5	*p*-$CH_3OC_6H_4CH_2$ (**2g**)	Ph (**3a**)	A	10	**4g**	99
6	$PhCH_2$ (**2a**)	$CO_2C_2H_5$ (**3b**)	A	15	**4h**	98
7	$PhCH_2$ (**2a**)	*p*-$CH_3OC_6H_4$ (**3c**)	A	20	**4i**	100
8	$PhCH_2$ (**2a**)	CH_2NHBoc (**3d**)	A	30	**4j**	95
9	$PhCH_2$ (**2a**)	CH_2OH (**3e**)	A	50	**4k**	99
10	$PhCH_2$ (**2a**)	cyclohexane-1-ol (**3f**)	A	40	**4l**	95
11	$PhCH_2$ (**2a**)	*t*-Bu (**3g**)	A	50	**4m**	98
12	$PhCH_2$ (**2a**)	*n*-Hex (**3h**)	B	40	**4n**	98
13	$PhCH_2$ (**2a**)	cyclohexyl (**3i**)	B	50	**4o**	100
14	$PhCH_2$ (**2a**)	CO_2H (**3j**)	B	20	**4p**	91
15	$PhCH_2$ (**2a**)	CH_2NH_2 (**3k**)	B	180	**4q**	97
16	$NH_2C_2H_4$ (**2h**)	Ph (**3a**)	B	20	**4r**	98
17	$NH_2C_6H_{12}$ (**2i**)	Ph (**3a**)	B	120	**4s**	93
18	$CH_3NHC_6H_{12}$ (**2j**)	Ph (**3a**)	B	50	**4t**	96

[a] Reaction conditions: **2** (0.50 mmol), **3** (0.55 mmol), **1a** (0.5 mol%), with conditions A or B in CH_2Cl_2/H_2O (1:1) (1 mL) at rt. [b] A: $CuSO_4 \cdot 5H_2O$ (0.5 mol%), Na ascorbate (1.5 mol%). B: $CuSO_4 \cdot 5H_2O$ (1.5 mol%), Na ascorbate (4.5 mol%). [c] Isolated yield.

min in excellent yields (entries 6 and 7). The *N*-Boc group at the propargylic position of the alkyne substrate did not affect the reaction rates (entry 8). Propargyl alcohols were also suitable for this reaction system, yielding product in less than 50 min (entries 9 and 10). The reaction of the *t*-butyl substituted alkyne was completed in 50 min (entry 11). However, the reaction of the *n*-hexyl or cyclohexyl substituted alkynes was not completed within the same time. These substrates required an increase in copper and sodium ascorbate loading (1.5 and 4.5 mol%, respectively; conditions B) for completion within 50 min (entries 12 and 13). The cycloadditions of propynoic acid also proceeded efficiently under these higher copper loading conditions (entry 14).

Noteworthy was the result obtained in the biphasic CuAAC reaction of propargyl amine (entry 15) because the CuAAC reaction generally fails or gives low yield in the presence of free amino groups as a consequence of the coordination between the Cu(I) ion and the amino group.[7a,21] Under higher reagent loading conditions, the triazole product **4q** was successfully obtained in 97% yield. In addition, the reactions between free amine containing azides **2h**–**j** and the phenyl acetylene (**3a**) proceeded efficiently in this reaction system (entries 16–18).

We demonstrated the utility and efficiency of the phase transfer agent assisted biphasic CuAAC reaction by applying it to the synthesis of an immunostimulant α-GalCer analog **5**.[22] Because this synthesis required a highly lipophilic alkyne **6**, the

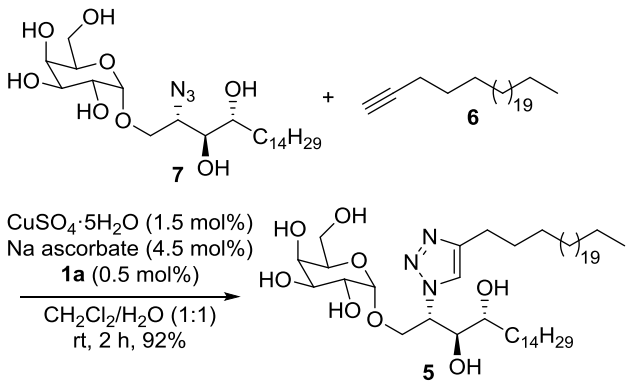

Scheme 1. Efficient synthesis of α-GalCer analog **5** using the phase transfer agent assisted CuAAC reaction.

CuAAC reaction of azide **7** with **6** under the conventional reaction system was not met with great success. For example, when the reaction was performed in monophasic *t*-BuOH/H_2O solvent system, the triazole product **5** was obtained in only 20% after 24 h even in the presence of TTTA (**1a**). However, under the presented biphasic system, we successfully obtained **5** in 92% yield in a short reaction time (2 h).

III. Conclusion

In summary, we have developed a phase transfer agent assisted biphasic CuAAC reaction system. A biphasic reaction media consisting of water and an organic solvent ensures a complete dissolution of reagents and substrates, thus broadening the scope of possible substrates. Among the tested tris(triazolylmethyl)amine Cu ligands, TTTA (**1a**) and TBTA (**1b**) afforded the expected phase transfer activity. The developed biphasic reaction system is highly efficient, especially when a lipophilic substrate is involved. The present system is widely applicable to substrates with various functionalities including a free amino group, making the CuAAC reaction more reliable.

IV. Experimental

IV-1. General.

All chemicals were reagent grade and used as purchased. The reactions were monitored with TLC analysis using silica gel 60 F-254 thin layer plates. Compounds on the TLC plates were sprayed with either potassium permanganate or phosphomolybdic acid and visualized under UV light. Flash column chromatography was conducted on silica gel 60 (230–400 mesh). Optical rotations were measured using a sodium lamp (D line 589.3 nm). Melting points were measured using an electrothermal capillary melting point apparatus and are uncorrected. ^{1}H NMR (400 MHz) and ^{13}C NMR (100 MHz) spectra were recorded in δ units relative to the deuterated solvent. IR spectra were measured on a Fourier Transform Infrared spectrometer. High-resolution mass spectra (HRMS) were recorded using FAB. Inductively coupled plasma mass spectrometry (ICP-MS) analysis was performed for copper quantitation.

IV-2. Experimental procedure and spectroscopic data analysis

Preparation of the Starting Materials.

Azides **2a**–**2g** were synthesized according to procedures provided by Alvarez *et al*.[23] Azides **2h**,[24] **2i**–**2j**,[25] and alkyne **3d**[26] was also prepared according to the procedures in the literature. The NMR data were in agreement with those published for benzyl azide (**2a**),[23] 1-azidooctane (**2b**),[23] azidocyclohexane (**2c**),[23] ethyl 2-azidoacetate (**2d**),[27] 1-(azidomethyl)-4-nitrobenzene (**2e**),[28] 1-(azidomethyl)-4-bromobenzene (**2f**),[29] 1-(azidomethyl)-4-methoxybenzene (**2g**),[28] 2-azidoethan-1-amine (**2h**),[24] 6-azidohexan-1-amine (**2i**),[25] 6-azido-*N*-methylhexan-1-amine (**2j**)[25] and *tert*-butyl prop-2-ynylcarbamate (**3d**).[26]

Measurement of partition ratio of TTTA (1a) between CH_2Cl_2 and H_2O.

In a vial fitted with a screw cap, TTTA (**1a**, 85.6 mg, 0.2 mmol) was dissolved in CH_2Cl_2/H_2O (1:1, 2 mL) and stirred at rt for 1 or 12 hr. After phase separation, 0.5 mL of each layer was carefully sampled and the solvents were evaporated. The **1a** in each residue was measured by ^1H NMR in $CDCl_3$ using 1,1,2,2-tetrachloroethane as an internal standard. In the sample taken from the H_2O layer, no peak of **1a** was identified.

General procedure for CuAAC reactions.

In a vial fitted with a screw cap, freshly prepared stock solutions of $CuSO_4 \cdot 5H_2O$

(50 L, 50 mM stock solution in DDW, 0.5 mol%), TTTA (**1a**, 50 L, 50 mM stock solution in CH_2Cl_2, 0.5 mol%), and sodium ascorbate (50 L, 150 mM stock solution in DDW, 1.5 mol%) were added to a mixture of azide **2** (0.5 mmol, 1.0 equiv) and acetylene **3** (0.55 mmol, 1.1 equiv) in DDW (0.40 mL) and CH_2Cl_2 (0.45 mL). The reaction was allowed to proceed at rt and monitored by TLC. After total consumption of the starting azide, the reaction mixture was poured into saturated NH_4Cl aqueous solution (10 mL). The aqueous layer was extracted with CH_2Cl_2 (2 × 10 mL).

For the carboxylic acid containing compound **4p**, the mixture was acidified to pH 1 with 1N HCl aqueous solution and extracted with CH_2Cl_2 (5 × 10 mL).

For the free amine containing compounds **4q**–**4r**, the reaction mixture was poured into 25 % NH_4OH aqueous solution (10 mL) and extracted with CH_2Cl_2 (3 × 10 mL).

The combined organic layers were dried over $MgSO_4$, and concentrated *in vacuo*. When required, the product was purified by flash column chromatography on silica gel.

1-Benzyl-4-phenyl-1*H*-1,2,3-triazole (4a): white solid (117.3 mg, 100%); m.p. 130–132 ℃; ^{1}H NMR (400 MHz, $CDCl_3$) δ 7.79–7.77 (m, 2H), 7.66 (s, 1H), 7.28–7.26 (m, 8H), 5.51 (s, 2H); ^{13}C NMR (100 MHz, $CDCl_3$) δ 148.0, 134.6, 130.4, 129.0 (2C), 128.7 (2C), 128.6, 128.0, 127.9 (2C), 125.5 (2C), 119.5, 54.0; IR (neat,

cm^{-1}) υ_{max} 3141, 3027, 2976, 1468, 1449, 1361, 1222, 1140, 1073, 1044, 766, 727, 693; HRMS (FAB): calcd. for $C_{15}H_{14}N_3$ $[M+H]^+$ 236.1188, found 236.1189.

1-Octyl-4-phenyl-1*H*-1,2,3-triazole (4b): white solid (128.6 mg, 100%); m.p. 78–80 °C; ^{1}H NMR (400 MHz, $CDCl_3$) δ 7.80–7.78 (m, 2H), 7.72 (s, 1H), 7.38–7.34 (m, 2H), 7.29–7.25 (m, 1H), 4.31 (t, J = 7.2 Hz, 2H), 1.91–1.84 (m, 2H), 1.28–1.21 (m, 10H), 0.83 (t, J = 6.7 Hz, 3H); ^{13}C NMR (100 MHz, $CDCl_3$) δ 147.5, 130.6, 128.6 (2C), 127.9, 125.5 (2C), 119.4, 50.2, 31.5, 30.2, 28.9, 28.8, 26.3, 22.4, 13.9; IR (neat, cm^{-1}) υ_{max} 3120, 3092, 3064, 2954, 2917, 2849, 1484, 1463, 1356, 1215, 1190, 1078, 1051, 976, 839, 760, 693; HRMS (FAB): calcd. for $C_{16}H_{24}N_3$ $[M+H]^+$ 258.1970, found 258.1976.

1-Cyclohexyl-4-phenyl-1*H*-1,2,3-triazole (4c): white solid (110.2 mg, 97%); m.p. 107–108 °C; ^{1}H NMR (400 MHz, $CDCl_3$) δ 7.80–7.78 (m, 2H), 7.75 (s, 1H), 7.37–7.33 (m, 2H), 7.27–7.23 (m, 1H), 4.39 (tt, J = 11.8, 3.7 Hz, 1H), 2.17–2.14 (m, 2H), 1.87–1.67 (m, 5H), 1.44–1.19 (m, 3H); ^{13}C NMR (100 MHz, $CDCl_3$) δ 147.0, 130.7, 128.6 (2C), 127.7, 125.4 (2C), 117.3, 59.9, 33.3 (2C), 24.94 (2C), 24.89; IR (neat, cm^{-1}) υ_{max} 3126, 2936, 2854, 1480, 1452, 1374, 1223, 1054, 1000, 894, 826, 761, 691; HRMS (FAB): calcd. for $C_{14}H_{18}N_3$ $[M+H]^+$ 228.1501, found 228.1503.

Ethyl 2-(4-phenyl-1*H*-1,2,3-triazol-1-yl)acetate (4d): white solid (113.3 mg, 98%); m.p. 93–94 °C; ^{1}H NMR (400 MHz, $CDCl_3$) δ 7.89 (s, 1H), 7.80–7.78 (m,

2H), 7.38–7.35 (m, 2H), 7.30–7.26 (m, 1H), 5.13 (s, 2H), 4.19 (q, *J* = 7.2 Hz, 2H), 1.23 (t, *J* = 7.2 Hz, 3H); ^{13}C NMR (100 MHz, $CDCl_3$) δ 166.1, 147.7, 130.2, 128.6 (2C), 127.9, 125.5 (2C), 121.1, 62.1, 50.6, 13.7; IR (neat, cm^{-1}) υ_{max} 3135, 2948, 1752, 1465, 1442, 1346, 1214, 1197, 1074, 1014, 763, 692; HRMS (FAB): calcd. for $C_{12}H_{14}N_3O_2$ $[M+H]^+$ 232.1086, found 232.1087.

1-(4-Nitrobenzyl)-4-phenyl-1*H*-1,2,3-triazole (4e): white solid (134.4 mg, 96%); m.p. 157–159 ℃; ^{1}H NMR (400 MHz, $CDCl_3$) δ 8.20–8.18 (m, 2H), 7.79–7.74 (m, 3H), 7.42–7.29 (m, 5H), 5.66 (s, 2H); ^{13}C NMR (100 MHz, $CDCl_3$) δ 148.6, 148.0, 141.7, 130.1, 128.9 (2C), 128.5 (2C), 128.4, 125.7 (2C), 124.3 (2C), 119.7, 53.1; IR (neat, cm^{-1}) υ_{max} 3127, 3083, 1606, 1517, 1347, 1222, 1077, 1045, 861, 803, 761, 729, 690; HRMS (FAB): calcd. for $C_{15}H_{13}N_4O_2$ $[M+H]^+$ 281.1039, found 281.1034.

1-(4-Bromobenzyl)-4-phenyl-1*H*-1,2,3-triazole (4f): white solid (150.4 mg, 96%); m.p. 150–152 ℃; ^{1}H NMR (400 MHz, $CDCl_3$) δ 7.78–7.76 (m, 2H), 7.66 (s, 1H), 7.48–7.45 (m, 2H), 7.39–7.37 (m, 2H), 7.31–7.27 (m, 1H), 7.14–7.12 (m, 2H), 5.47 (s, 2H); ^{13}C NMR (100 MHz, $CDCl_3$) δ 148.3, 133.7, 132.2 (2C), 130.3, 129.6 (2C), 128.8 (2C), 128.2, 125.6 (2C), 122.8, 119.5, 53.4; IR (neat, cm^{-1}) υ_{max} 3107, 3083, 1483, 1461, 1431, 1350, 1219, 1073, 1047, 1010, 799, 961, 687; HRMS (FAB): calcd. for $C_{15}H_{13}BrN_3$ $[M+H]^+$ 314.0293, found 314.0292.

1-(4-Methoxybenzyl)-4-phenyl-1*H*-1,2,3-triazole (4g): white solid (131.1 mg,

99%); m.p. 139–140 ℃; ^{1}H NMR (400 MHz, $CDCl_3$) δ 7.77–7.75 (m, 2H), 7.62 (s, 1H), 7.35 (t, J = 7.7 Hz, 2H), 7.28–7.21 (m, 3H), 6.86 (d, J = 8.6 Hz, 2H), 5.44 (s, 2H), 3.76 (s, 3H); ^{13}C NMR (100 MHz, $CDCl_3$) δ 159.8, 147.9, 130.5, 129.5 (2C), 128.6 (2C), 128.0, 126.6, 125.5 (2C), 119.3, 114.4 (2C), 55.2, 53.6; IR (neat, cm^{-1}) υ_{max} 3107, 3083, 1483, 1461, 1219, 1073, 1010, 816, 799, 761, 687; HRMS (FAB): calcd. for $C_{16}H_{16}N_3O$ $[M+H]^+$ 266.1293, found 266.1291.

Ethyl 1-benzyl-1*H*-1,2,3-triazole-4-carboxylate (4h): white solid (113.3 mg, 98%); m.p. 84–86 ℃; ^{1}H NMR (400 MHz, $CDCl_3$) δ 7.98 (s, 1H), 7.25–7.17 (m, 5H), 5.48 (s, 2H), 4.25 (q, J = 7.2 Hz, 2H), 1.24 (t, J = 7.2 Hz, 3H); ^{13}C NMR (100 MHz, $CDCl_3$) δ 160.3, 140.1, 133.7, 128.9 (2C), 128.6, 127.9 (2C), 127.2, 60.8, 54.0, 13.9; IR (neat, cm^{-1}) υ_{max} 3126, 2983, 1715, 1539, 1368, 1226, 1044, 1022, 776, 716, 693; HRMS (FAB): calcd. for $C_{12}H_{14}N_3O_2$ $[M+H]^+$ 232.1086, found 232.1088.

1-Benzyl-4-(4-methoxyphenyl)-1*H*-1,2,3-triazole (4i): white solid (132.3 mg, 100%); m.p. 142–144 ℃; ^{1}H NMR (400 MHz, $CDCl_3$) δ 7.71–7.69 (m, 2H), 7.56 (s, 1H), 7.37–7.27 (m, 5H), 6.92–6.89 (m, 2H), 5.52 (s, 2H), 3.80 (s, 3H); ^{13}C NMR (100 MHz, $CDCl_3$) δ 159.5, 147.9, 134.7, 129.0 (2C), 128.6, 127.9 (2C), 126.9 (2C), 123.2, 118.7, 114.1 (2C), 55.2, 54.0; IR (neat, cm^{-1}) υ_{max} 3138, 3040, 2949, 2838, 2098, 1614, 1557, 1495, 1454, 1436, 1349, 1249, 1170, 1070, 1027, 973, 832, 794, 717; HRMS (FAB): calcd. for $C_{16}H_{16}N_3O$ $[M+H]^+$ 266.1293, found

266.1286.

***tert*-Butyl ((1-benzyl-1*H*-1,2,3-triazol-4-yl)methyl)carbamate (4j)**: light yellow solid (137.0 mg, 95%); m.p. 91–93 ℃; ^{1}H NMR (400 MHz, $CDCl_3$) δ 7.40 (s, 1H), 7.37–7.23 (m, 5H), 5.48 (s, 2H), 5.04 (brs, 1H, NH), 4.34 (d, J = 5.9 Hz, 2H), 1.39 (s, 9H); ^{13}C NMR (100 MHz, $CDCl_3$) δ 155.7, 145.7, 134.5, 128.9 (2C), 128.5, 127.8 (2C), 121.7, 79.3, 53.9, 35.9, 28.2 (3C); IR (neat, cm^{-1}) υ_{max} 3405, 3111, 3063, 2978, 2954, 1688, 1515, 1454, 1268, 1169, 1123, 1054, 796, 717, 695; HRMS (FAB): calcd. for $C_{15}H_{21}N_4O_2$ $[M+H]^+$ 289.1665, found 289.1666.

(1-Benzyl-1*H*-1,2,3-triazol-4-yl)methanol (4k): white solid (93.4 mg, 99%); m.p. 77–79 ℃; ^{1}H NMR (400 MHz, $CDCl_3$) δ 7.43 (s ,1H), 7.31–7.28 (m, 3H), 7.21–7.19 (m, 2H), 5.42 (s, 2H), 4.67 (s, 2H), 3.71 (brs, 1H, OH); ^{13}C NMR (100 MHz, $CDCl_3$) δ 148.2, 134.4, 129.0 (2C), 128.6, 128.0 (2C), 121.8, 55.9, 54.0; IR (neat, cm^{-1}) υ_{max} 3252, 3140, 2934, 1457, 1222, 1129, 1036, 1012, 837, 788, 717, 691; HRMS (FAB): calcd. for $C_{10}H_{12}N_3O$ $[M+H]^+$ 190.0980, found 190.0980.

1-(1-Benzyl-1*H*-1,2,3-triazol-4-yl)cyclohexan-1-ol (4l): white solid (122.1 mg, 95%); m.p. 125–126 ℃; ^{1}H NMR (400 MHz, $CDCl_3$) δ 7.35 (s, 1H), 7.31–7.25 (3H), 7.19–7.17 (m, 2H), 5.40 (s, 2H), 3.05 (brs, 1H, OH), 1.91–1.25 (m, 10H); ^{13}C NMR (100 MHz, $CDCl_3$) δ 156.0, 134.6, 128.8 (2C), 128.4, 127.9 (2C), 119.5, 69.3, 53.8, 37.9 (2C), 25.2, 21.7 (2C); IR (neat, cm^{-1}) υ_{max} 3293, 2933, 2856, 1497, 1454, 1334, 1250, 1217, 1158, 1055, 979, 795, 727; HRMS (FAB): calcd. for

$C_{15}H_{20}N_3O$ $[M+H]^+$ 258.1606, found 258.1599.

1-Benzyl-4-(*tert*-butyl)-1*H*-1,2,3-triazole (4m): white solid (105.1 mg, 98%); m.p. 84–86 ℃; ^{1}H NMR (400 MHz, $CDCl_3$) δ 7.29–7.24 (m, 3H), 7.19–7.17 (m, 2H), 7.15 (s, 1H), 5.39 (s, 2H), 1.25 (s, 9H); ^{13}C NMR (100 MHz, $CDCl_3$) δ 157.8, 134.9, 128.7 (2C), 128.2, 127.7 (2C), 118.3, 53.6, 30.5, 30.1 (3C); IR (neat, cm^{-1}) υ_{max} 3119, 2961, 2865, 1531, 1495, 1457, 1361, 1341, 1231, 1202, 1051, 821, 713, 673; HRMS (FAB): calcd. for $C_{13}H_{18}N_3$ $[M+H]^+$ 216.1501, found 216.1498.

1-Benzyl-4-hexyl-1*H*-1,2,3-triazole (4n): white solid (119.0 mg, 98%); m.p. 52–54 ℃; ^{1}H NMR (400 MHz, $CDCl_3$) δ 7.35–7.29 (m, 3H), 7.23–7.21 (m, 2H), 7.15 (s, 1H), 5.45 (s, 2H), 2.65 (t, J = 7.8 Hz, 2H), 1.64–1.56 (m, 2H), 1.34–1.25 (m, 6H), 0.83 (t, J = 6.7 Hz, 3H); ^{13}C NMR (100 MHz, $CDCl_3$) δ 148.6, 134.9, 128.8 (2C), 128.3, 127.7 (2C), 120.4, 53.6, 31.3, 29.1, 28.7, 25.5, 22.3, 13.8; IR (neat, cm^{-1}) υ_{max} 3112, 3065, 2957, 2919, 2853, 1553, 1493, 1456, 1433, 1325, 1212, 1130, 1051, 1029, 856, 703, 691; HRMS (FAB): calcd. for $C_{15}H_{22}N_3$ $[M+H]^+$ 244.1814, found 244.1816.

1-Benzyl-4-cyclohexyl-1*H*-1,2,3-triazole (4o): white solid (120.4 mg, 100%); m.p. 109–111 ℃; ^{1}H NMR (400 MHz, $CDCl_3$) δ 7.37–7.31 (m, 3H), 7.24–7.22 (m, 2H), 7.12 (s, 1H), 5.46 (s, 2H), 2.72–2.71 (m, 1H), 2.01–1.99 (m, 2H), 1.77–1.66 (m, 3H), 1.37–1.29 (m, 4H), 1.22–1.18 (m, 1H); ^{13}C NMR (100 MHz, $CDCl_3$) δ 153.9, 134.9, 128.8 (2C), 128.3, 127.8 (2C), 119.1, 53.7, 35.1, 32.8 (2C), 25.9 (2C),

25.8; IR (neat, cm^{-1}) υ_{max} 3121, 2925, 2851, 1540, 1495, 1450, 1264, 1208, 1128, 1049, 821, 754, 721, 699; HRMS (FAB): calcd. for $C_{15}H_{20}N_3$ $[M+H]^+$ 242.1657, found 242.1660.

1-Benzyl-1*H*-1,2,3-triazole-4-carboxylic acid (4p): white solid (92.1 mg, 91%); m.p. 184–185 °C; ^1H NMR (400 MHz, $(CD_3)_2SO$) δ 12.92 (brs, 1H, CO_2H) 8.75 (s, 1H), 7.40–7.33 (m, 5H), 5.64 (s, 2H); ^{13}C NMR (100 MHz, $(CD_3)_2SO$) δ 161.6, 140.1, 135.6, 128.9, 128.8 (2C), 128.2, 128.0 (2C), 53.0; IR (neat, cm^{-1}) υ_{max} 3115, 2556, 1681, 1540, 1495, 1425, 1232, 1049, 944, 895, 783, 714, 687; HRMS (FAB): calcd. for $C_{10}H_{10}N_3O_2$ $[M+H]^+$ 204.0773, found 204.0767.

(1-Benzyl-1*H*-1,2,3-triazol-4-yl)methanamine (4q): white solid (91.2 mg, 97%); m.p. 106–109 °C; ^1H NMR (400 MHz, $(CD_3)_2SO$) δ 7.92 (s, 1H), 7.39–7.30 (m, 5H), 5.56 (s, 2H), 3.75 (s, 2H), 2.31 (brs, 2H, NH_2); ^{13}C NMR (100 MHz, $(CD_3)_2SO$) δ 150.1, 136.2, 128.7 (2C), 128.0, 127.9 (2C), 121.8, 52.7, 37.2; IR (neat, cm^{-1}) υ_{max} 3345, 3137, 2917, 1604, 1494, 1454, 1328, 1212, 1124, 1050, 898, 802, 726, 693, 668; HRMS (FAB): calcd. for $C_{10}H_{13}N_4$ $[M+H]^+$ 189.1140, found 189.1135.

2-(4-Phenyl-1*H*-1,2,3-triazol-1-yl)ethan-1-amine (4r): white solid (92.0 mg, 98%); m.p. 75–77 °C; ^1H NMR (400 MHz, $(CD_3)_2SO$) δ 8.54 (s, 1H), 7.84 (d, J = 7.3 Hz, 2H), 7.44 (t, J = 7.5 Hz, 2H), 7.32 (t, J = 7.3 Hz, 1H), 4.36 (t, J = 6.2 Hz, 2H), 3.02 (m, 2H); ^{13}C NMR (100 MHz, $(CD_3)_2SO$) δ 146.1, 130.9, 128.8 (2C),

127.7, 125.1 (2C), 121.6, 52.7, 41.7; IR (neat, cm^{-1}) υ_{max} 3338, 3125, 2952, 1461, 1217, 1075, 1039, 828, 760, 693; HRMS (FAB): calcd. for $C_{10}H_{13}N_4$ $[M+H]^+$ 189.1140, found 189.1135.

6-(4-Phenyl-1*H*-1,2,3-triazol-1-yl)hexan-1-amine (4s): white solid (113.7 mg, 93%); m.p. 68–71 ℃; ^{1}H NMR (400 MHz, C_5D_5N) δ 8.41 (s, 1H), 8.17 (d, J = 7.4 Hz, 2H), 7.46 (t, J = 7.6 Hz, 2H), 7.33 (t, J = 7.4 Hz, 1H), 4.36 (t, J = 7.1 Hz, 2H), 2.65 (t, J = 6.8 Hz, 2H), 1.85–1.78 (m, 2H), 1.37–1.21 (m, 6H); ^{13}C NMR (100 MHz, C_5D_5N) δ 147.7, 132.0, 129.3 (2C), 128.2, 126.0 (2C), 121.0, 50.2, 42.1, 33.3, 30.4, 26.4 (2C); IR (neat, cm^{-1}) υ_{max} 3286, 3118, 3008, 2924, 2849, 1578, 1483, 1462, 1215, 1077, 838, 758, 692; HRMS (FAB): calcd. for $C_{14}H_{21}N_4$ $[M+H]^+$ 245.1766, found 245.1768.

***N*-Methyl-6-(4-phenyl-1*H*-1,2,3-triazol-1-yl)hexan-1-amine (4t)**: white solid (124.1 mg, 96%); m.p. 58–60 ℃; ^{1}H NMR (400 MHz, $(CD_3)_2SO$) δ 8.57 (s, 1H), 7.84 (d, J = 7.5 Hz, 2H), 7.44 (t, J = 7.6 Hz, 2H), 7.32 (t, J = 7.2 Hz, 1H), 4.38 (t, J = 7.0 Hz, 2H), 2.39–2.38 (m, 2H), 2.23 (s, 3H), 1.89–1.82 (m, 2H), 1.38–1.26 (m, 6H); ^{13}C NMR (100 MHz, $(CD_3)_2SO$) δ 146.2, 130.9, 128.8 (2C), 127.7, 125.0 (2C), 121.1, 51.4, 49.4, 36.1, 29.6, 29.0, 26.2, 25.8; IR (neat, cm^{-1}) υ_{max} 3297, 3118, 3091, 2925, 2850, 2787, 1462, 1439, 1357, 1215, 1077, 1051, 838, 759, 692; HRMS (FAB): calcd. for $C_{15}H_{23}N_4$ $[M+H]^+$ 259.1923, found 259.1917.

Azide 7: Prepared according to the previously described procedure in which a glycosylation donor was changed to a galactosyl derivative.[30] TMSI (858 L, 6.03 mmol) was added to a solution of 1,2,3,4,6-penta-*O*-trimethylsilyl-α-D-galactose[31] (3.26 g, 6.03 mmol) in CH_2Cl_2 (60 mL) at 0 ℃. The reaction mixture was stirred under N_2 atmosphere for 15 min before benzene (60 mL) was added. The solvent was removed under reduced pressure and the glycosyl iodide intermediate obtained was dissolved in CH_2Cl_2 (60 mL) and kept under N_2 atmosphere. In a separate flask, a mixture of activated 4 Å molecular sieves (1.50 g), *n*-Bu_4NI (4.47 g, 12.1 mmol), *i*-Pr_2NEt (1.58 mL, 9.05 mmol) and (2*S*,3*S*,4*R*)-2-azido-3,4-*O*-isopropylidene-1,3,4-octadecanetriol[32] (770 mg, 2.01 mmol) in CH_2Cl_2 (60 mL) was prepared and stirred under an argon atmosphere at rt for 15 min. The solution of glycosyl iodide in CH_2Cl_2 was then added drop-wise over 5 min and the resulting mixture was stirred overnight. After removal of the solvent under reduced pressure, Et_2O (60 mL) and H_2O (60 mL) were added and the phases were separated. The organic phase was concentrated under reduced pressure. MeOH (60 mL) and PTSA·H_2O (39.9 mg, 0.21 mmol) were added to the crude mixture and stirred at rt for 5 h. The reaction was quenched by the addition of $NaHCO_3$ (300 mg, 3.57 mmol), filtered, and then concentrated under reduced pressure. The crude mixture was purified by flash column chromatography ($CHCl_3$/MeOH, 6:1) to afford azide **7** (650 mg, 64%, α-anomer only) as a white solid. m.p. 195 ℃ (dec.); $[\alpha]^{25}_D$ +103.9 (*c* 0.3,

$CHCl_3$/MeOH, 1:1); ^{1}H NMR (400 MHz, $CDCl_3$/CD_3OD, 2:1) δ 4.69 (d, J = 3.5 Hz, 1H), 3.90 (dd, J = 10.8 Hz, 3.2 Hz, 1H), 3.75–3.46 (m, 8H), 3.40–3.36 (m, 2H), 1.42–1.33 (m, 2H), 1.21–1.04 (m, 25H), 0.65 (t, J = 6.6 Hz, 3H); ^{13}C NMR (100 MHz, $CDCl_3$/CD_3OD, 2:1) δ 99.2, 73.5, 71.6, 70.5, 69.8, 69.5, 68.4, 67.3, 61.4, 61.3, 31.8, 31.5, 29.33, 29.26, 29.21, 28.9, 25.4, 22.2, 13.5; IR (neat, cm^{-1}) υ_{max} 3325, 2917, 2851, 2100, 1569, 1469, 1262, 1137, 1065, 1023, 696, 763, 717; HRMS (FAB): calcd. for $C_{24}H_{48}N_3O_8$ $[M+H]^+$ 506.3441, found 506.3438.

α-GalCer analog 5. In a vial fitted with a screw cap, freshly prepared stock solutions of $CuSO_4 \cdot 5H_2O$ (30 L, 50 mM stock solution in DDW, 1.5 mol%), TTTA (**1a**, 10 L, 50 mM stock solution in CH_2Cl_2, 0.5 mol%), and sodium ascorbate (30 L, 150 mM stock solution in DDW, 4.5 mol%) were added to a mixture of **7** (50.5 mg, 0.1 mmol) and **6** (40 mg, 0.11 mmol) in DDW (0.44 mL) and CH_2Cl_2 (0.49 mL). The reaction was allowed to proceed at rt for 2 h. The crude reaction mixture was filtered and rinsed with Et_2O (10 mL) and DDW (10 mL). The resulting solid was dried *in vacuo* to afford **5** (78.6 mg, 92%) as a white solid. m.p. 166–168 ℃; $[\alpha]^{25}_D$ +45.9 (*c* 0.3, pyridine); ^{1}H NMR (400 MHz, C_5D_5N) δ 8.28 (s, 1H), 7.07 (d, J = 6.6 Hz, 1H, NH), 6.70 (m, 1H, OH), 6.56 (m, 1H, OH), 6.51 (m, 1H, OH), 6.43 (d, J = 6.3 Hz, 1H, OH), 6.32 (m, 1H, OH), 5.97 (m, 1H, OH), 4.97 (dd, J = 11.5, 4.2 Hz, 1H), 4.69 (dd, J = 11.3, 6.8 Hz, 1H), 4.61 (m, 1H), 4.51–4.34 (m, 6H), 4.14 (m, 1H), 2.77 (t, J = 7.7 Hz, 2H), 2.16 (m, 1H), 1.81–1.58

(m, 6H), 1.31–1.25 (m, 63H), 0.86 (t, J = 6.9 Hz, 6H); ^{13}C NMR (100 MHz, C_5D_5N) δ 147.8, 122.1, 101.7, 76.7, 73.2, 72.2, 71.5, 71.0, 70.2, 67.4, 62.8, 62.7, 34.3, 32.1, 30.2, 30.00, 29.96, 29.89, 29.73, 29.62, 29.58, 26.3, 26.2, 22.9, 14.2; IR (neat, cm^{-1}) υ_{max} 3360, 2916, 2848, 1729, 1464, 1149, 1069, 1029, 794, 719; HRMS (FAB): calcd. for $C_{50}H_{98}N_3O_8$ $[M+H]^+$ 868.7354, found 868.7348.

V. References

(1) (a) R. Huisgen, in *1,3-Dipolar Cycloaddition Chemistry*, ed. A. Padwa, Wiley, New York, 1984, 1. (b) A. Michael, *J. Prakt. Chem.* **1893**, *48*, 94–95; (c) R. Huisgen, *Angew. Chem. Int. Ed. Engl*. **1963**, *2*, 565–598.

(2) (a) V. V. Rostovtsev, L. G. Green, V. V. Fokin, K. B. Sharpless, *Angew. Chem. Int. Ed*. **2002**, *41*, 2596–2599; (b) C. W. Tornøe, C. Christensen, M. Medal, *J. Org. Chem*. **2002**, *67*, 3057–3064.

(3) H. C. Kolb, M. G. Finn, K. B. Sharpless, *Angew. Chem. Int. Ed*. **2001**, *40*, 2004–2021.

(4) For reviews, see: (a) J. E. Moses, A. D. Moorhouse, *Chem. Soc. Rev.* **2007**, *36*, 1249–1262; (b) H. C. Kolb, K. B. Sharpless, *Drug Discovery Today* **2003**, *8*, 1128–1137; (c) G. C. Tron, T. Pirali, R. A. Billington, P. L. Canonico, G. Sorba, A. A. Genazzani, *Med. Res. Rev.* **2008**, *28*, 278–308; (d) W. H. Binder, R. Sachsenhofer, *Macromol. Rapid Commun.* **2007**, *28*, 15–54; (e) J. A. Johnson, M. G. Finn, J. T. Koberstein, N. J. Turro, *Macromol. Rapid Commun*. **2008**, *29*, 1052–1072; (f) E. Lallana, R. Riguera, E. Fernandez-Megia, *Angew. Chem. Int. Ed*. **2011**, *50*, 8794–8804.

(5) For reviews, see: (a) M. Medal, C. W. Tornøe, *Chem. Rev*. **2008**, *108*, 2952–3015; (b) J. E. Hein, V. V. Fokin, *Chem. Soc. Rev*. **2010**, *39*, 1302–1315; (c) L.

Liang, D. Astruc, *Coord. Chem. Rev*. **2011**, *255*, 2933–2945.

(6) For review see: S. Díez-González, *Curr. Org. Chem*. **2011**, *15*, 2830–2845.

(7) For selected examples, see: (a) T. R. Chan, R. Hilgraf, K. B. Sharpless, V. V. Fokin, *Org. Lett*. **2004**, *6*, 2853–2855; (b) S. Díez-González,S. P. Nolan, *Angew. Chem. Int. Ed*. **2008**, *47*, 8881–8884; (c) N. Candelon, D. Lastécouères, A. K. Diallo, J. R. Aranzaes, D. Astruc, J.-M. Vincent, *Chem. Commun*. **2008**, 741–743; (d) V. O. Rodionov, S. I. Presolski, S. Gardinier, Y.-H. Lim, M. G. Finn, *J. Am. Chem. Soc*. **2007**, *129*, 12696–12704; (e) K. Asano, S. Matsubara, *Org. Lett*. **2010**, *12*, 4988–4991.

(8) For selected examples, see: (a) E. Ozkal, S. Özçubukçu, C. Jimeno, M. A Pericàs, *Catal. Sci. Technol*. **2012**, *2*, 195–200; (b) A. Coelho, P. Diz, O. Caamaño, E. Sotelo, *Adv. Synth. Catal*. **2010**, *352*, 1179–1192; (c) T. R. Chan, V. V. Fokin, *QSAR Comb. Sci*. **2007**, *11*, 1274–1279; (d) S. Wallyn, M. Lammens, R. K. O'reilly, F. Du Prez, *J. Polym. Sci. Part A: Polym. Chem.* **2011**, *49*, 2878–2885.

(9) (a) G. A. Molander, J. Ham, *Org. Lett*. **2006**, *8*, 2767–2770; (b) M. Malkoch, K. Schleicher, E. Drockenmuller, C. J. Hawker, T. P. Russell, P. Wu, V. V. Fokin, *Macromolecules* **2005**, *38*, 3663–3678; (c) P. Wu, A. K. Feldman, A. K. Nugent, C. J. Hawker, A. Scheel, B. Voit, J. Pyun, J. M. J. Fréchet, K. B. Sharpless, V. V. Fokin, *Angew. Chem. Int. Ed*. **2004**, *43*, 3928–3932.

(10) C. Girard, E. Önen, M. Aufort, S. Beauvière, E. Samson, J. Herscovici, *Org. Lett*. **2006**, *8*, 1689–1692.

(11) (a) F. Pérez-Balderas, M. Ortega-Muñoz, J. Morales-Sanfrutos, F. Hernández-Mateo, F. G. Calvo-Flores, J. A. Calvo-Asín, J. Isac-García, F. Santoyo-González, *Org. Lett*. **2003**, *5*, 1951–1954; (b) R. Berg, J. Straub, E. Schreiner, S. Mader, F. Rominger, B. F. Straub, *Adv. Synth. Catal*. **2012**, *354*, 3445–3450; (c) Z. Gonda, Z. Novák, *Dalton Trans*. **2010**, *39*, 726–729.

(12) (a) B.-Y. Lee, S. R. Park, H. B. Jeon, K. S. Kim, *Tetrahedron Lett*. **2006**, *47*, 5105–5109; (b) H. K. Akula, M. K. Lakshman, *J. Org. Chem*. **2012**, *77*, 8896–8904; (c) A. Shigenaga, H. Hirakawa, J. Yamamoto, K. Ogura, M. Denda, K. Yamaguchi, D. Tsuji, K. Itoh, A. Otaka, *Tetrahedron* **2011**, *67*, 3984–3990.

(13) (a) B. Lygo, B. I. Andrews, *Acc. Chem. Res*. **2004**, *37*, 518–525; (b) M. Ikunaka, *Org. Process Res. Dev*. **2008**, *12*, 698–709; (c) S. D. Naik, L. K. Doraiswamy, *AIChE J*. **1998**, *44*, 612–646.

(14) (a) J.-A. Shin, Y.-G. Lim, K.-H. Lee, *J. Org. Chem*. **2012**, *77*, 4117–4122; (b) X. Xiong, L. Cai, *Catal. Sci. Technol*. **2013**, *3*, 1301–1307; (c) D. Kumar, V. B. Reddy, R. S. Varma, *Tetrahedron Lett*. **2009**, *50*, 2065–2068.

(15) M. N. Tahir, R. Qamar, A. Adnan, E. Cho, S. Jung, *Tetrahedron Lett*. **2013**, *54*, 3268–3273.

(16) P. S. Donnelly, S. D. Zanatta, S. C. Zammit, J. M. White, S. J. Williams, *Chem.*

Commun. **2008**, 2459–2461.

(17) There is a possibility that the Cu(II)-ligand complex can also be reduced directly to Cu(I) complex; see Ref 16.

(18) (a) J. E. Hein, J. C. Tripp, L. B. Krasnova, K. B. Sharpless, V. V. Fokin, *Angew. Chem. Int. Ed*. **2009**, *48*, 8018–8021; (b) C. Besanceney-Webler, H. Jiang, T. Zheng, L, Feng, D. Soriano del Amo, W. Wang, L. M. Klivansky, F. L. Marlow, Y. Liu, P. Wu, *Angew. Chem. Int. Ed*. **2011**, *50*, 8051–8056.

(19) The use of TBTA (**1b**) for performing the CuAAC reaction with the same Cu(I) sources in the same biphasic system has been reported. However, the phase transfer activity was not noticed; see Ref 12c.

(20) H.-M. Yang, H.-S. Wu, *Catal. Rev.-Sci. Eng*. 2003, **45**, 463–540.

(21) (a) C. Shao, R. Zhu, S. Luo, Q. Zhang, X. Wang, Y. Hu, *Tetrahedron Lett*. **2011**, *52*, 3782–3785; (b) S. Dodela, D. L. Hughes, S. A. Nepogodiev, M. Rejzek, R. A. Field, *Carbohydr. Res*. **2010**, *345*, 1123–1134; (c) N. Chopin, S. Decamps, A. Gouger, M. Médebielle, S. Picot, A.-L. Bienvenu, G. Pilet, *J. Fluor. Chem*. **2011**, *132*, 850–857; (d) L. S. Campbell-Verduyn, L. Mirfeizi, R. A. Dierckx, P. H. Elsinga, B. L. Feringa, *Chem. Commun*. **2009**, 2139–2141; (e) S. Ö zçubukçu, E. Ozkal, C. Jimeno, M. A. Pericàs, *Org. Lett*. **2009**, *11*, 4680–4683.

(22) T. Lee, M. Cho, S.-Y. Ko, H.-J. Youn, D. J. Baek, W.-J. Cho, C.-Y. Kang, S. Kim, *J. Med. Chem*. **2007**, *50*, 585–589.

(23) S. G. Alvarez, M. T. Alvarez, *Synthesis* **1997**, 413–414.

(24) M. K. Sinha, O. Reany, M. Yefet, M. Botoshansky, E. Keinan, *Chem. Eur. J.* **2012**, *18*, 5589–5605.

(25) F. Coutrot, E. Busseron, *Chem. Eur. J.* **2009**, *15*, 5186–5190.

(26) T. T. Denton, X. Zhang, J. R. Cashman, *J. Med. Chem.* **2005**, *48*, 224–239.

(27) F. Shi, J. P. Waldo, Y. Chen, R. C. Larock, *Org. Lett.* **2008**, *10*, 2409–2412.

(28) M. Lamani, P. Devadig, K. R. Prabhu, *Org. Biomol. Chem.* **2012**, *10*, 2753–2759.

(29) O. Berger, A. Kaniti, C. Tran van Ba, H. Vial, S. A. Ward, G. A. Biagini, P. G. Bray, P. M. O'Neill, *ChemMedChem* **2011**, *6*, 2094–2108.

(30) P. J. Jervis, N. Veerapen, G. Bricard, L. R. Cox, S. A. Porcelli, G. S. Besra, *Bioorg. Med. Chem. Lett.* **2010**, *20*, 3475–3478.

(31) A. S. Bhat, J. Gervay-Hague, *Org. Lett.* **2001**, *3*, 2081–2084.

(32) R. T. Dere, X. Zhu, *Org. Lett.* **2008**, *10*, 4641–4644.

VI. Acknowledgements

Reproduced from *RSC Adv.* **2014**, *4*, 26516–26523 with permission from the Royal Society of Chemistry.

Appendix I

Spectra of Compounds
(Part A)

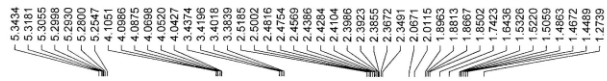

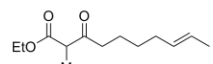

9

(400 MHz, $CDCl_3$)

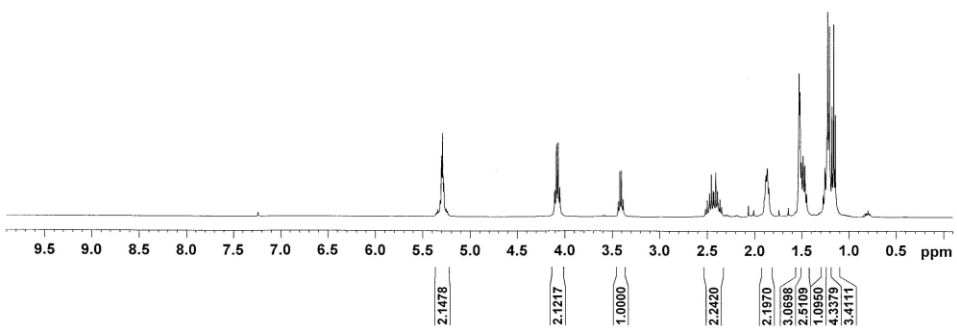

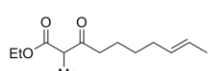

9

(100 MHz, $CDCl_3$)

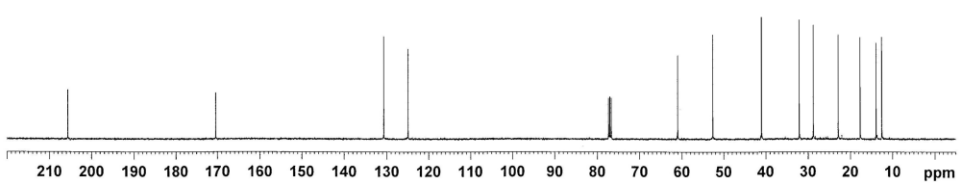

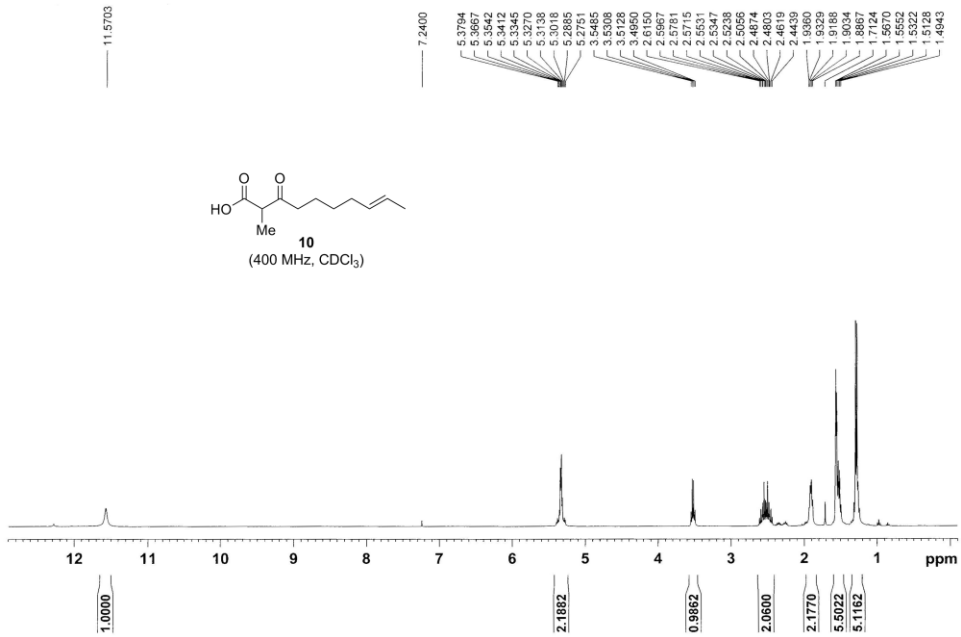
11.5703
7.2400
5.3794
5.3667
5.3542
5.3417
5.3345
5.3270
5.3138
5.3018
5.2885
5.2751
3.5485
3.5308
3.5128
3.4950
2.6150
2.5967
2.5781
2.5715
2.5531
2.5347
2.5238
2.5056
2.4874
2.4693
2.4513
2.4439
1.9360
1.9329
1.9188
1.9034
1.8867
1.7124
1.5670
1.5552
1.5322
1.5128
1.4943
HO
O
O
Me
10
(400 MHz, CDCl3)
12
11
10
9
8
7
6
5
4
3
2
1
ppm
1.0000
2.1882
0.9862
2.0600
2.1770
5.5022
5.1162

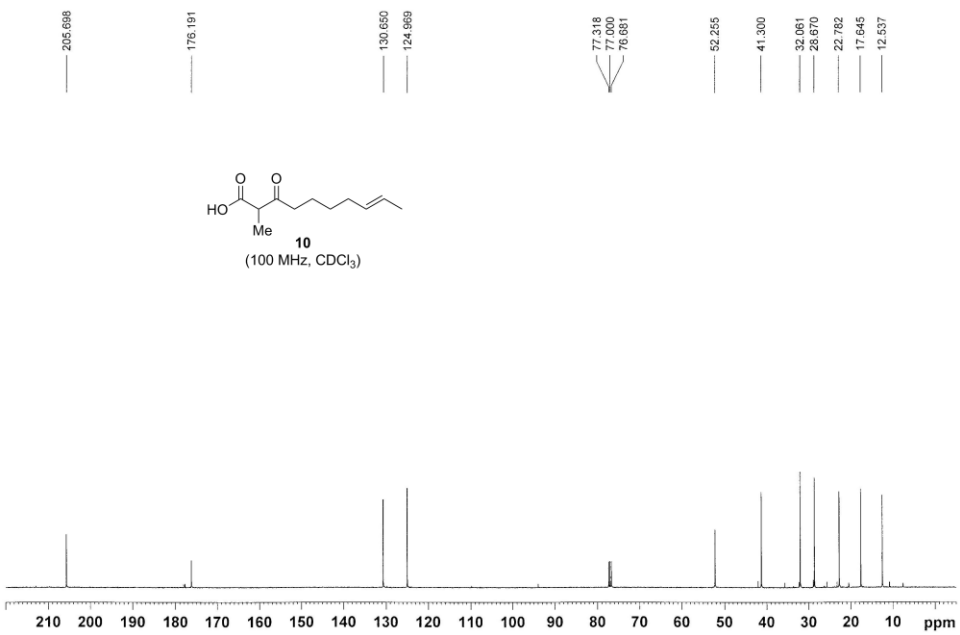
205.698
176.191
130.650
124.969
77.318
77.000
76.681
52.255
41.300
32.061
28.670
22.762
17.645
12.537
HO
O
O
Me
10
(100 MHz, CDCl3)
210
200
190
180
170
160
150
140
130
120
110
100
90
80
70
60
50
40
30
20
10
ppm

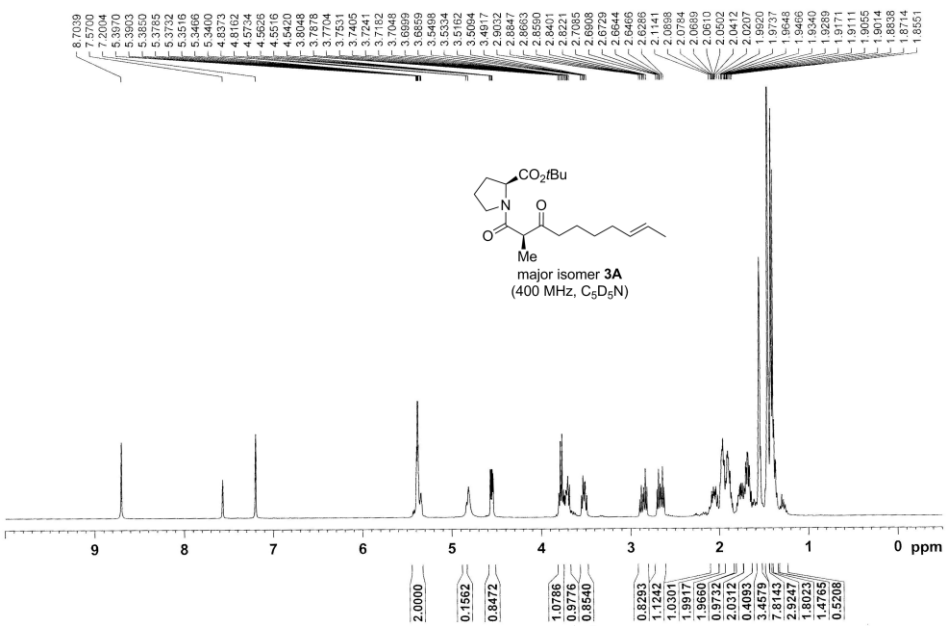
major isomer 3A
(400 MHz, C5D5N)

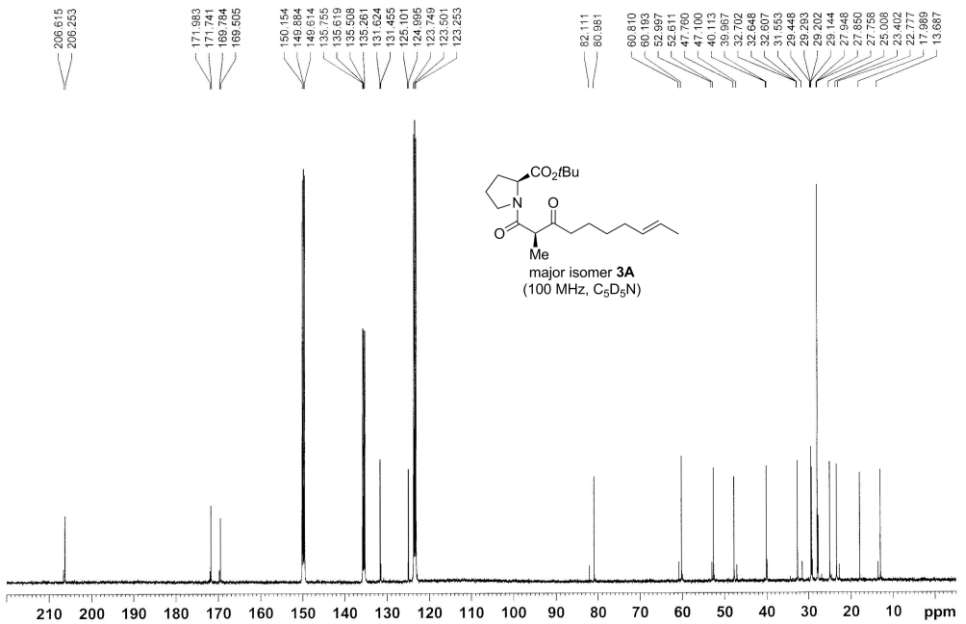
major isomer 3A
(100 MHz, C5D5N)

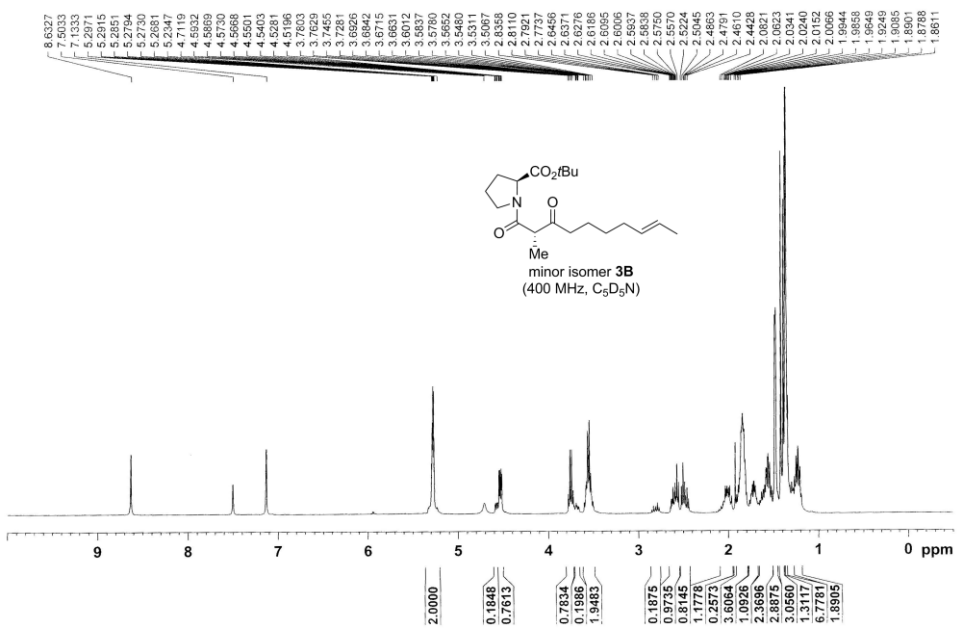
CO2tBu
N
O
O
Me
minor isomer 3B
(400 MHz, C5D5N)
ppm

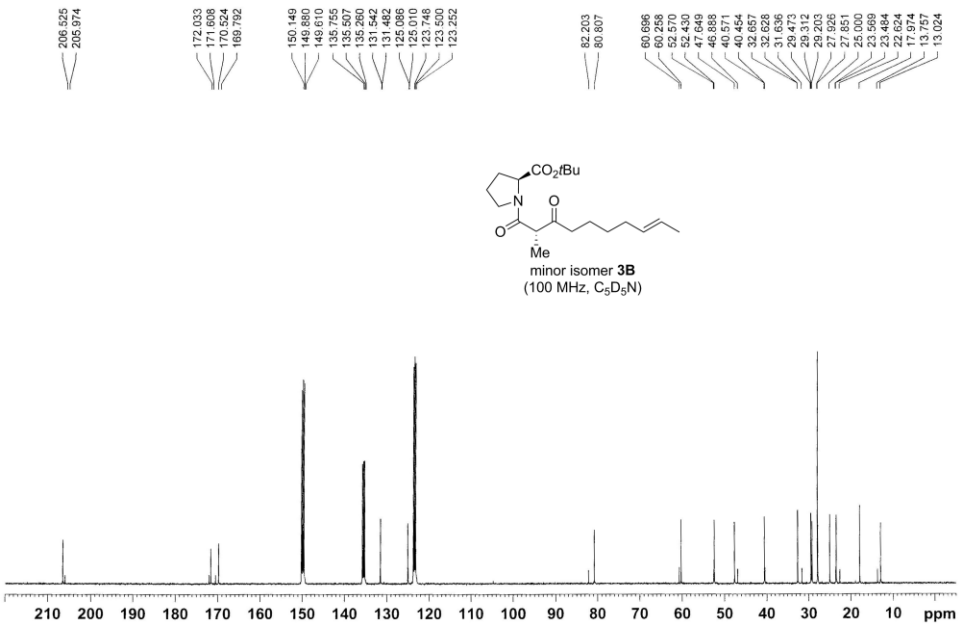
CO2tBu
N
O
O
Me
minor isomer 3B
(100 MHz, C5D5N)
ppm

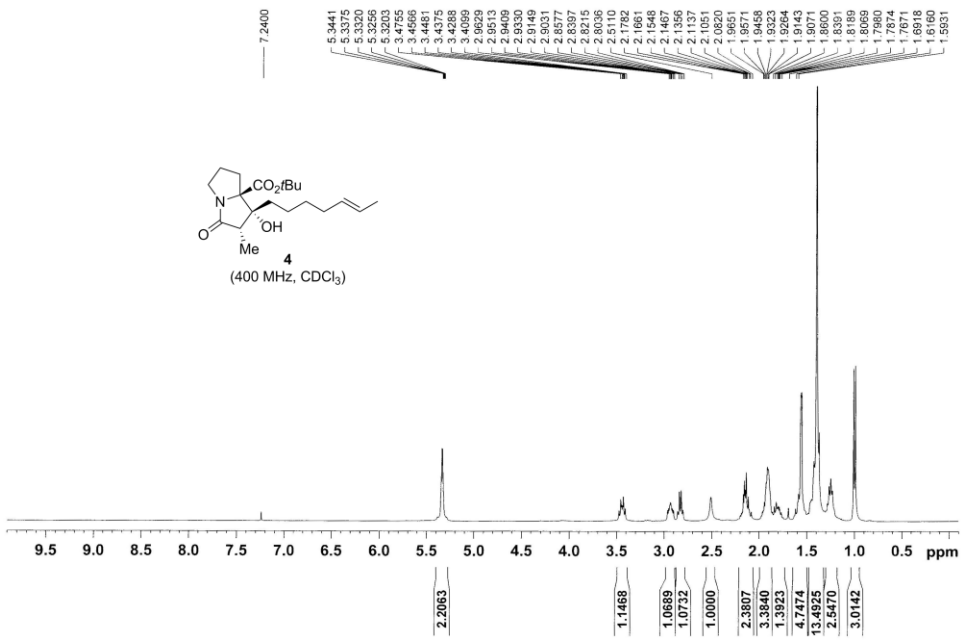
7.2400
5.3441
5.3375
5.3320
5.3256
5.3203
3.4755
3.4566
3.4481
3.4375
3.4288
3.4099
2.9629
2.9513
2.9409
2.9330
2.9149
2.9031
2.8577
2.8397
2.8215
2.8036
2.5110
2.1782
2.1661
2.1548
2.1467
2.1356
2.1137
2.1051
2.0820
1.9651
1.9571
1.9458
1.9323
1.9264
1.9143
1.9071
1.8900
1.8391
1.8189
1.8069
1.7980
1.7874
1.7671
1.6918
1.6160
1.5931
CO2tBu
N
O
OH
Me
4
(400 MHz, CDCl3)
9.5 9.0 8.5 8.0 7.5 7.0 6.5 6.0 5.5 5.0 4.5 4.0 3.5 3.0 2.5 2.0 1.5 1.0 0.5 ppm
2.2063
1.1468
1.0689
1.0732
1.0000
2.3807
3.3840
1.3923
4.7474
13.4925
2.5470
3.0142

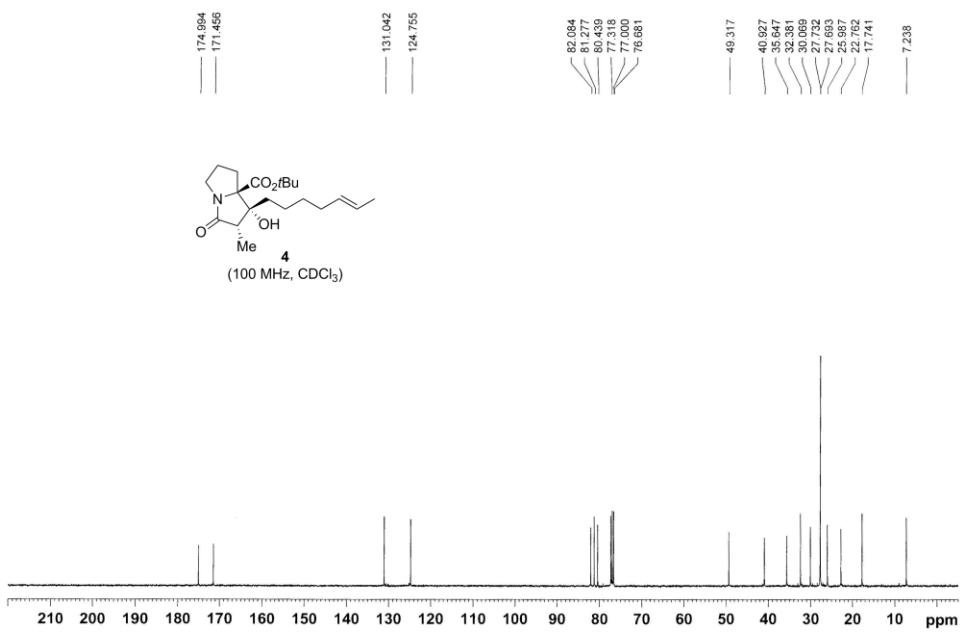
174.994
171.456
131.042
124.755
82.084
81.277
80.439
77.318
77.000
76.681
49.317
40.927
35.647
32.381
30.069
27.732
27.693
25.987
22.762
17.741
7.238
CO2tBu
N
O
OH
Me
4
(100 MHz, CDCl3)
210 200 190 180 170 160 150 140 130 120 110 100 90 80 70 60 50 40 30 20 10 ppm

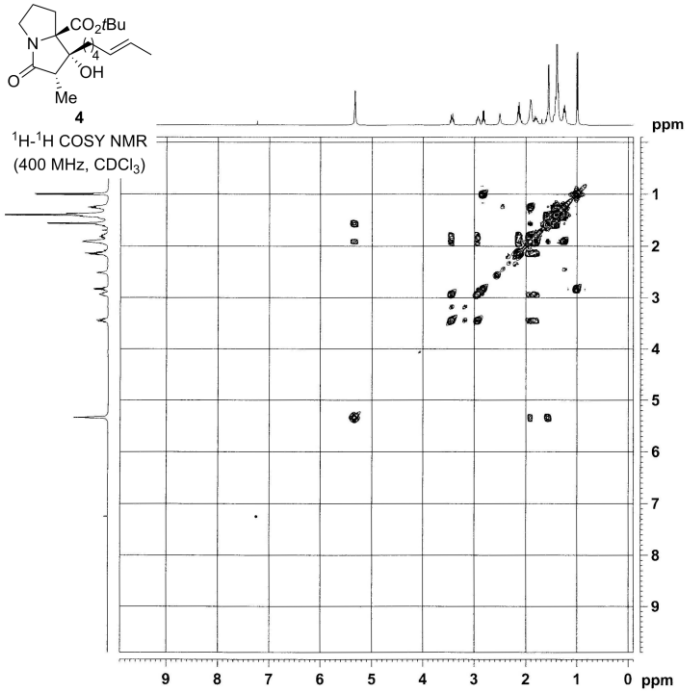


```
Current Data Parameters
NAME            1230 (KJN)
EXPNO                 11
PROCNO                 1

F2 - Acquisition Parameters
Date_           20150107
Time                9.00
INSTRUM            spect
PROBHD     5 mm Multinucl
PULPROG         cosygf45
TD                  2048
SOLVENT             CDCl3
NS                     8
DS                    16
SWH              5592.841 Hz
FIDRES           2.730880 Hz
AQ               0.1831412 sec
RG                    10.1
DW                89.400 usec
DE                 6.00 usec
TE                300.0 K
d0             0.00000300 sec
D1             2.00000000 sec
IN0            0.00017880 sec
MCREST         0.00000000 sec
MCWRK          2.00000000 sec

======== CHANNEL f1 ========
NUC1                   1H
P1                 12.50 usec
PL1                 5.50 dB
SFO1         400.1320159 MHz

F1 - Acquisition parameters
ND0                    1
TD                   256
SFO1           400.132 MHz
FIDRES       21.847036 Hz
SW               13.977 ppm
FnMODE                QF

F2 - Processing parameters
SI                  1024
SF           400.1300144 MHz
WDW                 SINE
SSB                    0
LB                  0.00 Hz
GB                     0
PC                  1.00

F1 - Processing parameters
SI                  1024
MC2                   QF
SF           400.1300142 MHz
WDW                 SINE
SSB                    0
LB                  0.00 Hz
GB                     0
```

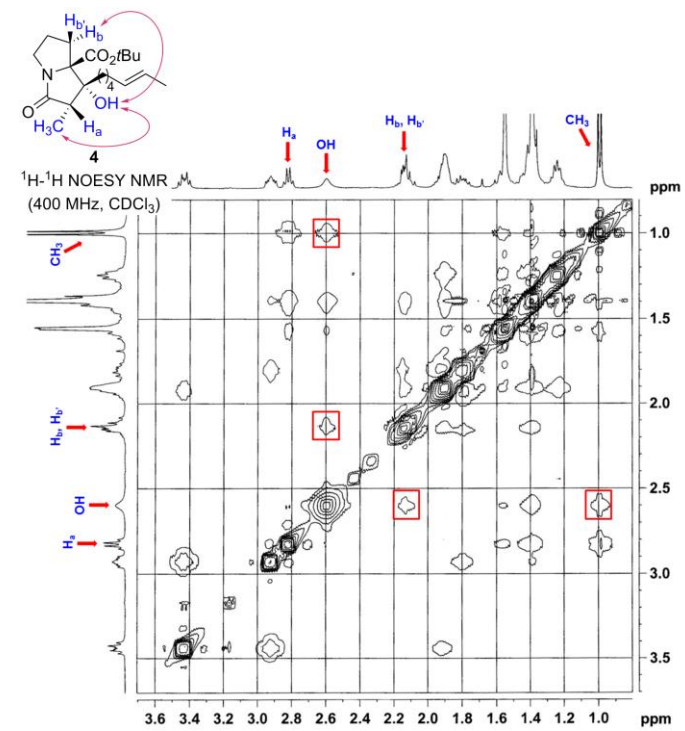


```
Current Data Parameters
NAME            1230 (KJN)
EXPNO                 14
PROCNO                 1

F2 - Acquisition Parameters
Date_           20150115
Time               11.11
INSTRUM            spect
PROBHD     5 mm Multinucl
PULPROG          noesyph
TD                  2048
SOLVENT             CDCl3
NS                    16
DS                    16
SWH              5592.841 Hz
FIDRES           2.730880 Hz
AQ               0.1831412 sec
RG                    20.2
DW                89.400 usec
DE                 6.00 usec
TE                300.0 K
d0             0.00007374 sec
D1             2.00000000 sec
D8             1.00000000 sec
IN0            0.00017880 sec
MCREST         0.00000000 sec
MCWRK          1.00000000 sec
ST1CNT                128

======== CHANNEL f1 ========
NUC1                   1H
P1                 12.30 usec
PL1                 5.50 dB
SFO1         400.1320159 MHz

F1 - Acquisition parameters
ND0                    1
TD                   256
SFO1           400.132 MHz
FIDRES       21.847036 Hz
SW               13.977 ppm
FnMODE       States-TPPI

F2 - Processing parameters
SI                  2048
SF           400.1300134 MHz
WDW                 SINE
SSB                    2
LB                  0.00 Hz
GB                     0
PC                  1.00

F1 - Processing parameters
SI                  1024
MC2          States-TPPI
SF           400.1300120 MHz
WDW                 SINE
SSB                    2
LB                  0.00 Hz
GB                     0
```

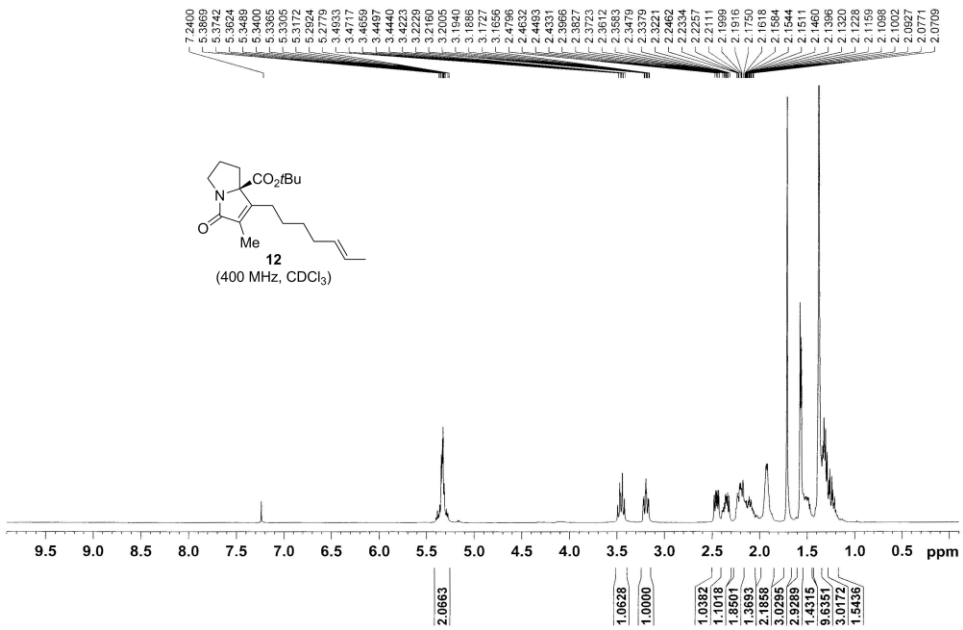
7.2400
5.3869
5.3742
5.3624
5.3489
5.3400
5.3365
5.3175
5.3172
5.2904
5.2779
3.4933
3.4717
3.4659
3.4497
3.4440
3.4223
3.2229
3.2160
3.2005
3.1940
3.1886
3.1727
3.1656
2.4796
2.4632
2.4493
2.4351
2.3966
2.3827
2.3723
2.3612
2.3583
2.3479
2.3379
2.3221
2.2462
2.2334
2.2257
2.2111
2.1999
2.1916
2.1750
2.1618
2.1584
2.1544
2.1511
2.1460
2.1395
2.1320
2.1228
2.1098
2.1002
2.0927
2.0771
2.0709
CO2tBu
N
O
Me
12
(400 MHz, CDCl3)
9.5 9.0 8.5 8.0 7.5 7.0 6.5 6.0 5.5 5.0 4.5 4.0 3.5 3.0 2.5 2.0 1.5 1.0 0.5 ppm
2.0663
1.0628
1.0000
1.0382
1.1018
1.8501
1.3693
2.1858
3.0295
2.9289
1.4315
9.6351
3.0172
1.5436

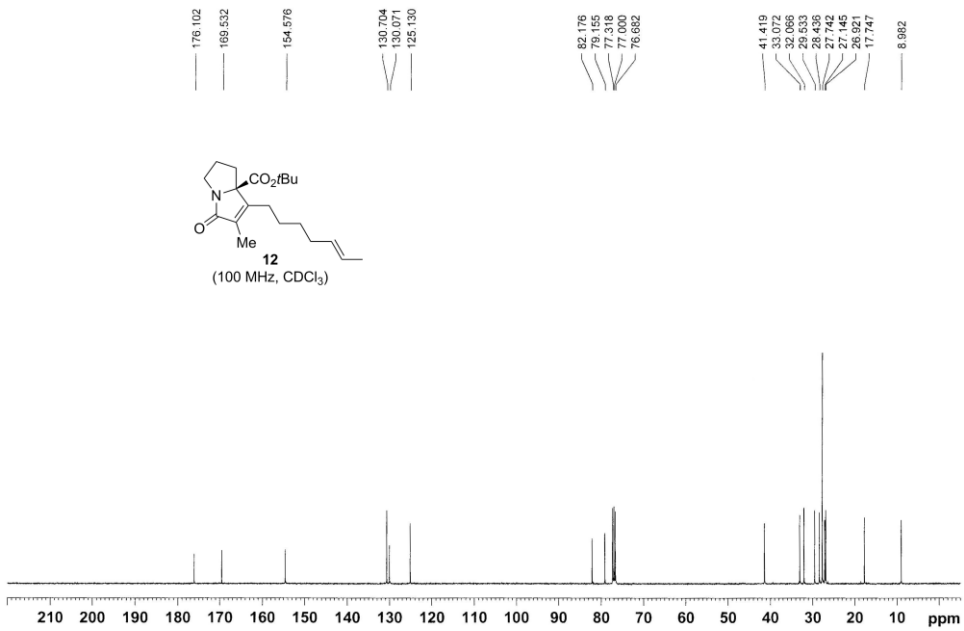
176.102
169.532
154.576
130.704
130.071
125.130
82.176
79.155
77.318
77.000
76.682
41.419
33.072
32.066
29.533
28.436
27.742
27.445
26.921
17.747
8.982
CO2tBu
N
O
Me
12
(100 MHz, CDCl3)
210 200 190 180 170 160 150 140 130 120 110 100 90 80 70 60 50 40 30 20 10 ppm

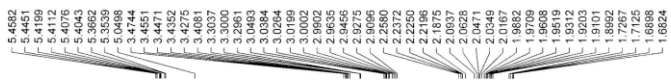

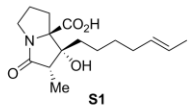

S1

(400 MHz, CD_3OD)

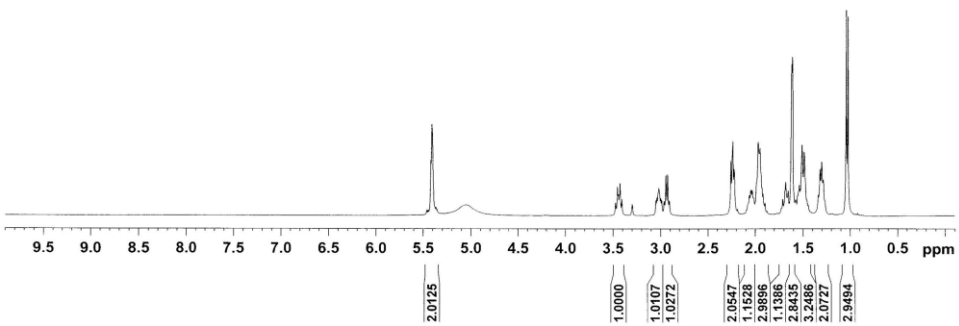

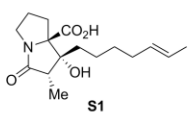

S1

(100 MHz, CD_3OD)

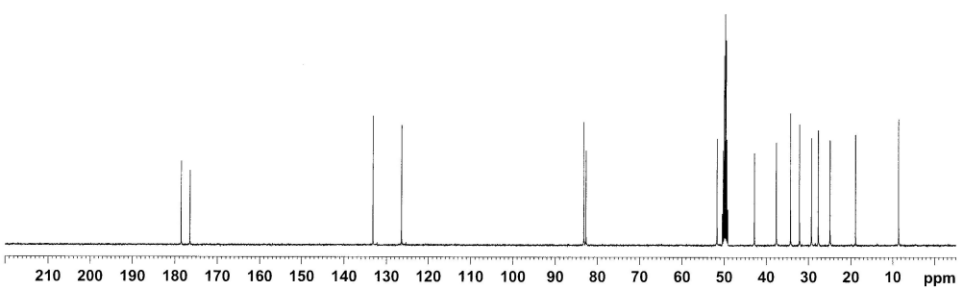

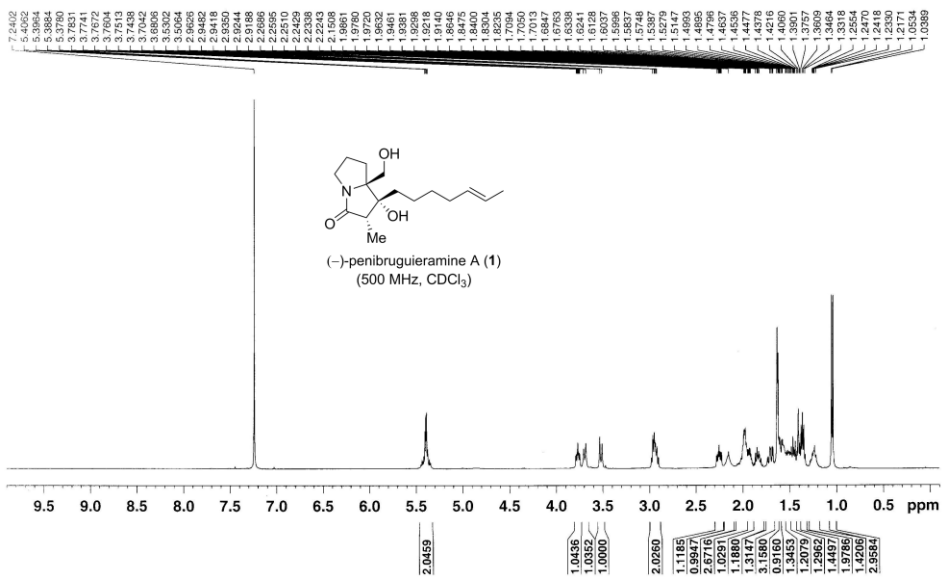
OH
N
O
OH
Me
(–)-penibruguieramine A (1)
(500 MHz, CDCl3)
9.5 9.0 8.5 8.0 7.5 7.0 6.5 6.0 5.5 5.0 4.5 4.0 3.5 3.0 2.5 2.0 1.5 1.0 0.5 ppm
2.0459
1.0436
1.0352
1.0000
2.0260
1.1185
0.9947
2.6716
1.0291
1.1880
1.3147
3.1580
0.9160
1.3453
1.2079
1.2962
1.4497
1.9786
1.4206
2.9584

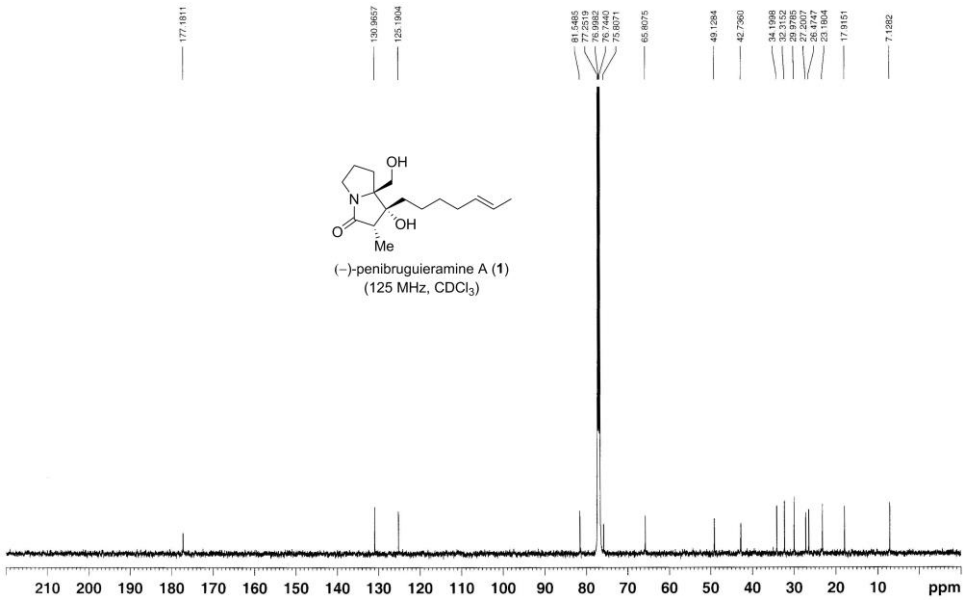
177.1811
130.9657
125.1904
81.5485
77.3553
76.9982
76.7440
75.8671
65.8075
49.1284
42.7360
34.1998
32.3152
29.7595
27.2007
26.4747
23.1804
17.9151
7.1282
OH
N
O
OH
Me
(–)-penibruguieramine A (1)
(125 MHz, CDCl3)
210 200 190 180 170 160 150 140 130 120 110 100 90 80 70 60 50 40 30 20 10 ppm

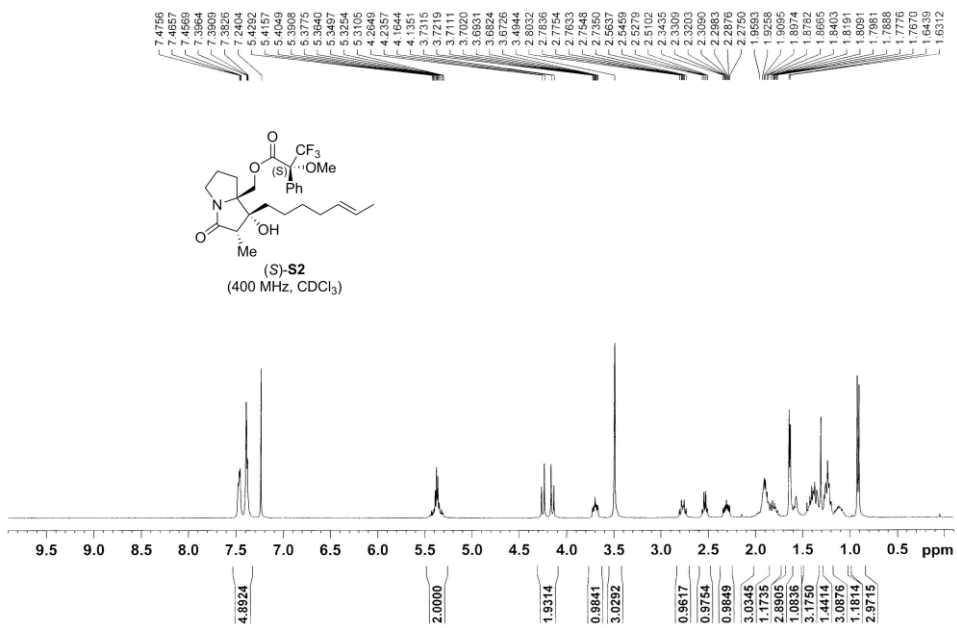
(S)-S2
(400 MHz, CDCl3)
9.5 9.0 8.5 8.0 7.5 7.0 6.5 6.0 5.5 5.0 4.5 4.0 3.5 3.0 2.5 2.0 1.5 1.0 0.5 ppm
4.8924
2.0000
1.9314
0.9841
3.0292
0.9617
0.9754
0.9849
3.0345
1.1735
2.8905
1.0836
3.1750
1.4414
3.0876
1.1814
2.9715

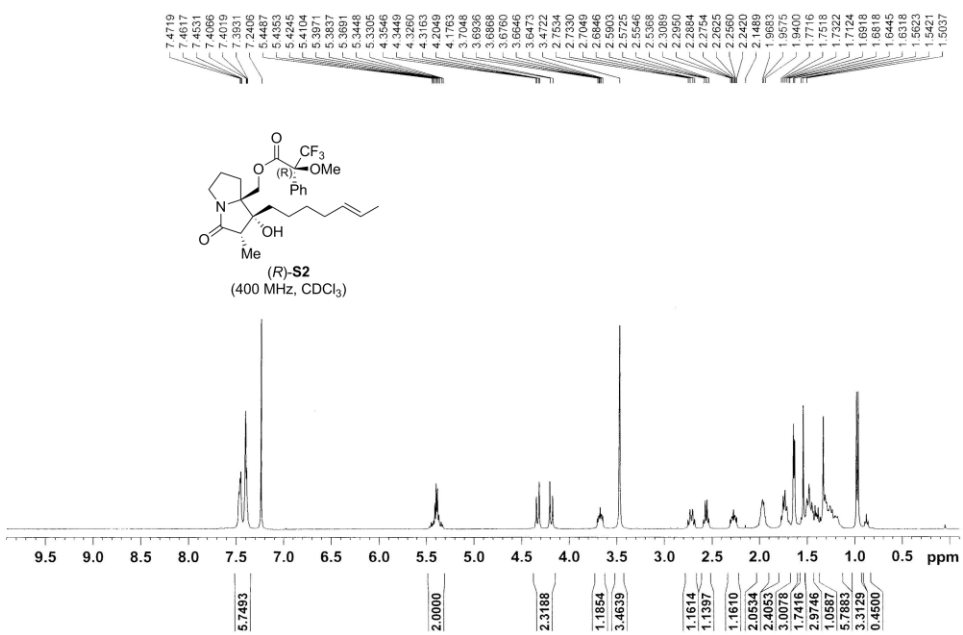
(R)-S2
(400 MHz, CDCl3)
9.5 9.0 8.5 8.0 7.5 7.0 6.5 6.0 5.5 5.0 4.5 4.0 3.5 3.0 2.5 2.0 1.5 1.0 0.5 ppm
5.7493
2.0000
2.3188
1.1854
3.4639
1.1614
1.1397
1.1610
2.0534
2.4053
3.0078
1.7416
2.9746
1.0587
5.7883
3.3129
0.4500

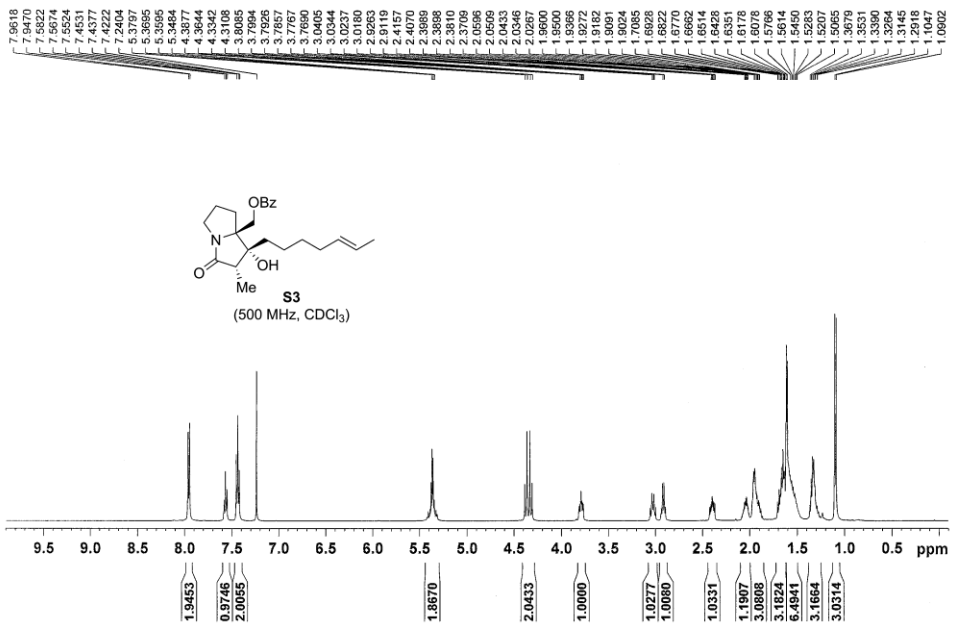
OBz
N
O
OH
Me
S3
(500 MHz, CDCl3)
ppm

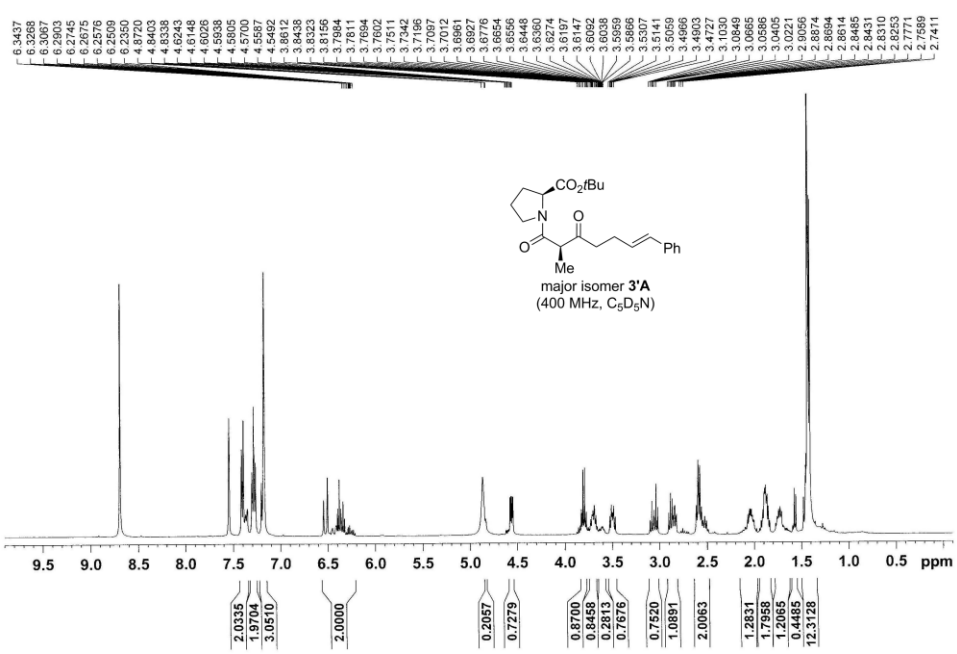
CO2tBu
N
O
O
Ph
Me
major isomer 3'A
(400 MHz, C5D5N)
ppm

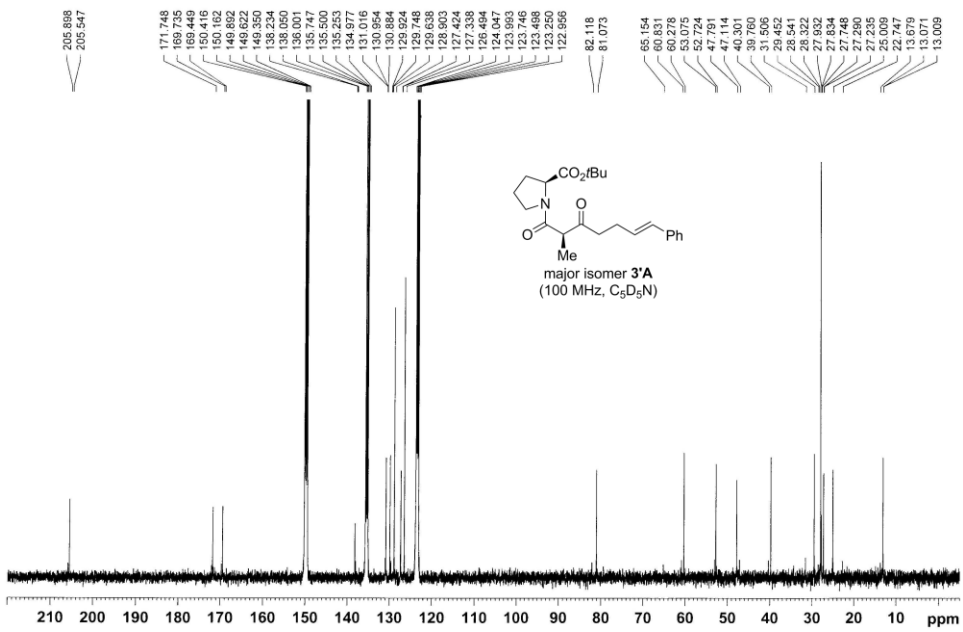
205.898
205.547
171.748
169.735
169.449
150.416
150.162
149.892
149.622
149.350
138.234
138.050
136.001
135.747
135.500
135.253
134.977
131.016
130.954
130.884
129.924
129.748
129.638
128.903
127.424
127.338
126.494
124.047
123.993
123.746
123.498
123.250
122.956
82.118
81.073
65.154
60.831
60.278
53.775
52.724
47.791
47.114
40.301
39.760
31.506
29.452
28.541
28.322
27.932
27.834
27.748
27.290
27.235
25.009
22.747
13.679
13.071
13.009
CO2tBu
N
O
O
Ph
Me
major isomer 3'A
(100 MHz, C5D5N)
210 200 190 180 170 160 150 140 130 120 110 100 90 80 70 60 50 40 30 20 10 ppm

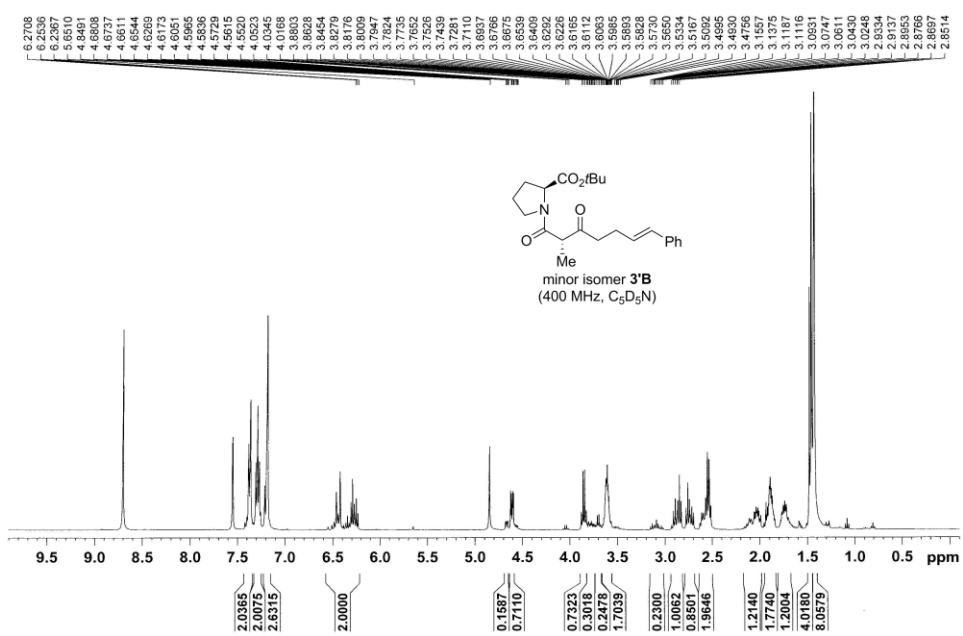
6.2708
6.2536
6.2357
5.6510
4.8491
4.6808
4.6737
4.6611
4.6544
4.6289
4.6173
4.6051
4.5965
4.5836
4.5729
4.5615
4.5520
4.0523
4.0345
4.0168
3.8803
3.8628
3.8454
3.8279
3.8178
3.8009
3.7947
3.7824
3.7735
3.7652
3.7526
3.7439
3.7281
3.7110
3.6937
3.6766
3.6675
3.6539
3.6409
3.6292
3.6228
3.6165
3.6113
3.6063
3.5985
3.5893
3.5828
3.5730
3.5650
3.5334
3.5167
3.5092
3.4995
3.4930
3.4756
3.1557
3.1375
3.1187
3.1116
3.0931
3.0747
3.0611
3.0430
3.0248
2.9534
2.9137
2.8953
2.8766
2.8697
2.8514
CO2tBu
N
O
O
Ph
Me
minor isomer 3'B
(400 MHz, C5D5N)
9.5 9.0 8.5 8.0 7.5 7.0 6.5 6.0 5.5 5.0 4.5 4.0 3.5 3.0 2.5 2.0 1.5 1.0 0.5 ppm
2.0365
2.0075
2.6315
2.0000
0.1587
0.7110
0.7323
0.3018
0.2478
1.7039
0.2300
1.0062
0.8501
1.9646
1.2140
1.7740
1.2004
4.0180
8.0579

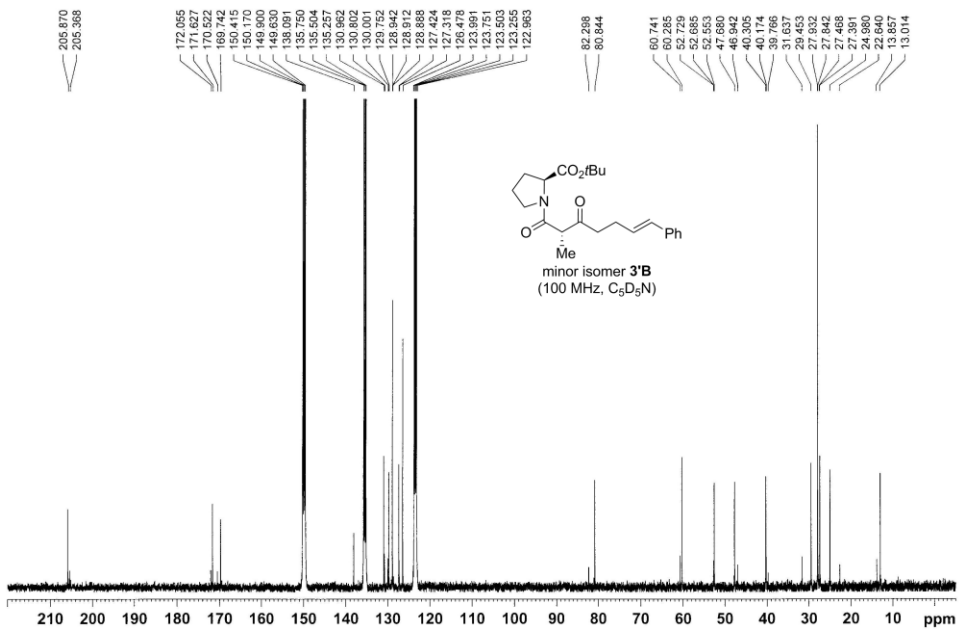
205.870
205.368
172.055
171.627
170.522
169.742
150.415
150.170
149.900
149.630
138.091
135.750
135.504
135.257
130.962
130.802
130.001
129.752
128.942
128.912
128.888
127.424
127.213
126.478
123.991
123.751
123.503
123.255
122.963
82.298
80.844
60.741
60.285
52.729
52.685
52.553
47.680
46.942
40.305
40.174
39.766
31.637
29.453
27.932
27.842
27.468
27.301
24.980
22.640
13.857
13.014
CO2tBu
N
O
O
Ph
Me
minor isomer 3'B
(100 MHz, C5D5N)
210 200 190 180 170 160 150 140 130 120 110 100 90 80 70 60 50 40 30 20 10 ppm

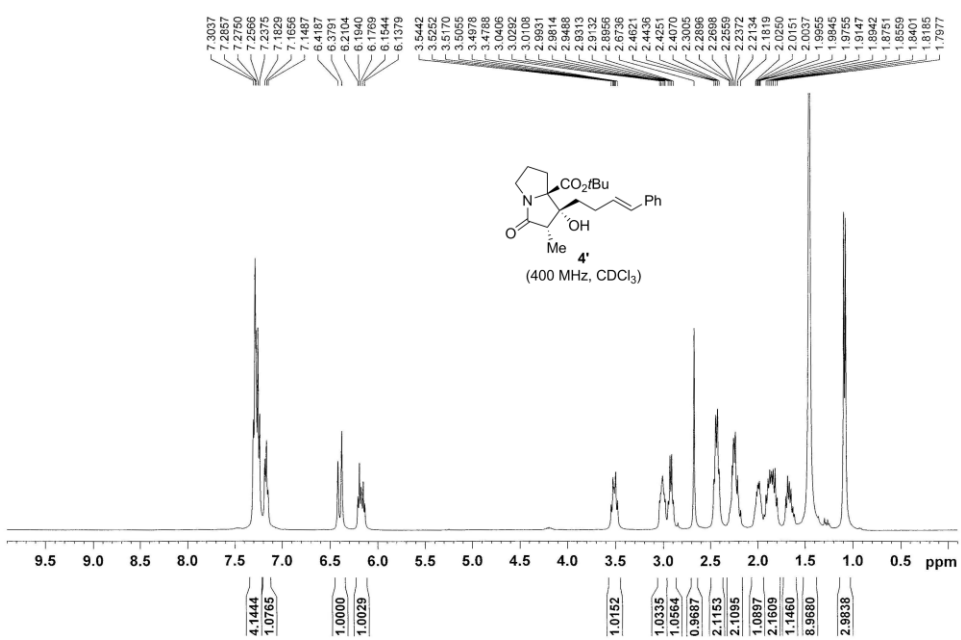
7.3037
7.2857
7.2760
7.2566
7.2375
7.1829
7.1656
7.1497
6.4187
6.3791
6.2104
6.1940
6.1789
6.1544
6.1379
3.5442
3.5252
3.5170
3.5055
3.4978
3.4788
3.0406
3.0292
3.0108
2.9931
2.9814
2.9488
2.9313
2.9132
2.8956
2.6736
2.4621
2.4436
2.4251
2.4070
2.3065
2.2886
2.2698
2.2559
2.2372
2.2134
2.1819
2.0250
2.0151
2.0037
1.9955
1.9845
1.9755
1.9147
1.8942
1.8751
1.8559
1.8401
1.8185
1.7977
CO2tBu
N
O
OH
Ph
Me
4'
(400 MHz, CDCl3)
9.5 9.0 8.5 8.0 7.5 7.0 6.5 6.0 5.5 5.0 4.5 4.0 3.5 3.0 2.5 2.0 1.5 1.0 0.5 ppm
4.1444
1.0765
1.0000
1.0029
1.0152
1.0335
1.0564
0.9687
2.1153
2.1095
1.0897
2.1609
1.1460
8.9680
2.9838

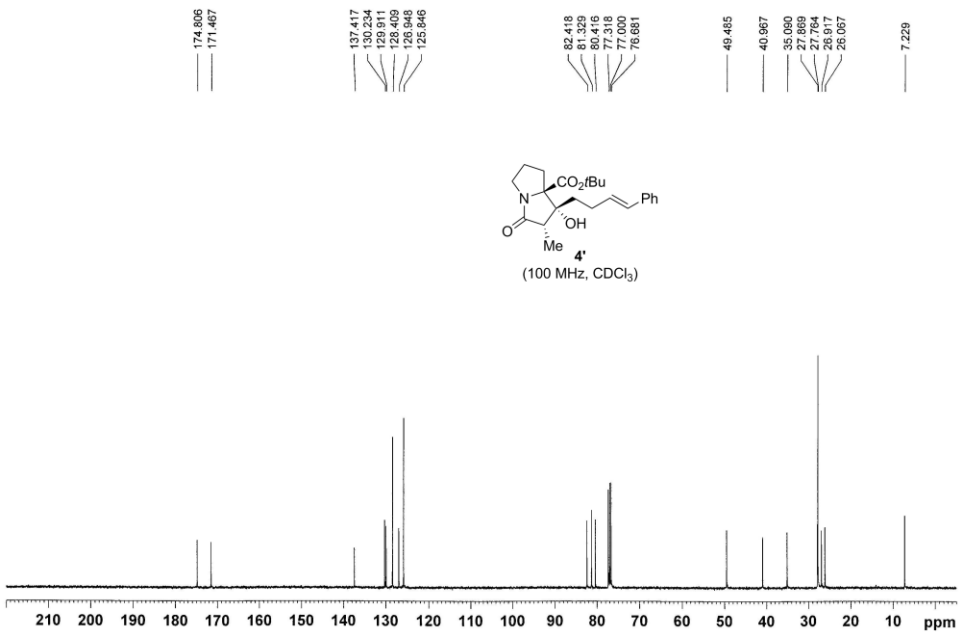
174.806
171.467
137.417
130.234
129.911
128.409
126.948
125.846
82.418
81.329
80.416
77.318
77.000
76.681
49.485
40.967
35.090
27.869
27.764
26.917
26.067
7.229
CO2tBu
N
Ph
OH
O
Me
4'
(100 MHz, CDCl3)
210 200 190 180 170 160 150 140 130 120 110 100 90 80 70 60 50 40 30 20 10 ppm

Appendix II

Spectra of Compounds
(Part B)

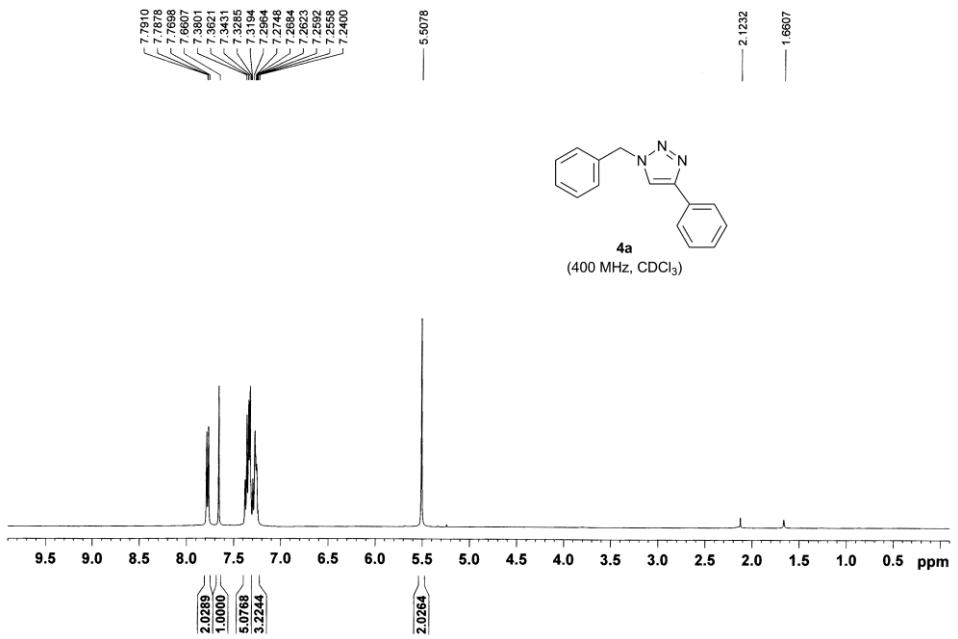
7.7910
7.7878
7.7698
7.6607
7.3801
7.3621
7.3431
7.3185
7.3164
7.2964
7.2748
7.2684
7.2623
7.2592
7.2558
7.2400
5.5078
2.1232
1.6607
4a
(400 MHz, CDCl3)
9.5 9.0 8.5 8.0 7.5 7.0 6.5 6.0 5.5 5.0 4.5 4.0 3.5 3.0 2.5 2.0 1.5 1.0 0.5 ppm
2.0289
1.0000
5.0768
3.2244
2.0264

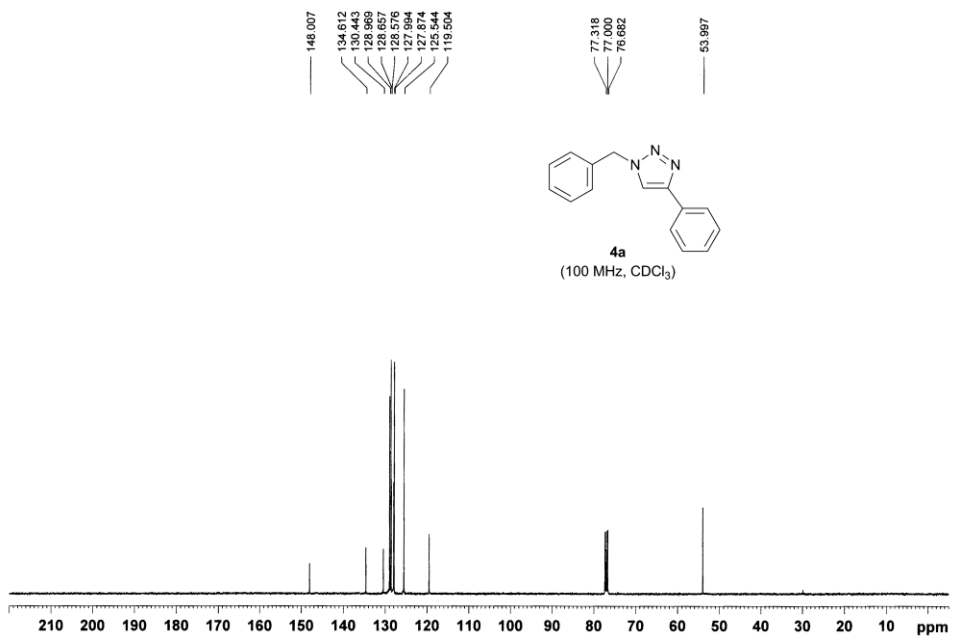
148.007
134.612
130.443
128.969
128.657
128.576
127.994
127.874
125.544
119.504
77.318
77.000
76.682
53.997
4a
(100 MHz, CDCl3)
210 200 190 180 170 160 150 140 130 120 110 100 90 80 70 60 50 40 30 20 10 ppm

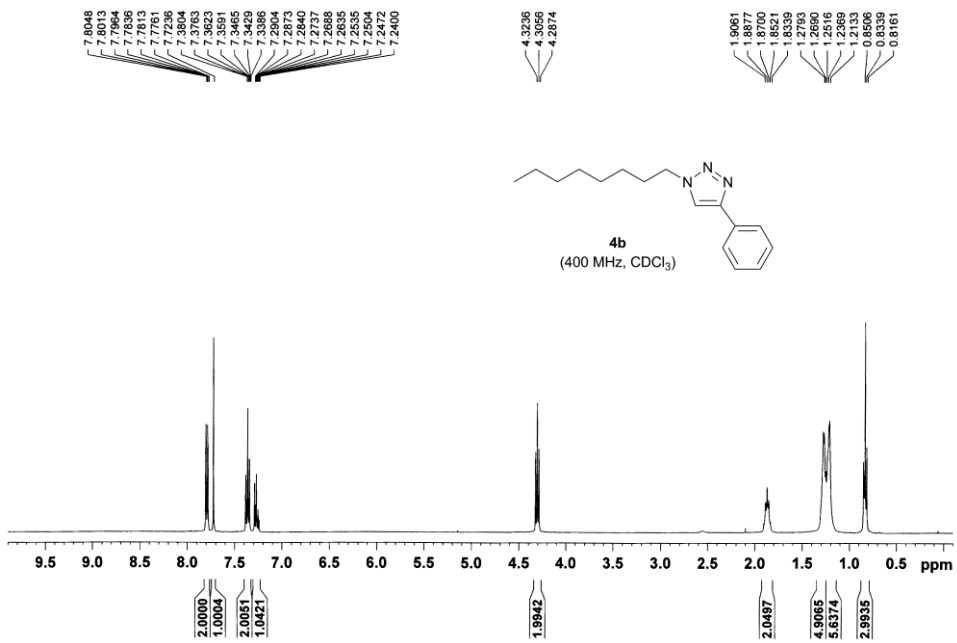
7.8048
7.8013
7.7964
7.7835
7.7813
7.7761
7.7236
7.3804
7.3763
7.3623
7.3591
7.3465
7.3429
7.3386
7.2904
7.2873
7.2840
7.2737
7.2688
7.2635
7.2535
7.2504
7.2472
7.2460
4.3236
4.3056
4.2874
1.9061
1.8877
1.8700
1.8521
1.8339
1.2703
1.2680
1.2516
1.2369
1.2133
0.8506
0.8339
0.8161
4b
(400 MHz, CDCl3)
9.5 9.0 8.5 8.0 7.5 7.0 6.5 6.0 5.5 5.0 4.5 4.0 3.5 3.0 2.5 2.0 1.5 1.0 0.5 ppm
2.0000
1.0004
2.0051
1.0421
1.9942
2.0497
4.9065
5.6374
2.9935

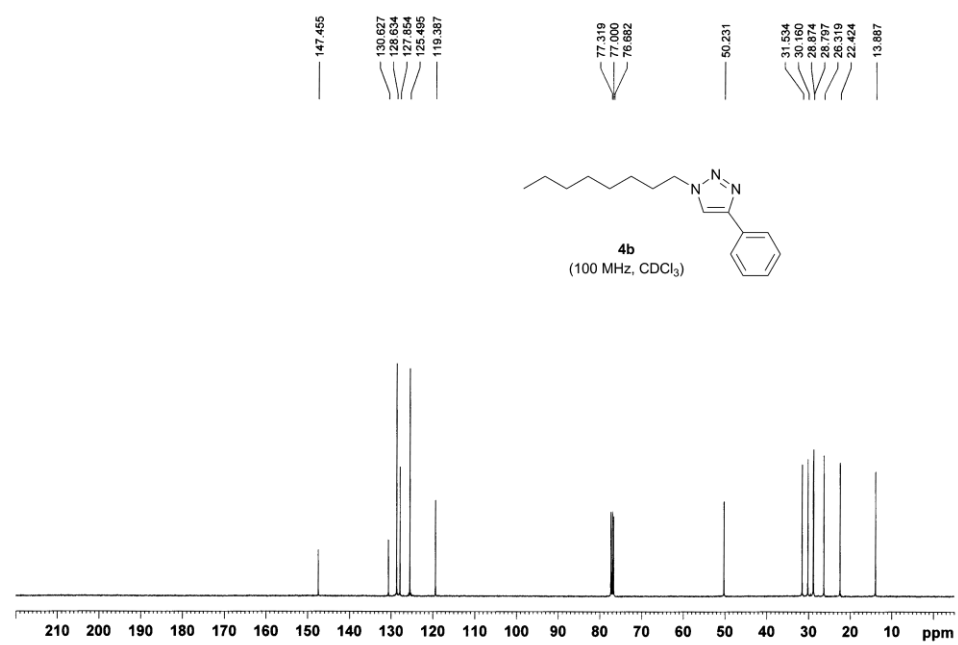
147.455
130.627
128.634
127.854
125.495
119.387
77.319
77.000
76.682
50.231
31.534
30.160
28.874
28.797
26.319
22.424
13.887
4b
(100 MHz, CDCl3)
210 200 190 180 170 160 150 140 130 120 110 100 90 80 70 60 50 40 30 20 10 ppm

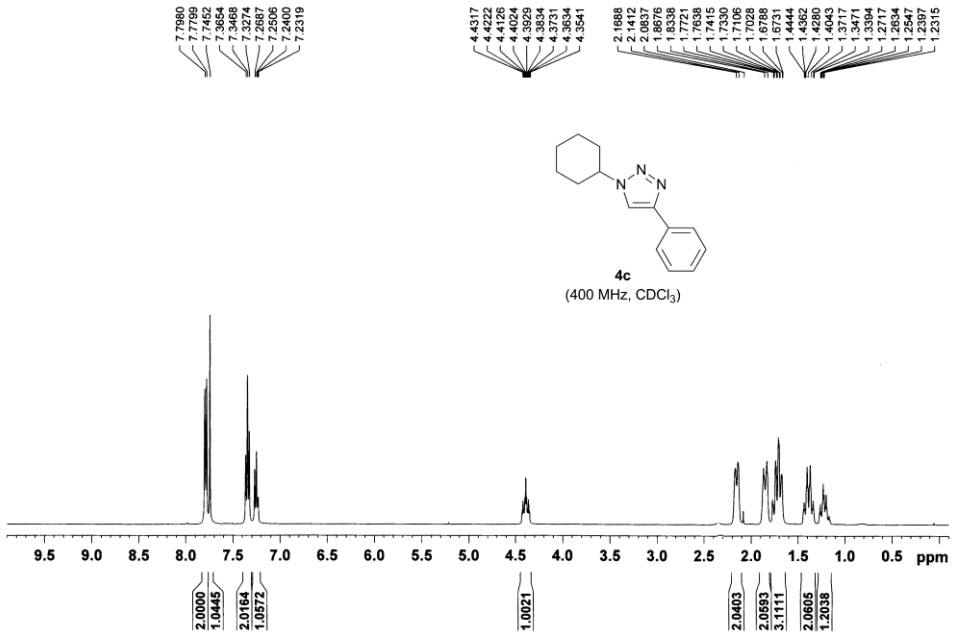
7.7980
7.7799
7.7452
7.3654
7.3468
7.3274
7.2687
7.2506
7.2400
7.2319
4.4317
4.4122
4.4026
4.4024
4.3929
4.3834
4.3731
4.3634
4.3541
2.1688
2.1412
2.0837
1.8676
1.8338
1.7721
1.7638
1.7415
1.7330
1.7106
1.7028
1.6788
1.6731
1.4444
1.4362
1.4280
1.4043
1.3717
1.3471
1.3394
1.2717
1.2634
1.2547
1.2397
1.2315
4c
(400 MHz, CDCl3)
9.5 9.0 8.5 8.0 7.5 7.0 6.5 6.0 5.5 5.0 4.5 4.0 3.5 3.0 2.5 2.0 1.5 1.0 0.5 ppm
2.0000
1.0445
2.0164
1.0572
1.0021
2.0403
2.0593
3.1111
2.0605
1.2038

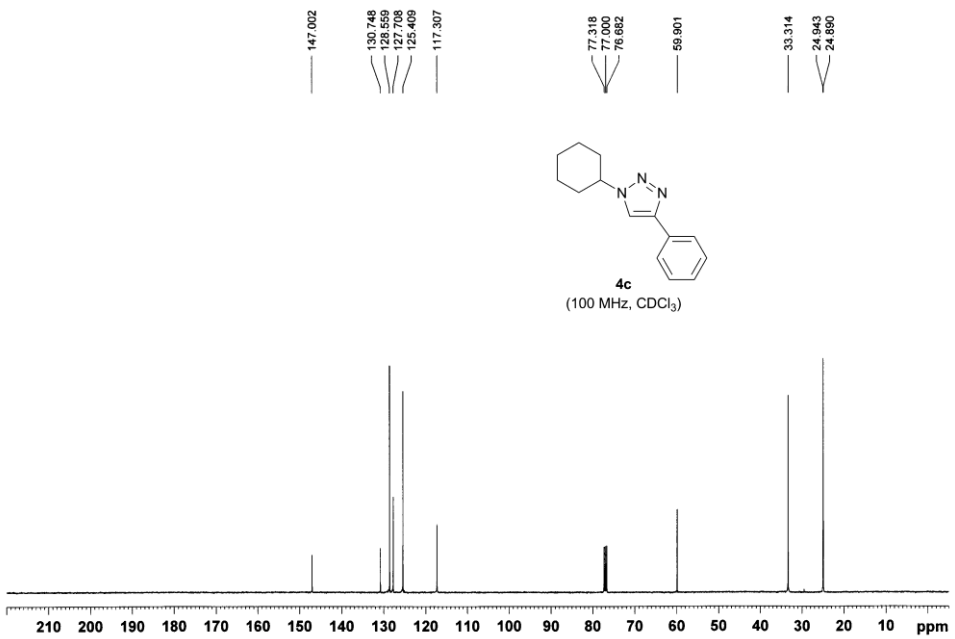
147.002
130.748
128.559
127.708
125.409
117.307
77.318
77.000
76.682
59.901
33.314
24.943
24.890
4c
(100 MHz, CDCl3)
210 200 190 180 170 160 150 140 130 120 110 100 90 80 70 60 50 40 30 20 10 ppm

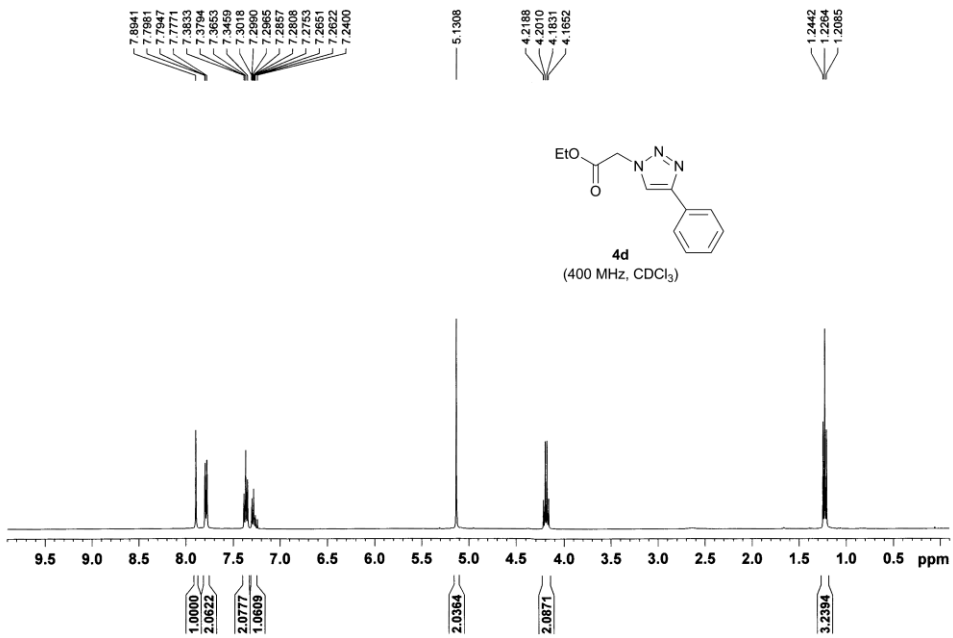
7.8941
7.7981
7.7947
7.7771
7.3833
7.3794
7.3653
7.3459
7.3018
7.2990
7.2965
7.2857
7.2808
7.2753
7.2651
7.2622
7.2400
5.1308
4.2188
4.2010
4.1831
4.1652
1.2442
1.2264
1.2085
EtO
O
N
N
N
4d
(400 MHz, CDCl3)
9.5 9.0 8.5 8.0 7.5 7.0 6.5 6.0 5.5 5.0 4.5 4.0 3.5 3.0 2.5 2.0 1.5 1.0 0.5 ppm
1.0000
2.0622
2.0777
1.0609
2.0364
2.0871
3.2394

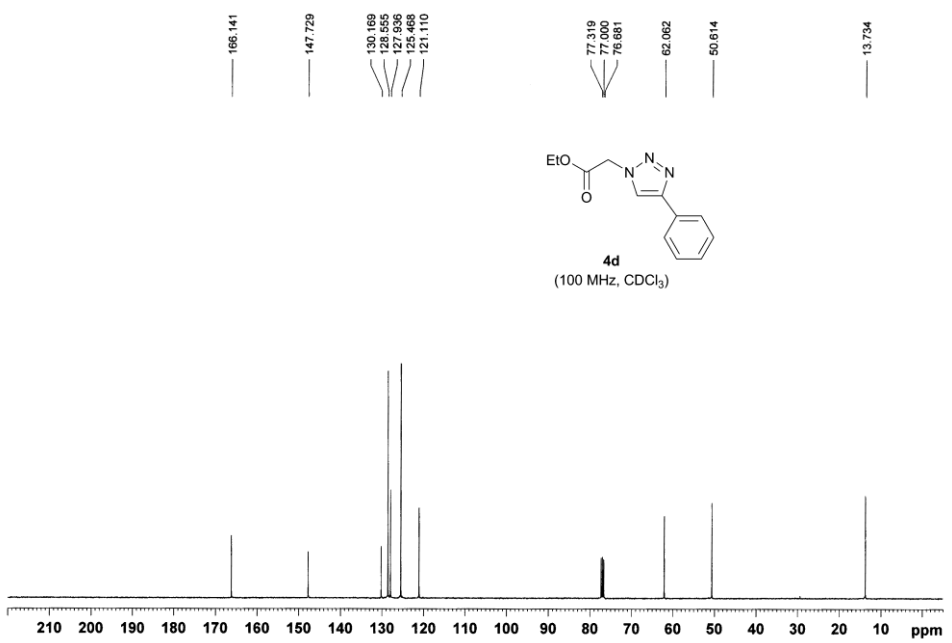
166.141
147.729
130.169
128.555
127.936
125.488
121.110
77.319
77.000
76.681
62.062
50.614
13.734
EtO
O
N
N
N
4d
(100 MHz, CDCl3)
210 200 190 180 170 160 150 140 130 120 110 100 90 80 70 60 50 40 30 20 10 ppm

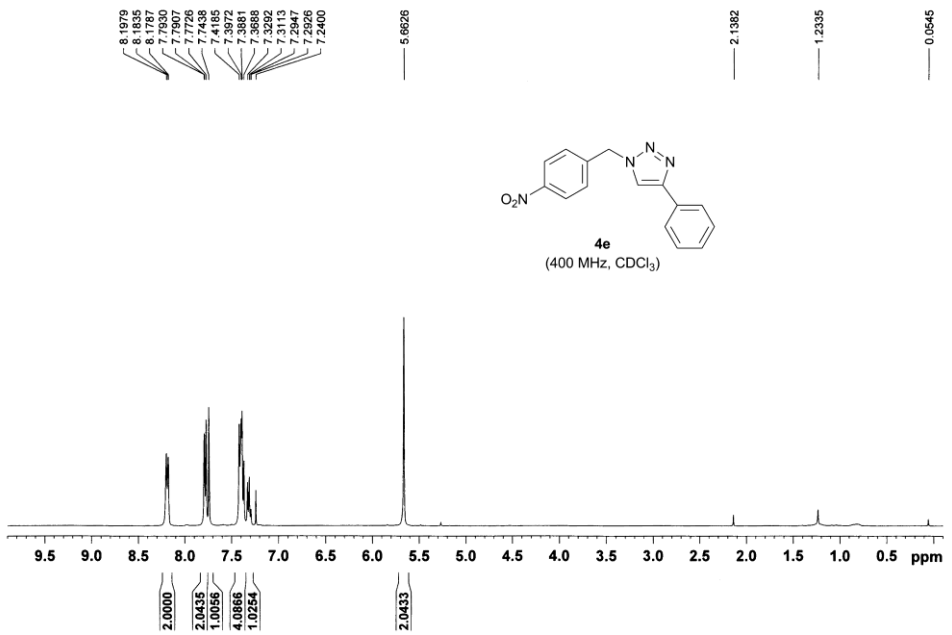
8.1979
8.1835
7.7737
7.7930
7.7907
7.7726
7.7438
7.4185
7.3972
7.3881
7.3688
7.3292
7.3113
7.2947
7.2926
7.2400
5.6626
2.1382
1.2335
0.0545
O2N
4e
(400 MHz, CDCl3)
9.5 9.0 8.5 8.0 7.5 7.0 6.5 6.0 5.5 5.0 4.5 4.0 3.5 3.0 2.5 2.0 1.5 1.0 0.5 ppm
2.0000
2.0435
1.0056
4.0866
1.0254
2.0433

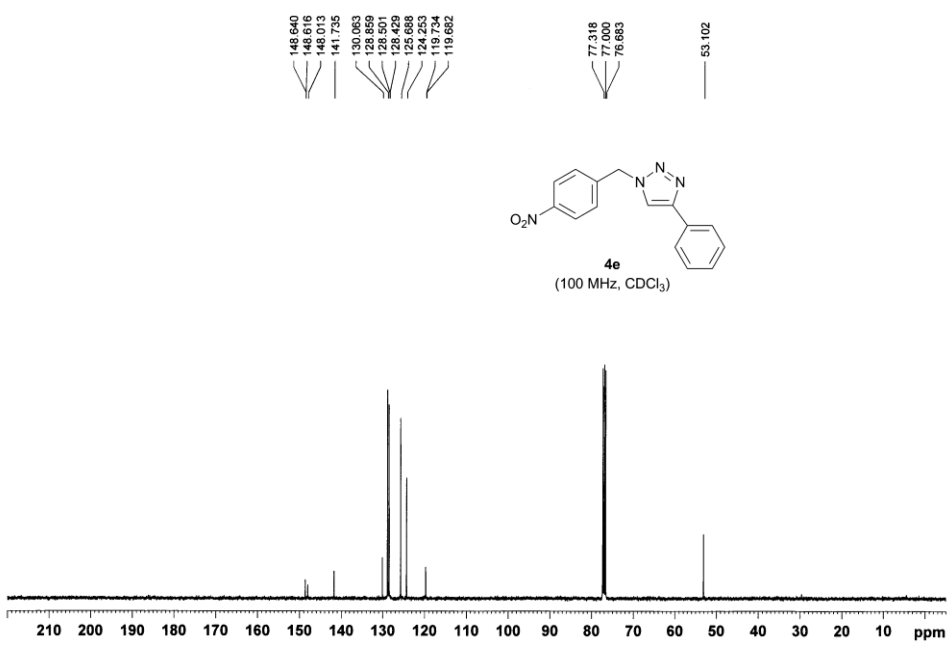
148.640
148.616
148.013
141.735
130.063
128.859
128.501
128.429
125.688
124.253
119.734
119.682
77.318
77.000
76.683
53.102
O2N
4e
(100 MHz, CDCl3)
210 200 190 180 170 160 150 140 130 120 110 100 90 80 70 60 50 40 30 20 10 ppm

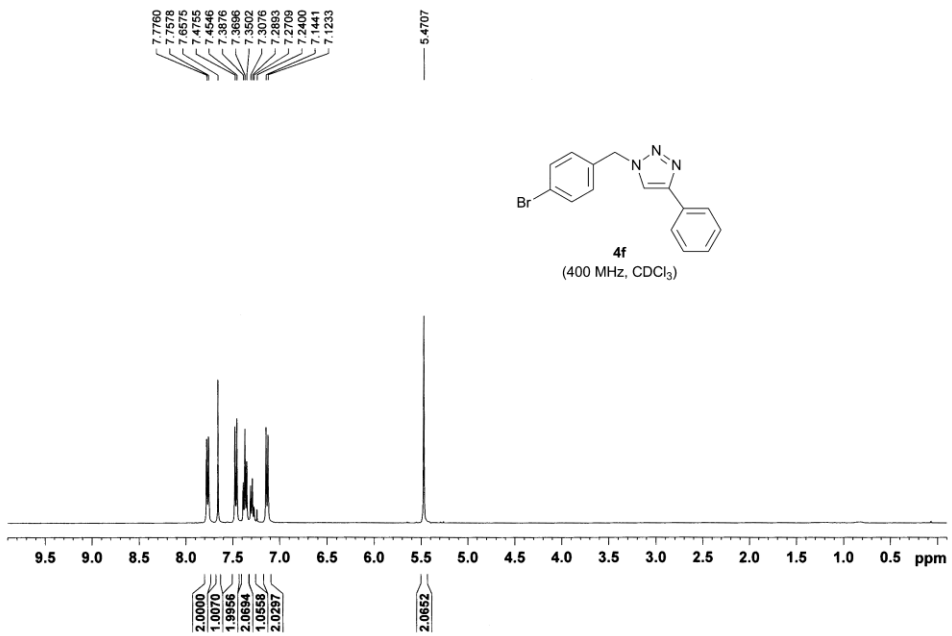
7.7760
7.7578
7.6575
7.4755
7.4546
7.3876
7.3696
7.3502
7.3076
7.2893
7.2709
7.2400
7.1441
7.1233
5.4707
Br
N
N
N
4f
(400 MHz, CDCl3)
9.5 9.0 8.5 8.0 7.5 7.0 6.5 6.0 5.5 5.0 4.5 4.0 3.5 3.0 2.5 2.0 1.5 1.0 0.5 ppm
2.0000
1.0070
1.9956
2.0694
1.0558
2.0297
2.0652

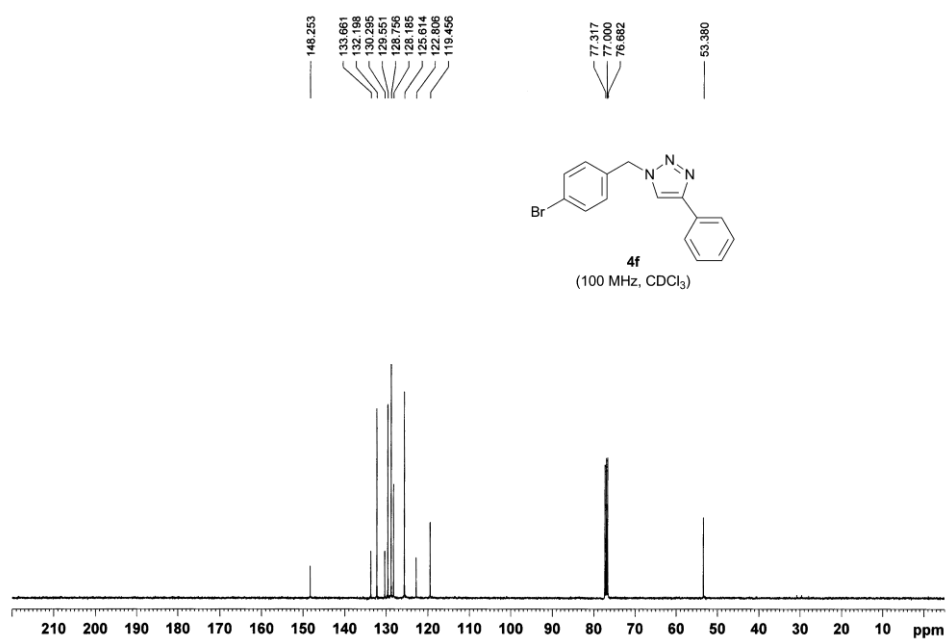
148.253
133.661
132.198
130.295
129.551
128.756
128.185
125.614
122.806
119.456
77.317
77.000
76.682
53.380
Br
N
N
N
4f
(100 MHz, CDCl3)
210 200 190 180 170 160 150 140 130 120 110 100 90 80 70 60 50 40 30 20 10 ppm

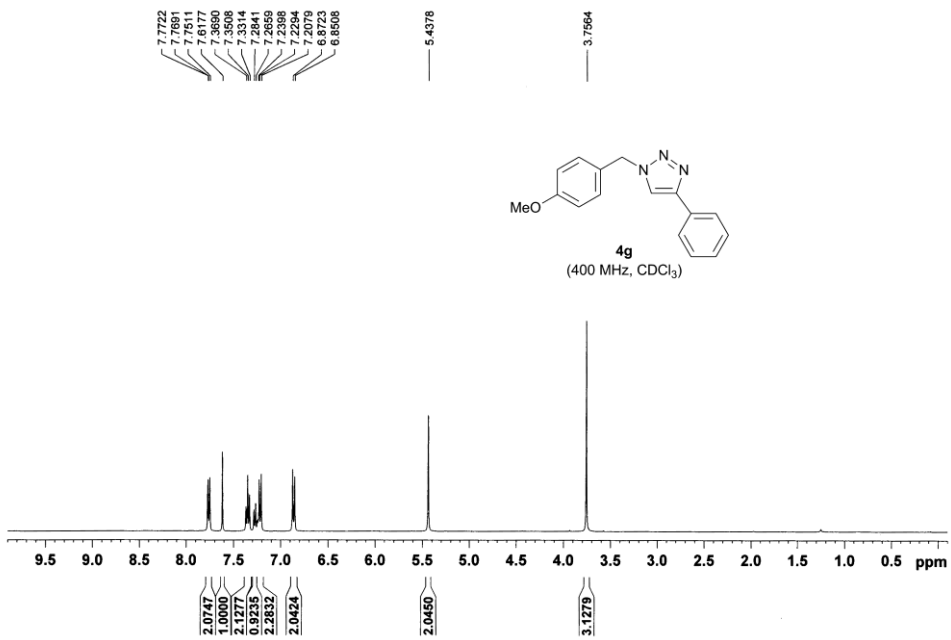
7.7722
7.7691
7.7511
7.6177
7.3690
7.3508
7.3314
7.2841
7.2659
7.2398
7.2294
7.2079
6.8723
6.8508
5.4378
3.7564
MeO
N
N
N
4g
(400 MHz, CDCl3)
9.5 9.0 8.5 8.0 7.5 7.0 6.5 6.0 5.5 5.0 4.5 4.0 3.5 3.0 2.5 2.0 1.5 1.0 0.5 ppm
2.0747
1.0000
2.1277
0.9235
2.2832
2.0424
2.0450
3.1279

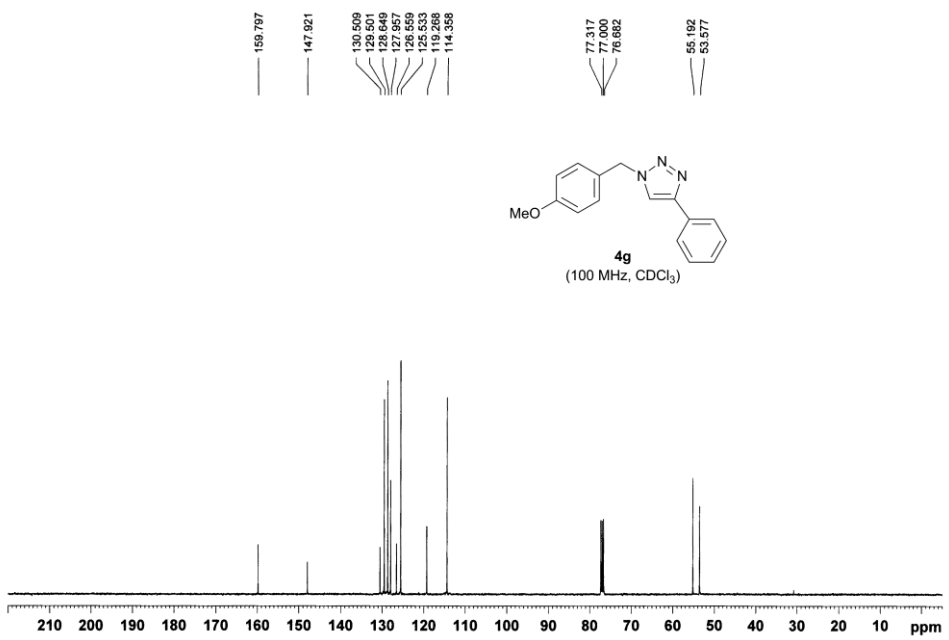
159.797
147.921
130.509
129.501
128.649
127.957
126.559
125.533
119.268
114.358
77.317
77.000
76.682
55.192
53.577
MeO
N
N
N
4g
(100 MHz, CDCl3)
210 200 190 180 170 160 150 140 130 120 110 100 90 80 70 60 50 40 30 20 10 ppm

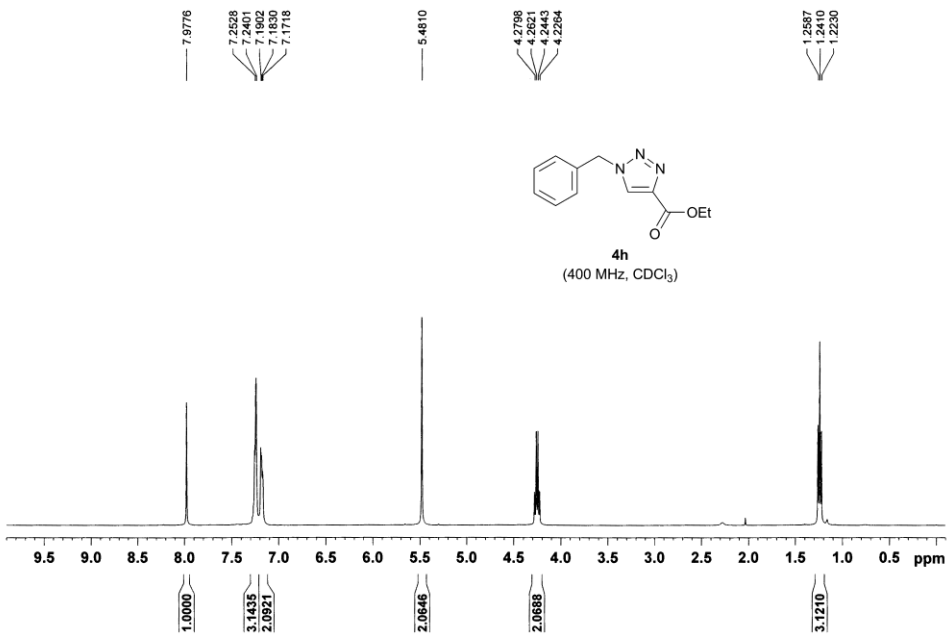
7.9776
7.2528
7.2401
7.1692
7.1630
7.1718
5.4810
4.2798
4.2621
4.2443
4.2264
1.2587
1.2410
1.2230
OEt
O
4h
(400 MHz, CDCl3)
9.5 9.0 8.5 8.0 7.5 7.0 6.5 6.0 5.5 5.0 4.5 4.0 3.5 3.0 2.5 2.0 1.5 1.0 0.5 ppm
1.0000
3.1435
2.0921
2.0646
2.0688
3.1210

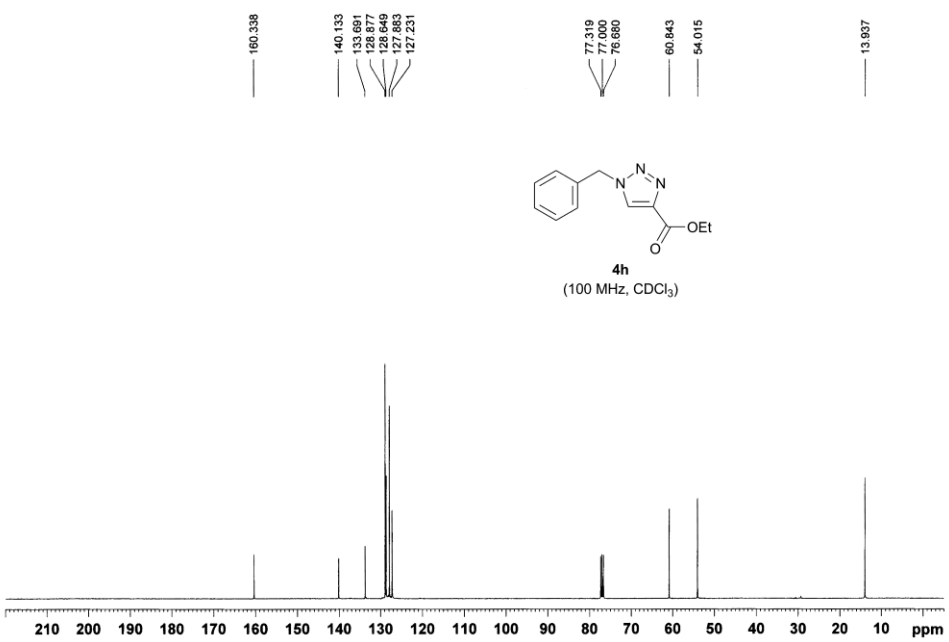
160.338
140.133
133.691
128.877
128.649
127.883
127.231
77.319
77.000
76.680
60.843
54.015
13.937
OEt
O
4h
(100 MHz, CDCl3)
210 200 190 180 170 160 150 140 130 120 110 100 90 80 70 60 50 40 30 20 10 ppm

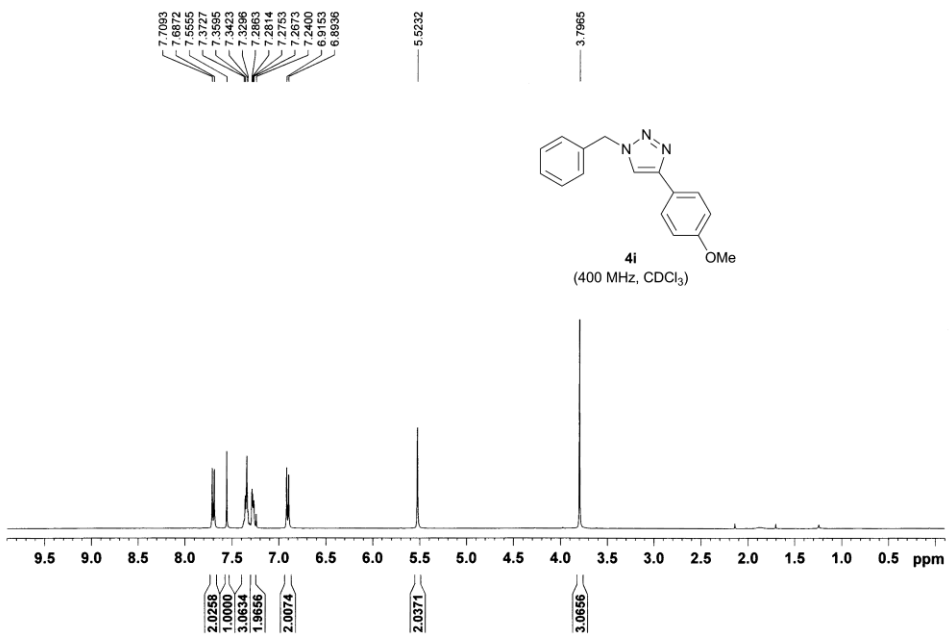
7.7093
7.6872
7.5555
7.3727
7.3595
7.3423
7.3296
7.2863
7.2814
7.2753
7.2673
7.2400
6.9153
6.8936
5.5232
3.7965
4i
(400 MHz, CDCl3)
9.5 9.0 8.5 8.0 7.5 7.0 6.5 6.0 5.5 5.0 4.5 4.0 3.5 3.0 2.5 2.0 1.5 1.0 0.5 ppm
2.0258
1.0000
3.0634
1.9656
2.0074
2.0371
3.0656

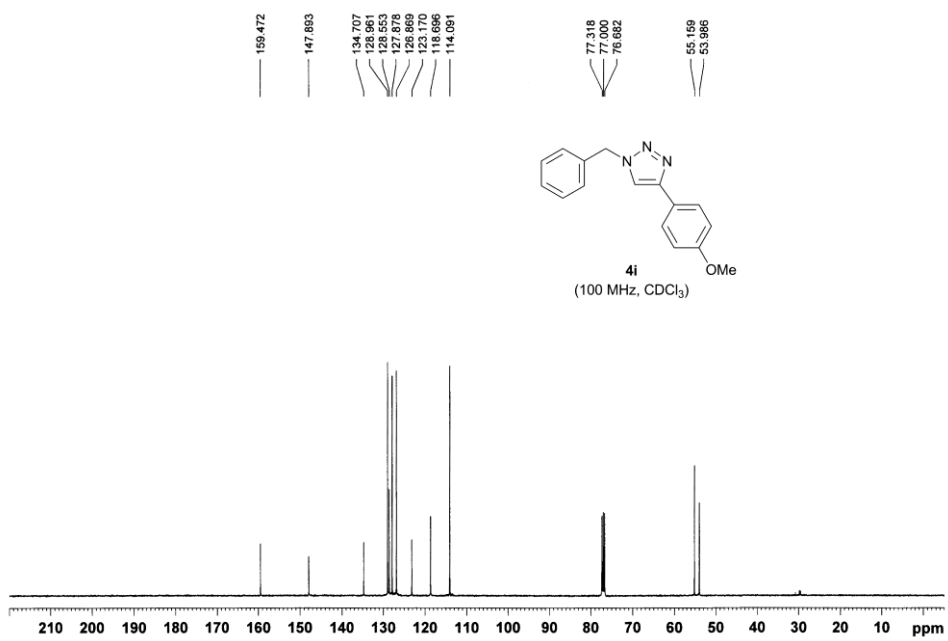
159.472
147.893
134.707
128.961
128.553
127.878
126.869
123.170
118.696
114.091
77.318
77.000
76.682
55.159
53.986
4i
(100 MHz, CDCl3)
210 200 190 180 170 160 150 140 130 120 110 100 90 80 70 60 50 40 30 20 10 ppm

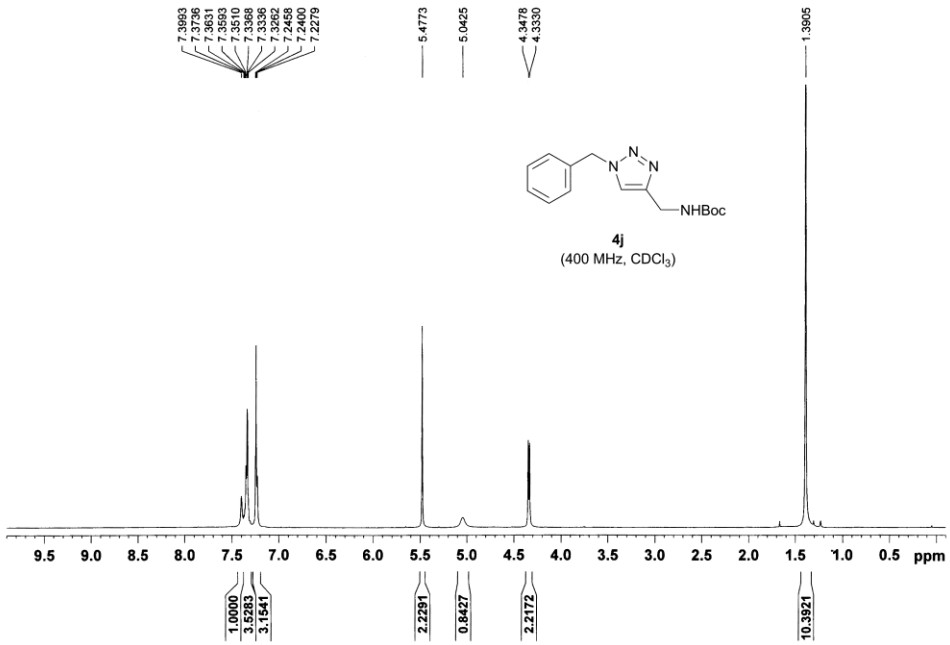
7.3993
7.3736
7.3631
7.3593
7.3510
7.3388
7.3336
7.3262
7.2458
7.2400
7.2279
5.4773
5.0425
4.3478
4.3330
1.3905
NHBoc
4j
(400 MHz, CDCl3)
9.5 9.0 8.5 8.0 7.5 7.0 6.5 6.0 5.5 5.0 4.5 4.0 3.5 3.0 2.5 2.0 1.5 1.0 0.5 ppm
1.0000
3.5283
3.1541
2.2291
0.8427
2.2172
10.3921

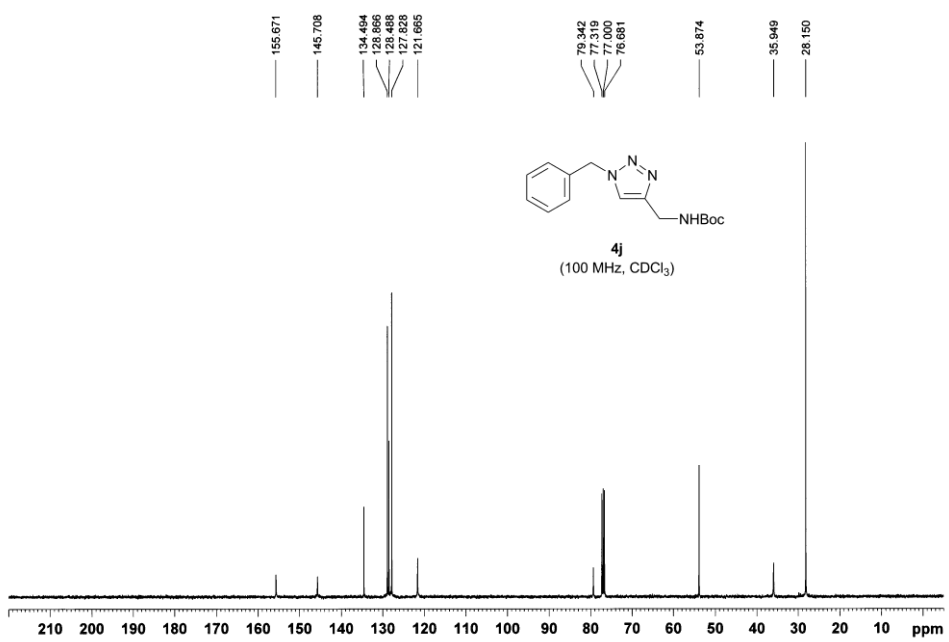
155.671
145.708
134.494
128.866
128.488
127.828
121.665
79.342
77.319
77.000
76.681
53.874
35.949
28.150
NHBoc
4j
(100 MHz, CDCl3)
210 200 190 180 170 160 150 140 130 120 110 100 90 80 70 60 50 40 30 20 10 ppm

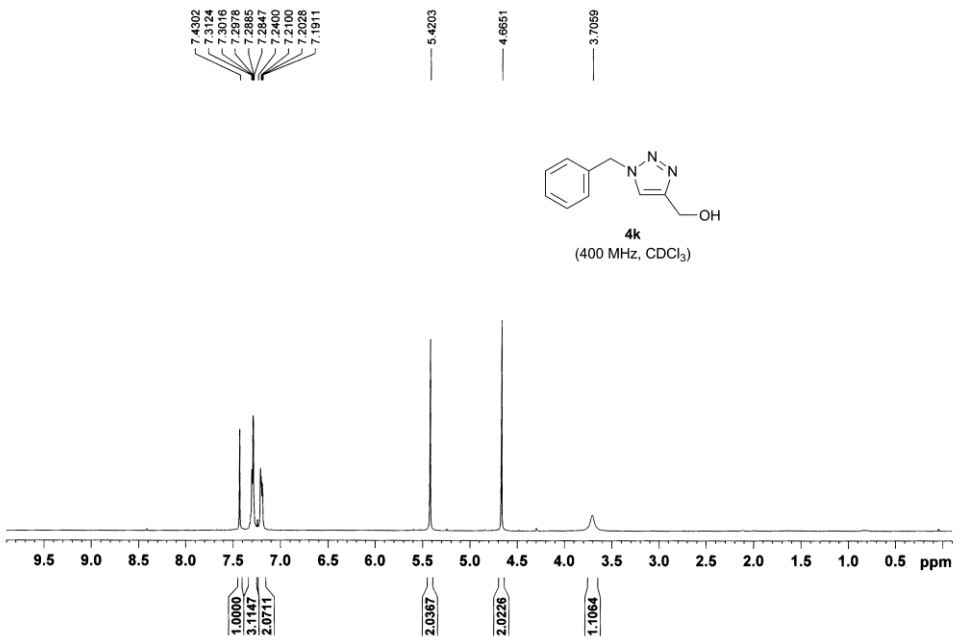
7.4302
7.3124
7.3016
7.2978
7.2885
7.2847
7.2400
7.2100
7.2028
7.1911
5.4203
4.6651
3.7059
OH
4k
(400 MHz, CDCl3)
9.5 9.0 8.5 8.0 7.5 7.0 6.5 6.0 5.5 5.0 4.5 4.0 3.5 3.0 2.5 2.0 1.5 1.0 0.5 ppm
1.0000
3.1147
2.0711
2.0367
2.0226
1.1064

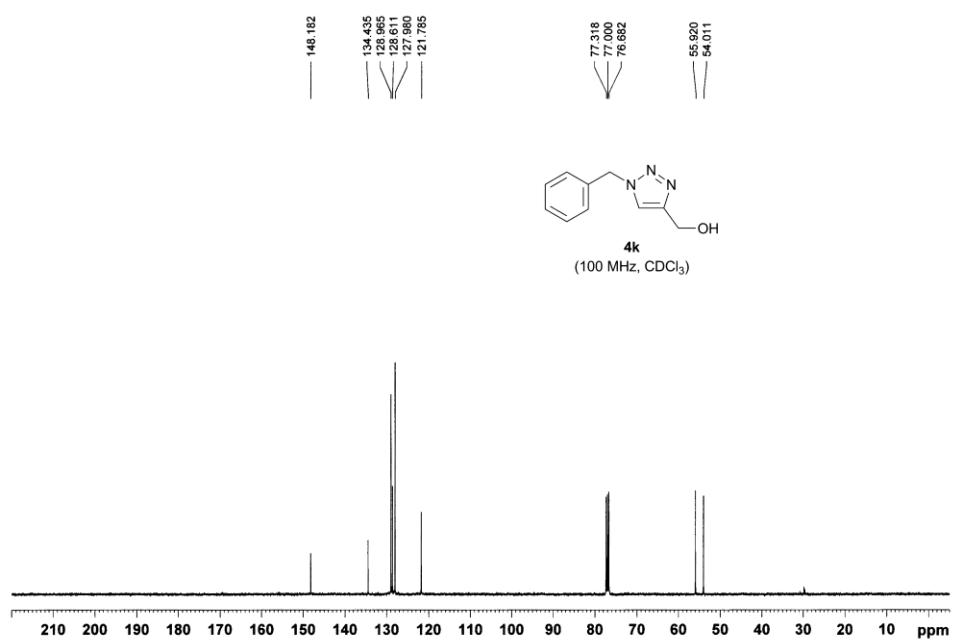
148.182
134.435
128.865
128.611
127.980
121.785
77.318
77.000
76.682
55.920
54.011
OH
4k
(100 MHz, CDCl3)
210 200 190 180 170 160 150 140 130 120 110 100 90 80 70 60 50 40 30 20 10 ppm

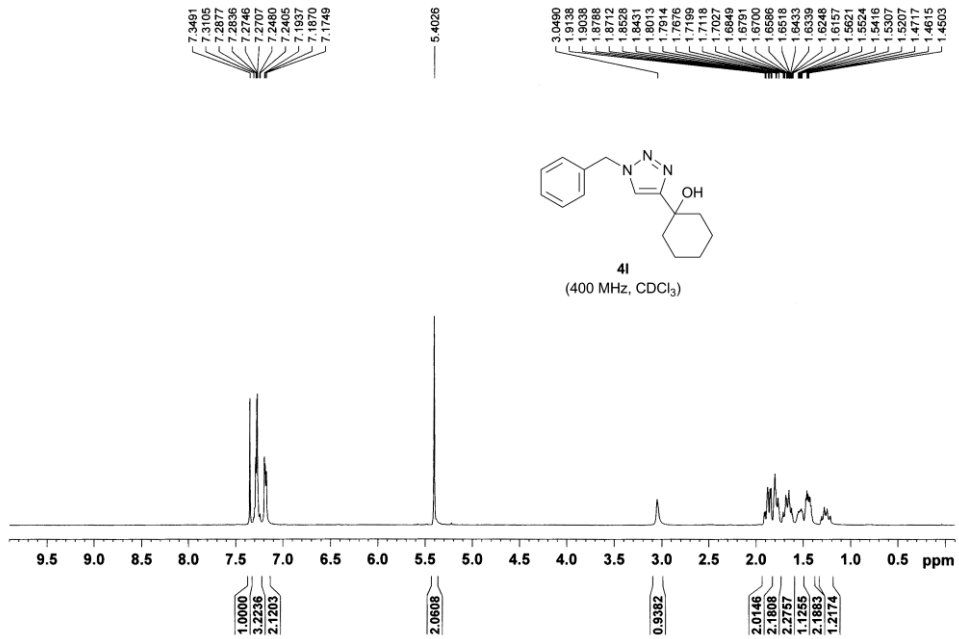
7.3491
7.3105
7.2877
7.2836
7.2746
7.2707
7.2480
7.2405
7.1937
7.1870
7.1749
5.4026
3.0490
1.9138
1.9038
1.8788
1.8712
1.8528
1.8431
1.8013
1.7914
1.7676
1.7199
1.7118
1.7027
1.6849
1.6791
1.6700
1.6586
1.6518
1.6433
1.6339
1.6248
1.6157
1.5621
1.5524
1.5416
1.5307
1.5207
1.4717
1.4615
1.4503
OH
4l
(400 MHz, CDCl3)
9.5 9.0 8.5 8.0 7.5 7.0 6.5 6.0 5.5 5.0 4.5 4.0 3.5 3.0 2.5 2.0 1.5 1.0 0.5 ppm
1.0000
3.2236
2.1203
2.0608
0.9382
2.0146
2.1808
2.2757
1.1255
2.1883
1.2174

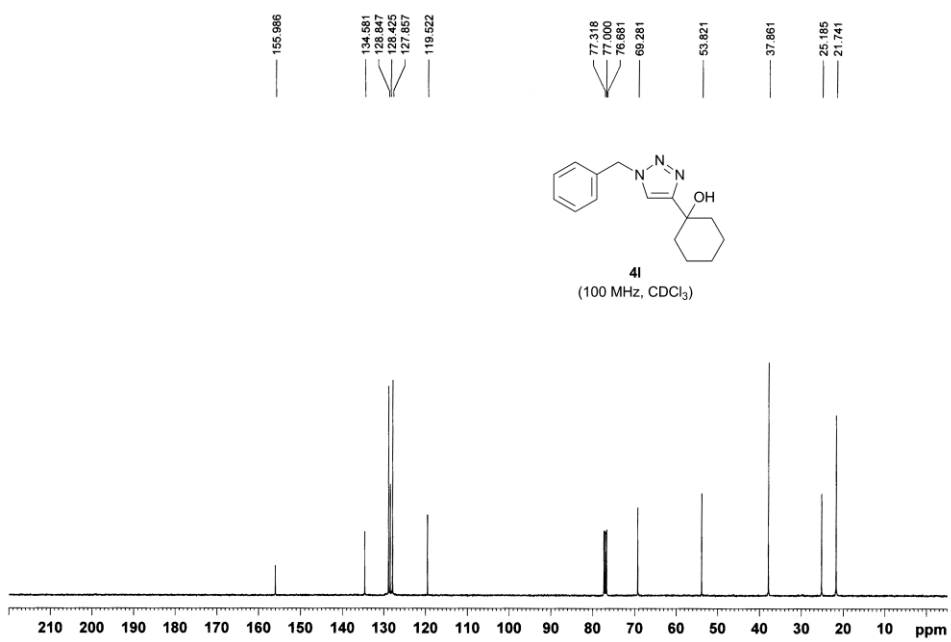
155.986
134.581
129.447
128.425
127.857
119.522
77.318
77.000
76.681
69.281
53.821
37.861
25.185
21.741
OH
4l
(100 MHz, CDCl3)
210 200 190 180 170 160 150 140 130 120 110 100 90 80 70 60 50 40 30 20 10 ppm

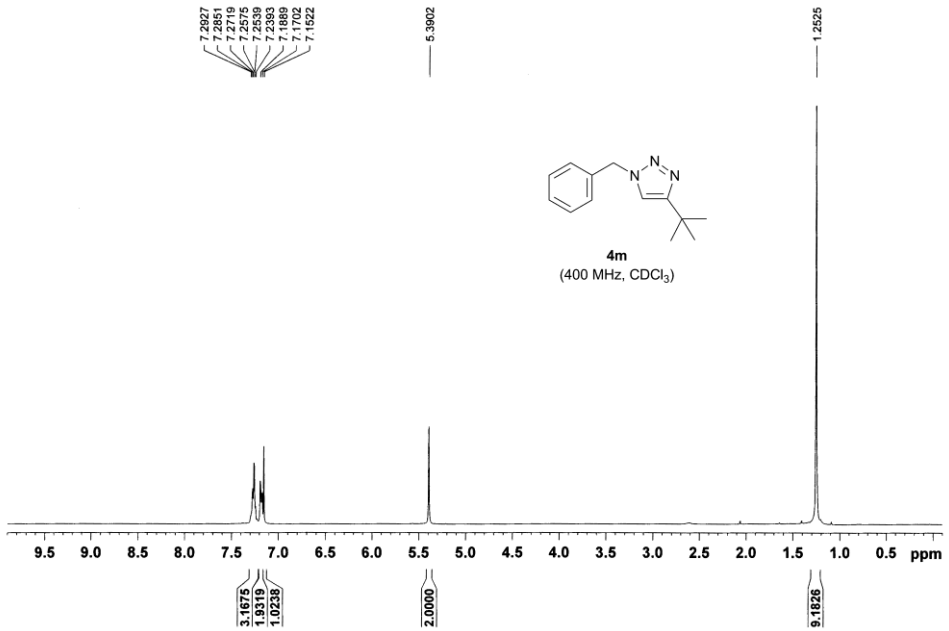
7.2927
7.2851
7.2710
7.2575
7.2539
7.2393
7.1889
7.1702
7.1522
5.3902
1.2525
4m
(400 MHz, CDCl3)
9.5 9.0 8.5 8.0 7.5 7.0 6.5 6.0 5.5 5.0 4.5 4.0 3.5 3.0 2.5 2.0 1.5 1.0 0.5 ppm
3.1675
1.9319
1.0238
2.0000
9.1826

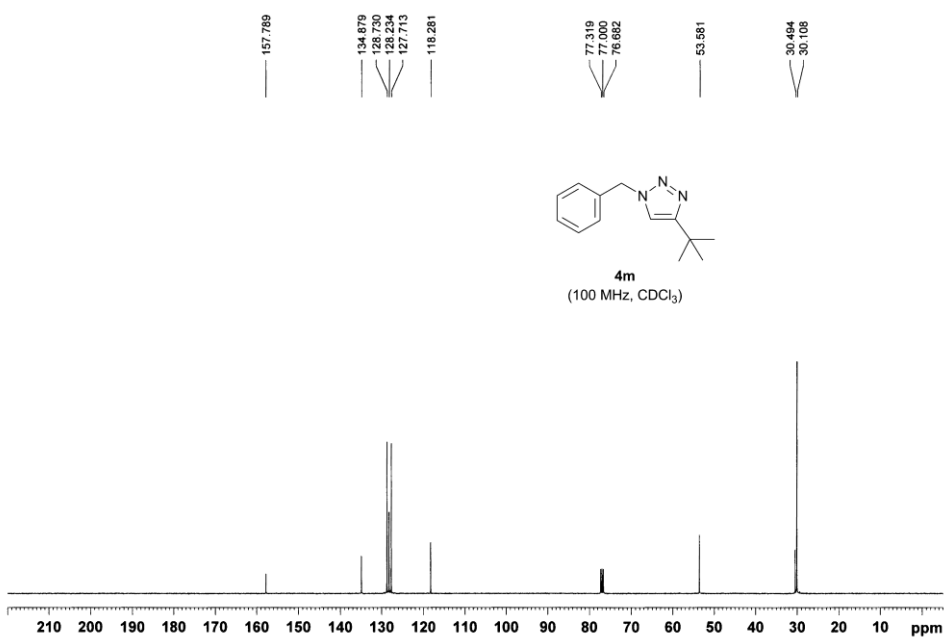
157.789
134.879
128.730
128.234
127.713
118.281
77.319
77.000
76.682
53.581
30.494
30.108
4m
(100 MHz, CDCl3)
210 200 190 180 170 160 150 140 130 120 110 100 90 80 70 60 50 40 30 20 10 ppm

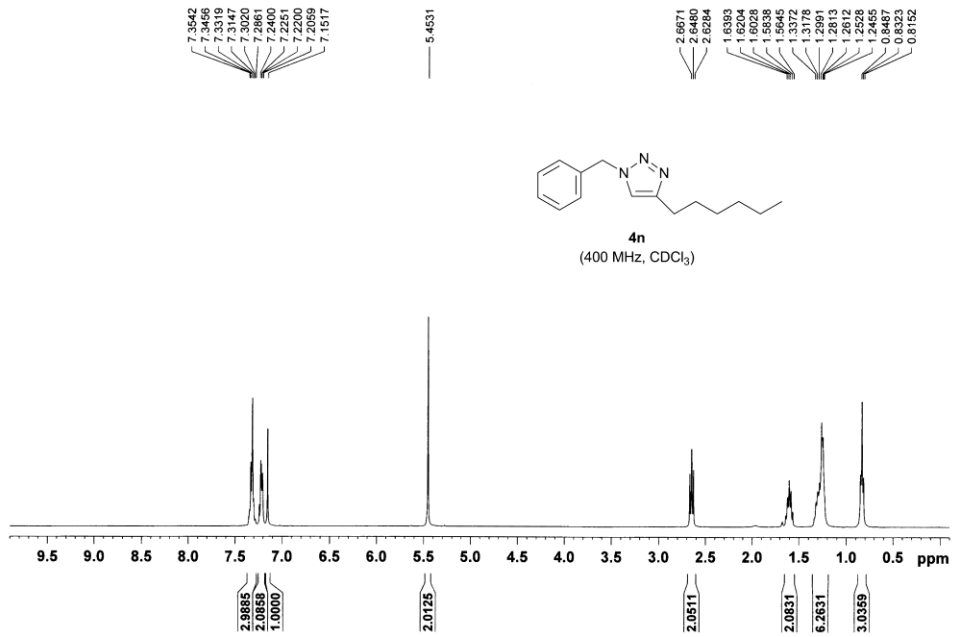
7.3542
7.3456
7.3319
7.3147
7.3020
7.2861
7.2400
7.2251
7.2200
7.2059
7.1517
5.4531
2.6671
2.6480
2.6284
1.6393
1.6204
1.6028
1.5838
1.5645
1.3372
1.3178
1.2991
1.2813
1.2612
1.2528
1.2455
0.8487
0.8323
0.8152
4n
(400 MHz, CDCl3)
9.5 9.0 8.5 8.0 7.5 7.0 6.5 6.0 5.5 5.0 4.5 4.0 3.5 3.0 2.5 2.0 1.5 1.0 0.5 ppm
2.9885
2.0858
1.0000
2.0125
2.0511
2.0831
6.2631
3.0359

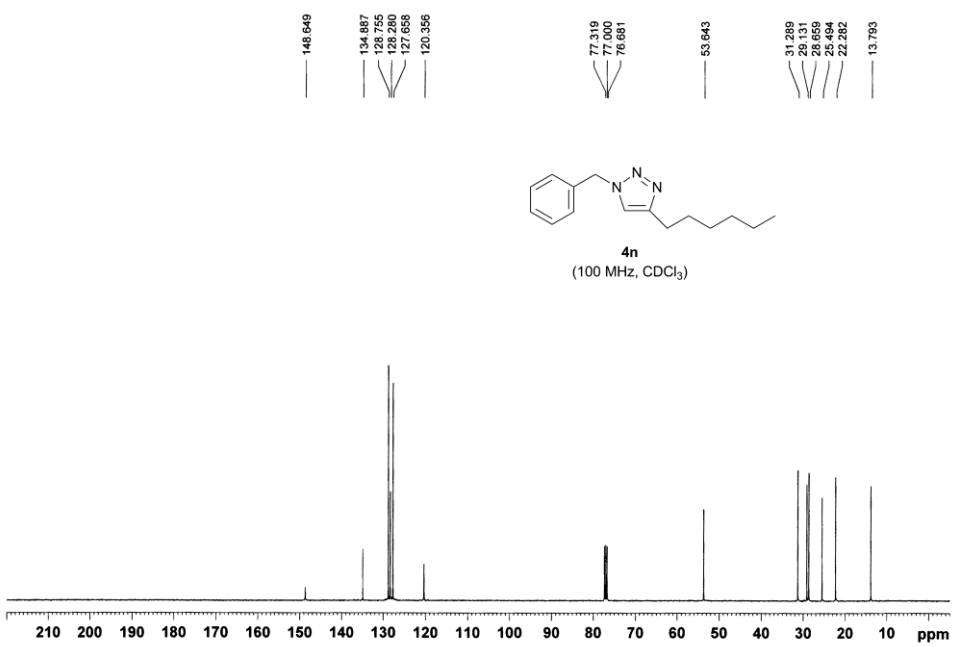
148.649
134.887
128.755
128.280
127.658
120.356
77.319
77.000
76.681
53.643
31.289
29.131
28.659
25.494
22.282
13.793
4n
(100 MHz, CDCl3)
210 200 190 180 170 160 150 140 130 120 110 100 90 80 70 60 50 40 30 20 10 ppm

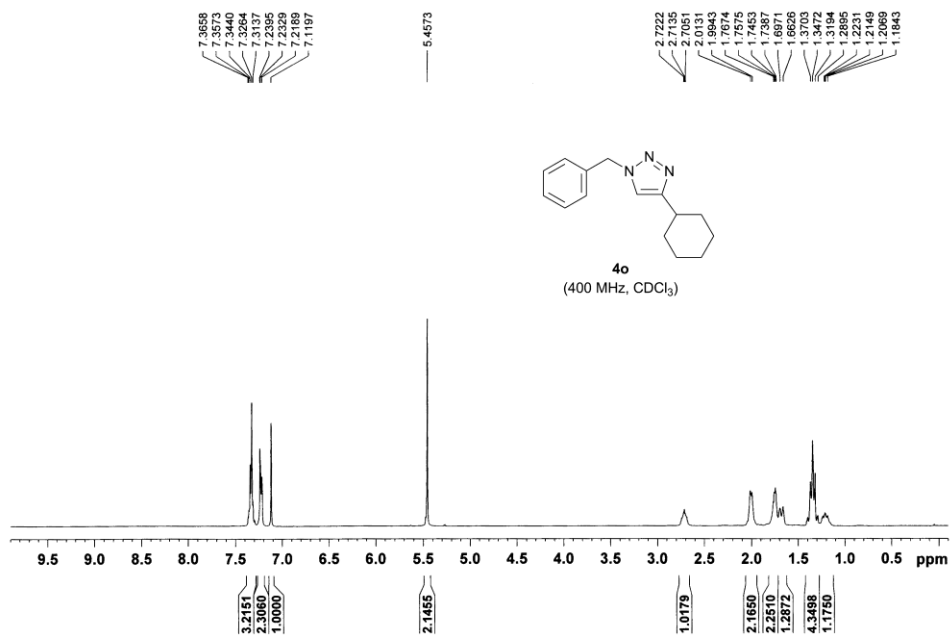
7.3658
7.3573
7.3440
7.3264
7.3137
7.2395
7.2329
7.2189
7.1197
5.4573
2.7222
2.7135
2.7051
2.6013
1.9943
1.7674
1.7575
1.7453
1.7387
1.6971
1.6626
1.3703
1.3472
1.3194
1.2895
1.2231
1.2149
1.2069
1.1643
4o
(400 MHz, CDCl3)
9.5 9.0 8.5 8.0 7.5 7.0 6.5 6.0 5.5 5.0 4.5 4.0 3.5 3.0 2.5 2.0 1.5 1.0 0.5 ppm
3.2151
2.3060
1.0000
2.1455
1.0179
2.1650
2.2510
1.2872
4.3498
1.1750

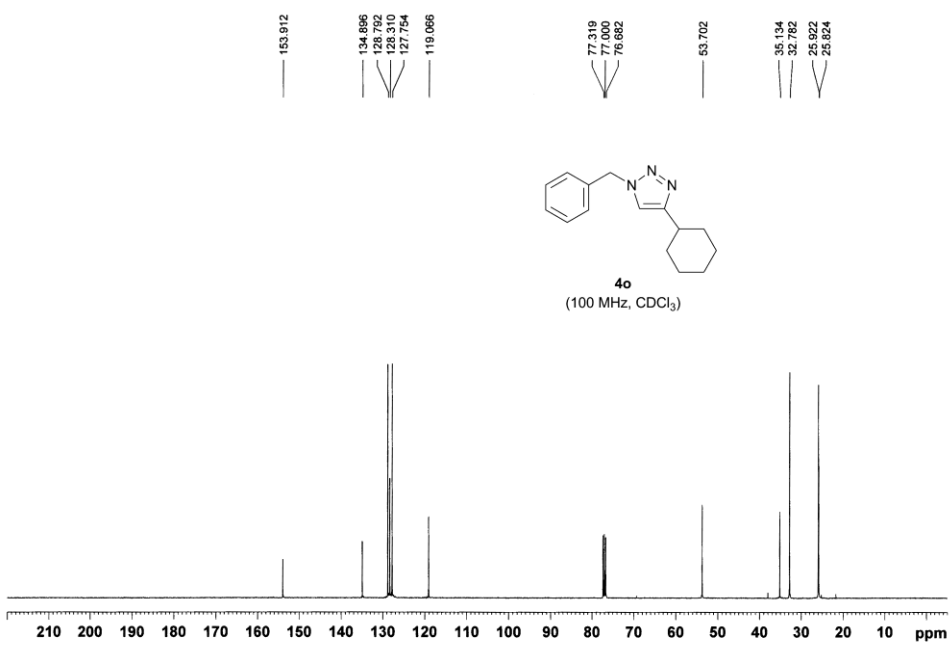
153.912
134.896
128.792
128.310
127.754
119.066
77.319
77.000
76.682
53.702
35.134
32.782
25.922
25.824
4o
(100 MHz, CDCl3)
210 200 190 180 170 160 150 140 130 120 110 100 90 80 70 60 50 40 30 20 10 ppm

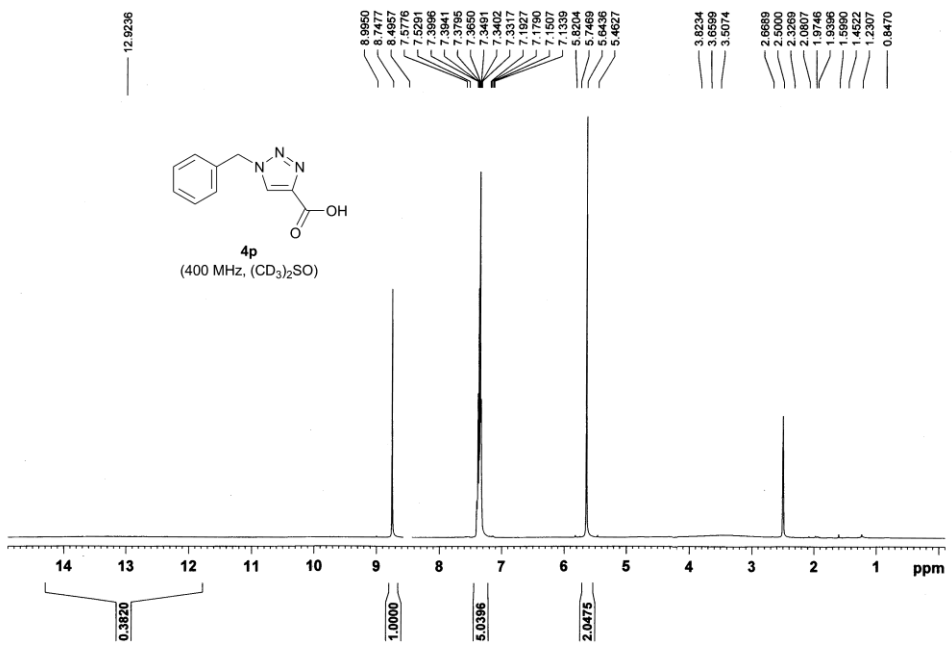
12.9236
8.9950
8.7477
8.4957
7.5776
7.5291
7.3996
7.3941
7.3755
7.3650
7.3491
7.3402
7.3317
7.1927
7.1790
7.1507
7.1339
5.8204
5.7469
5.6436
5.4627
3.8234
3.6599
3.5074
2.6689
2.5000
2.3269
2.0807
1.9746
1.9396
1.5990
1.4522
1.2307
0.8470
OH
O
4p
(400 MHz, (CD3)2SO)
14 13 12 11 10 9 8 7 6 5 4 3 2 1 ppm
0.3820
1.0000
5.0396
2.0475

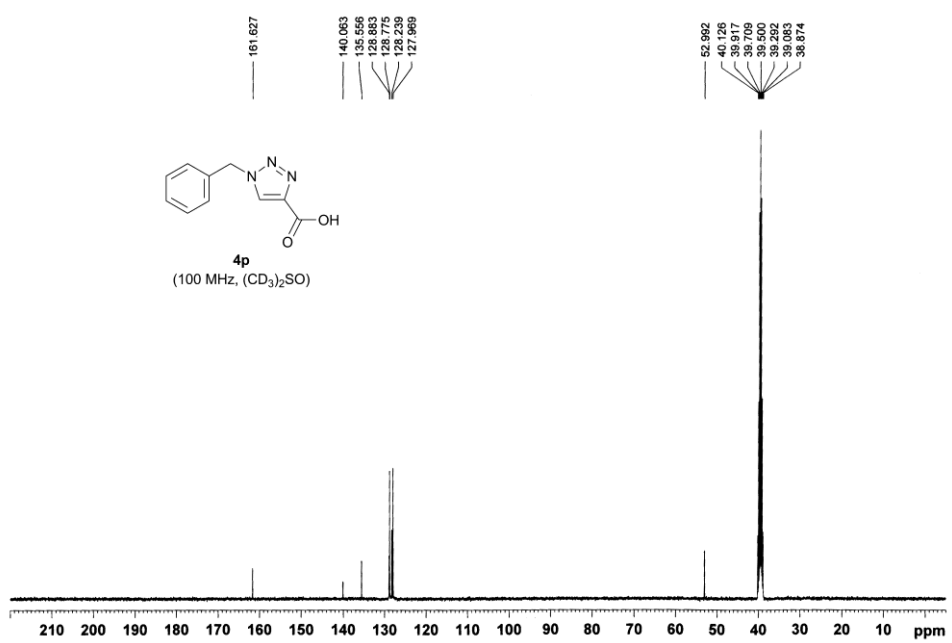
161.627
140.063
135.556
128.883
128.775
128.239
127.969
52.992
40.126
39.917
39.709
39.500
39.292
39.083
38.874
OH
O
4p
(100 MHz, (CD3)2SO)
210 200 190 180 170 160 150 140 130 120 110 100 90 80 70 60 50 40 30 20 10 ppm

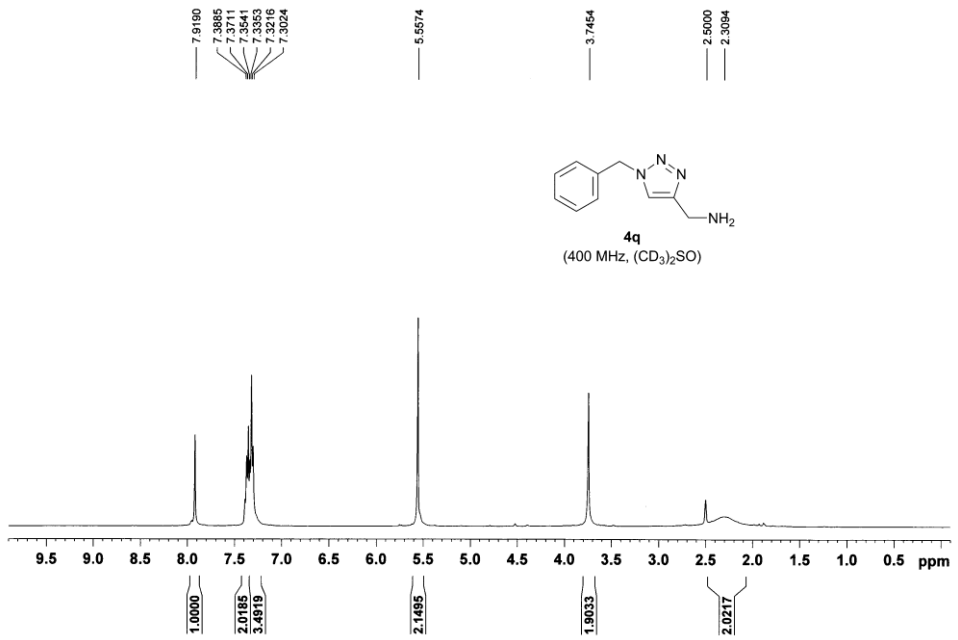
7.9190
7.3885
7.3711
7.3541
7.3353
7.3216
7.3024
5.5574
3.7454
2.5000
2.3094
NH2
4q
(400 MHz, (CD3)2SO)
9.5 9.0 8.5 8.0 7.5 7.0 6.5 6.0 5.5 5.0 4.5 4.0 3.5 3.0 2.5 2.0 1.5 1.0 0.5 ppm
1.0000
2.0185
3.4919
2.1495
1.9033
2.0217

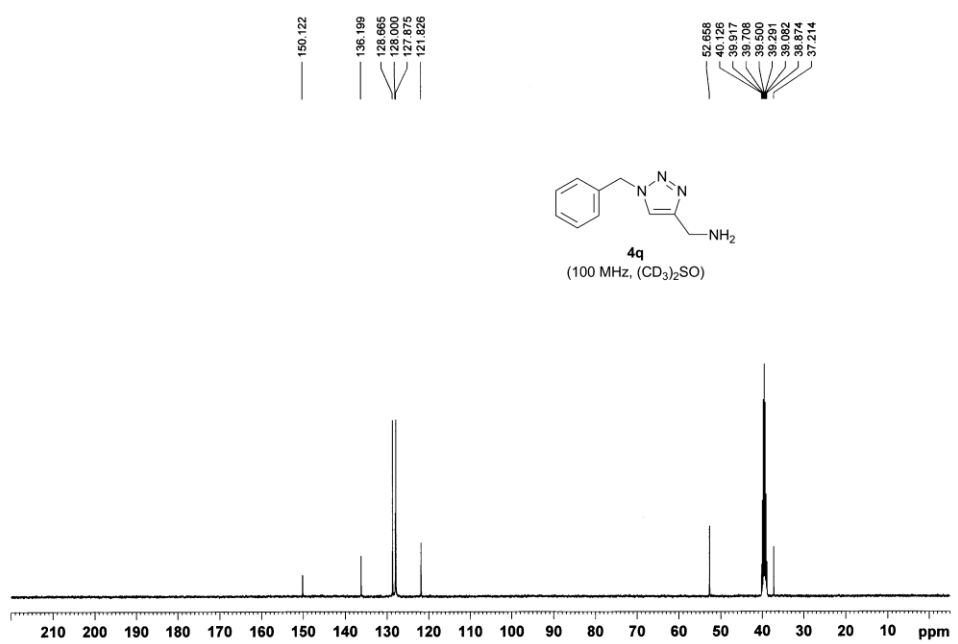
150.122
136.199
128.665
128.000
127.875
121.826
52.558
40.126
39.917
39.708
39.500
39.291
39.082
38.874
37.214
NH2
4q
(100 MHz, (CD3)2SO)
210 200 190 180 170 160 150 140 130 120 110 100 90 80 70 60 50 40 30 20 10 ppm

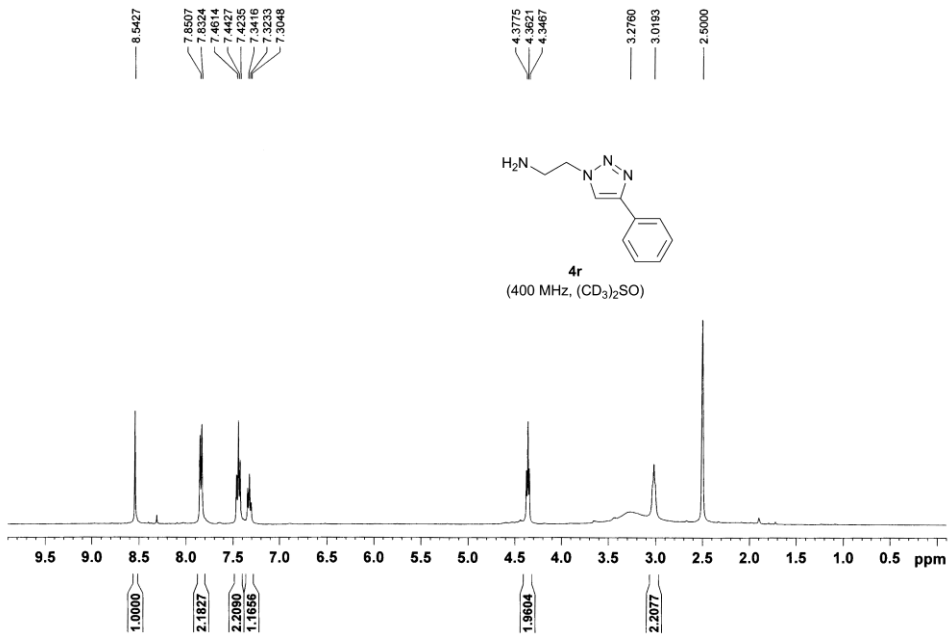
8.5427
7.8507
7.8324
7.4614
7.4427
7.4235
7.3416
7.3233
7.3048
4.3775
4.3621
4.3467
3.2760
3.0193
2.5000
4r
(400 MHz, (CD3)2SO)
9.5 9.0 8.5 8.0 7.5 7.0 6.5 6.0 5.5 5.0 4.5 4.0 3.5 3.0 2.5 2.0 1.5 1.0 0.5 ppm
1.0000
2.1827
2.2090
1.1656
1.9604
2.2077

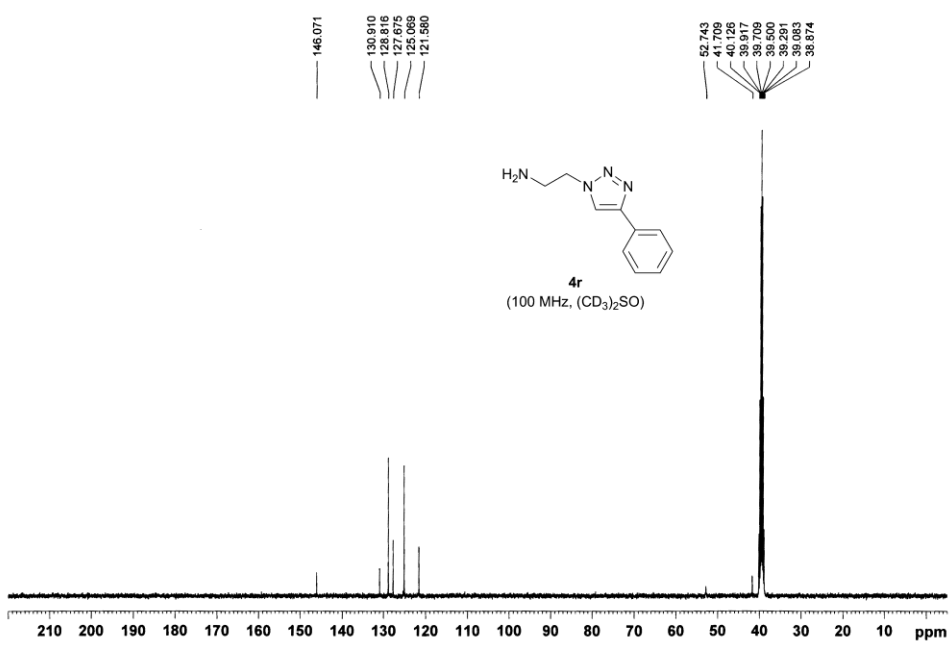
146.071
130.910
128.816
127.675
125.069
121.580
52.743
41.709
40.126
39.917
39.709
39.500
39.291
39.083
38.874
4r
(100 MHz, (CD3)2SO)
210 200 190 180 170 160 150 140 130 120 110 100 90 80 70 60 50 40 30 20 10 ppm

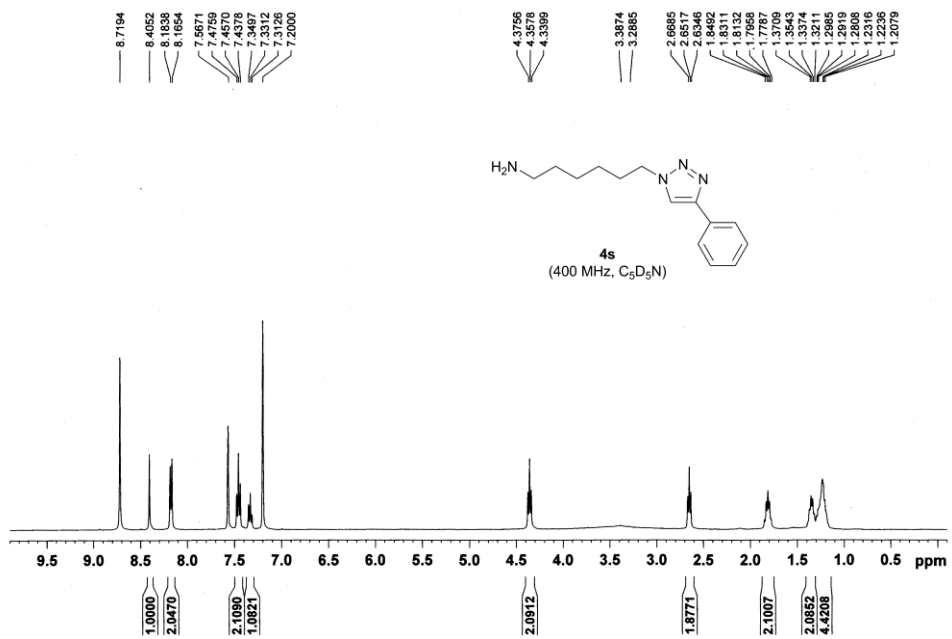
8.7194
8.4052
8.1838
8.1654
7.5671
7.4759
7.4570
7.4378
7.3497
7.3312
7.3126
7.2000
4.3756
4.3578
4.3399
3.3874
3.2885
2.6885
2.6517
2.6346
1.8462
1.8311
1.8132
1.7958
1.7787
1.3709
1.3543
1.3374
1.3211
1.2985
1.2919
1.2808
1.2316
1.2236
1.2079
H2N
N
N
N
4s
(400 MHz, C5D5N)
9.5 9.0 8.5 8.0 7.5 7.0 6.5 6.0 5.5 5.0 4.5 4.0 3.5 3.0 2.5 2.0 1.5 1.0 0.5 ppm
1.0000
2.0470
2.1090
1.0821
2.0912
1.8771
2.1007
2.0852
4.4208

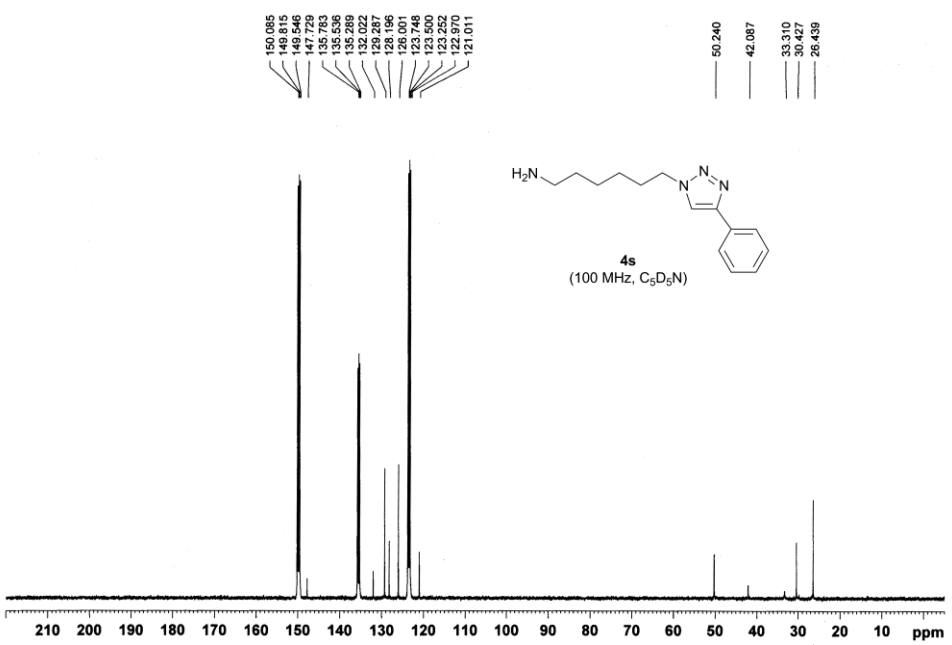
150.085
149.815
149.546
147.729
135.783
135.536
135.289
132.022
129.287
128.196
126.091
123.748
123.500
123.252
122.970
121.011
50.240
42.087
33.310
30.427
26.439
H2N
N
N
N
4s
(100 MHz, C5D5N)
210 200 190 180 170 160 150 140 130 120 110 100 90 80 70 60 50 40 30 20 10 ppm

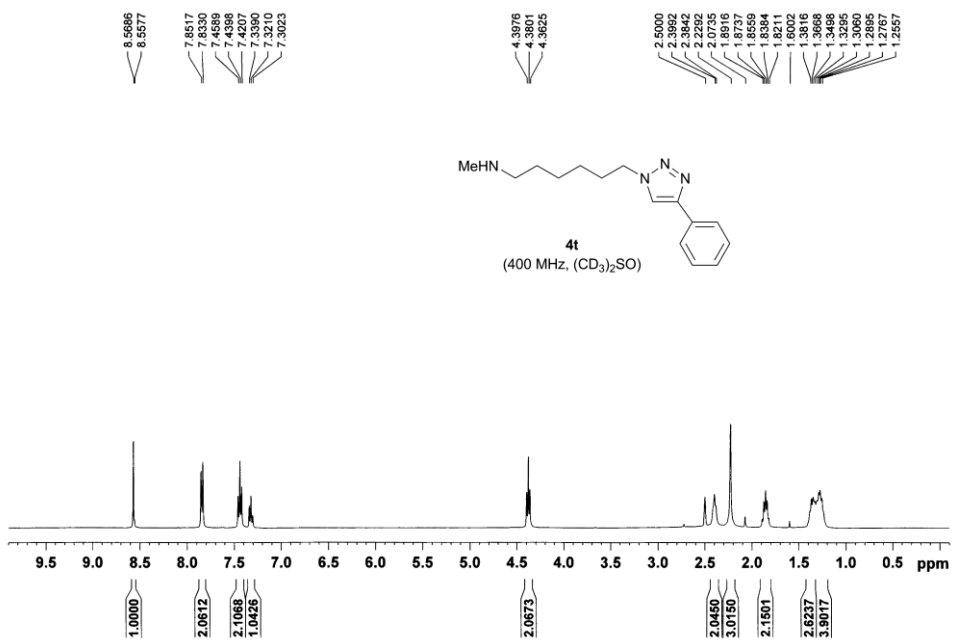
8.5686
8.5577
7.8517
7.8330
7.4589
7.4398
7.4207
7.3390
7.3210
7.3023
4.3976
4.3801
4.3625
2.5000
2.3992
2.3842
2.2292
2.0735
1.8516
1.8377
1.8559
1.8384
1.8211
1.6002
1.3816
1.3668
1.3498
1.3295
1.3060
1.2895
1.2767
1.2557
MeHN
N
N
N
4t
(400 MHz, (CD3)2SO)
9.5 9.0 8.5 8.0 7.5 7.0 6.5 6.0 5.5 5.0 4.5 4.0 3.5 3.0 2.5 2.0 1.5 1.0 0.5 ppm
1.0000
2.0612
2.1068
1.0426
2.0673
2.0450
3.0150
2.1501
2.6237
3.9017

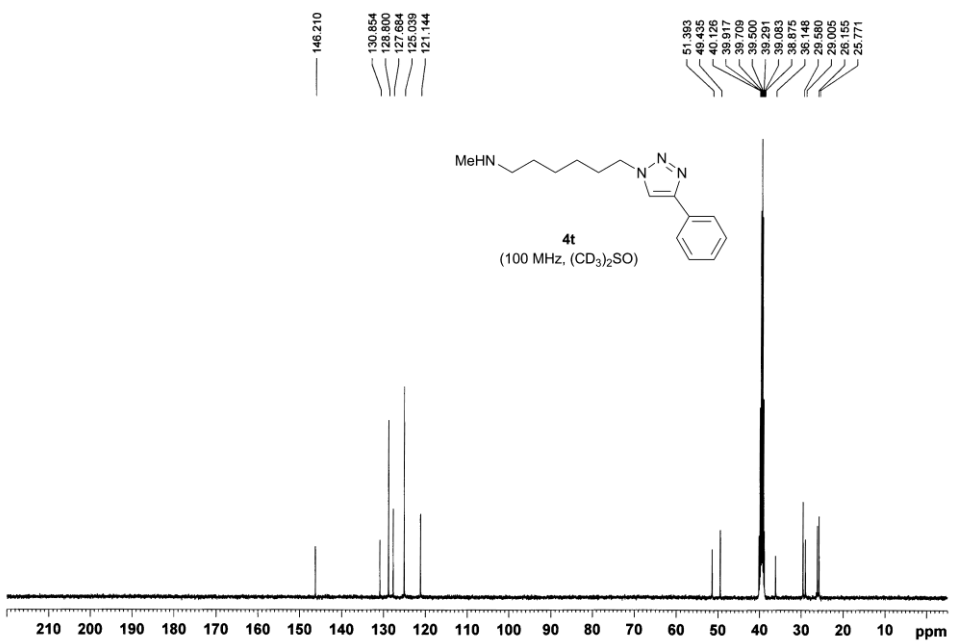
146.210
130.854
128.800
127.684
125.039
121.144
51.393
49.435
40.126
39.917
39.709
39.500
39.291
39.083
38.875
36.148
29.580
29.005
26.155
25.771
MeHN
N
N
N
4t
(100 MHz, (CD3)2SO)
210 200 190 180 170 160 150 140 130 120 110 100 90 80 70 60 50 40 30 20 10 ppm

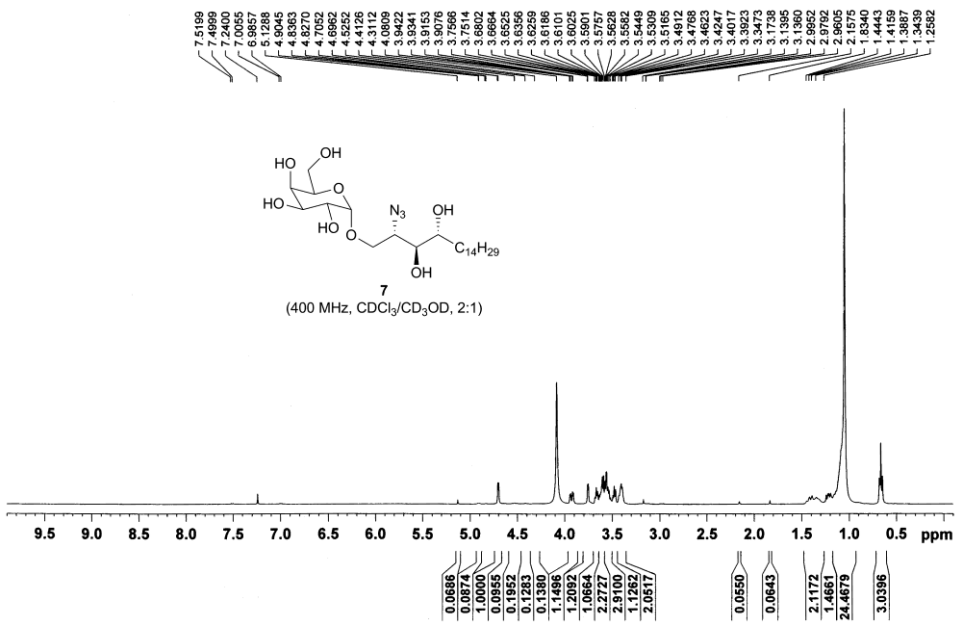
7.5199
7.4999
7.2400
7.0055
6.9857
5.1288
4.9045
4.8363
4.8270
4.7052
4.6962
4.5252
4.4126
4.3112
4.0809
3.9422
3.9341
3.9153
3.9076
3.7566
3.7514
3.6802
3.6664
3.6525
3.6356
3.6258
3.6186
3.6101
3.6025
3.5901
3.5757
3.5628
3.5582
3.5449
3.5309
3.5165
3.4912
3.4768
3.4623
3.4247
3.4017
3.3923
3.3473
3.3238
3.1385
3.1360
2.9952
2.9792
2.9605
2.1575
1.8340
1.4443
1.4159
1.3887
1.3439
1.2582
HO
OH
O
HO
HO
HO
O
N3
OH
C14H29
OH
7
(400 MHz, CDCl3/CD3OD, 2:1)
9.5 9.0 8.5 8.0 7.5 7.0 6.5 6.0 5.5 5.0 4.5 4.0 3.5 3.0 2.5 2.0 1.5 1.0 0.5 ppm
0.0686
0.0874
1.0000
0.0955
0.1952
0.1283
0.1380
1.1496
1.2092
1.0664
2.2727
2.9100
1.1262
2.0517
0.0550
0.0643
2.1172
1.4661
24.4679
3.0396

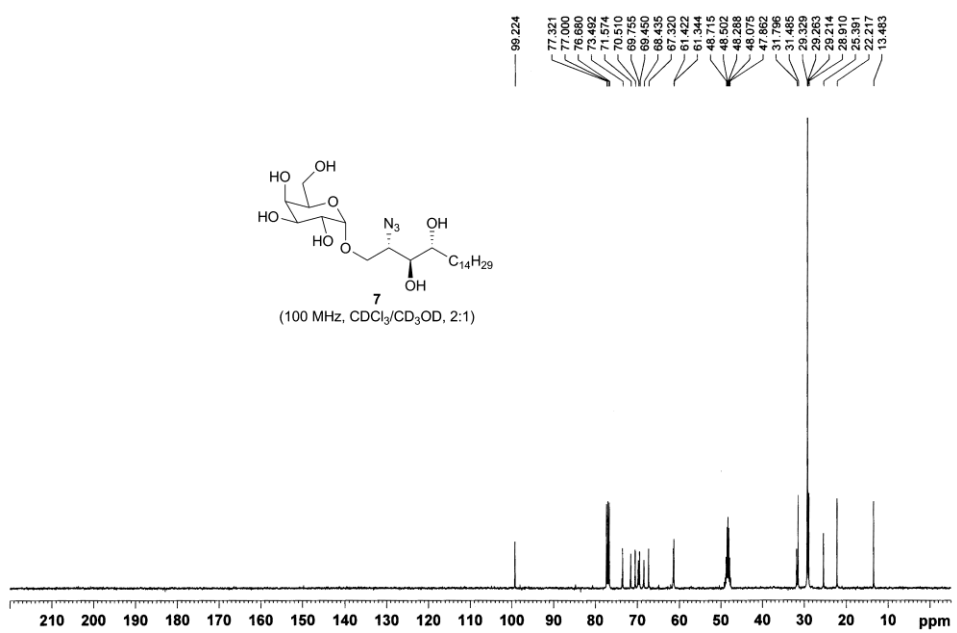
99.224
77.321
77.000
76.680
73.492
71.574
70.510
69.755
69.450
68.435
67.320
61.422
61.344
48.715
48.502
48.288
48.075
47.862
31.796
31.485
29.329
29.263
29.214
28.910
25.391
22.217
13.483
HO
OH
O
HO
HO
HO
O
N3
OH
C14H29
OH
7
(100 MHz, CDCl3/CD3OD, 2:1)
210 200 190 180 170 160 150 140 130 120 110 100 90 80 70 60 50 40 30 20 10 ppm

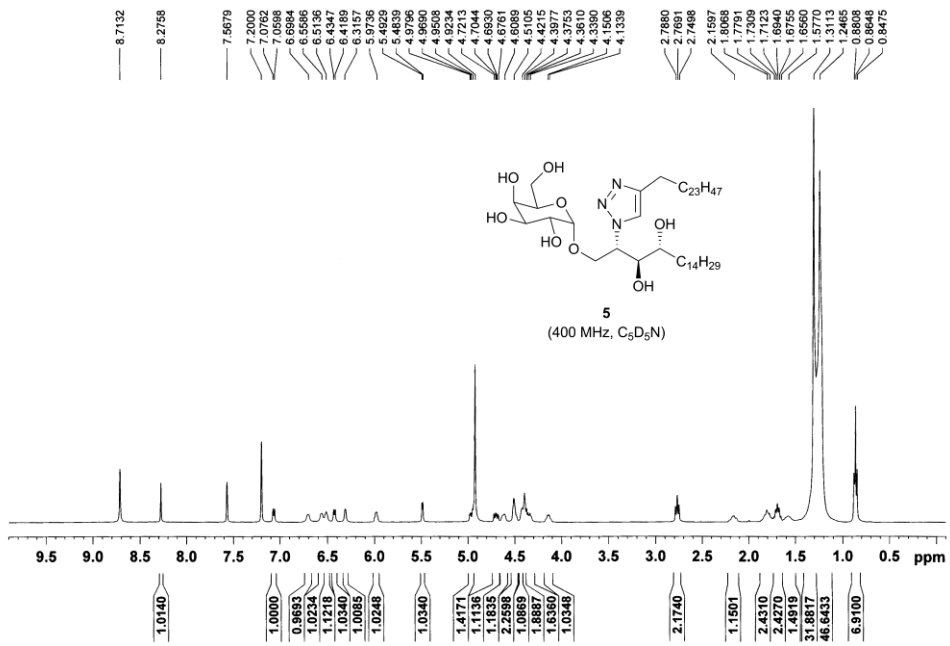
8.7132
8.2758
7.5679
7.2000
7.0762
7.0598
6.6984
6.5586
6.5136
6.4347
6.4159
6.3157
5.9736
5.4929
5.4839
4.9796
4.9690
4.9508
4.9234
4.7213
4.7044
4.6930
4.6761
4.6089
4.5105
4.4215
4.3977
4.3753
4.3610
4.3390
4.1506
4.1339
2.7880
2.7691
2.7498
2.1597
1.8068
1.7791
1.7309
1.7123
1.6940
1.6755
1.6560
1.5770
1.3113
1.2465
0.8808
0.8648
0.8475
HO
OH
O
HO
HO
O
N
N
N
C23H47
OH
C14H29
OH
5
(400 MHz, C5D5N)
9.5 9.0 8.5 8.0 7.5 7.0 6.5 6.0 5.5 5.0 4.5 4.0 3.5 3.0 2.5 2.0 1.5 1.0 0.5 ppm
1.0140
1.0000
0.9693
1.0234
1.1218
1.0340
1.0085
1.0248
1.0340
1.4171
1.1136
1.1835
2.2598
1.0869
1.8887
1.6360
1.0348
2.1740
1.1501
2.4310
2.4270
1.4919
31.8817
46.6433
6.9100

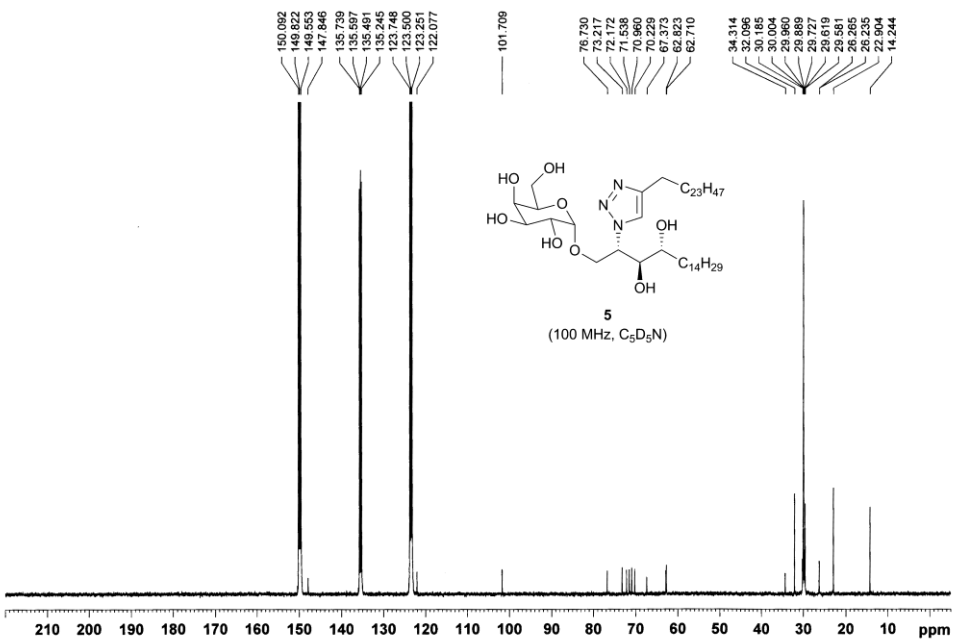
150.092
149.822
149.553
147.846
135.739
135.597
135.491
135.245
123.748
123.500
123.251
122.077
101.709
76.730
73.217
72.172
71.538
70.960
70.229
67.373
62.823
62.710
34.314
32.096
30.185
30.004
29.960
29.889
29.727
29.619
29.551
29.265
26.235
22.904
14.244
HO
OH
O
HO
HO
O
N
N
N
C23H47
OH
C14H29
OH
5
(100 MHz, C5D5N)
210 200 190 180 170 160 150 140 130 120 110 100 90 80 70 60 50 40 30 20 10 ppm

국 문 초 록

Part A. 분자 비대칭성 기억 현상과 동적 속도론적 분할 현상을 이용한 (−)-penibruguieramien A의 비대칭 전합성.

(–)-Penibruguieramine A는 해양 pyrrolizidine 알칼로이드로서, 2014년 Guo 연구진에 의해 중국 맹그로브지대 *Bruguiera gymnorrhiza*의 식내서성 균류인 *Penicillium* sp. GD6 로부터 분리·보고되었다. 이 천연물은 다른 천연물에서는 보고된 적 없는 흥미로운 골격인 1-hydroxyl-2-methyl pyrrolizidin-3-one 을 특징적으로 갖고 있어 전합성을 수행하기에 적합한 화합물로 생각되었다.

본 논문에서는 proline을 유일한 키랄 소스로 사용하여, '분자 비대칭성 기억 현상 (memory of chirality, MOC)'과 속도론적 분할 현상 (dynamic kinetic resolution, DKR)'을 이용한 첫 번째 전합성을 보고하고자 한다. MOC와 DKR은 화합물의 비대칭 합성에 있어 유용한 합성 방법이다. 하지만 천연물의 전합성에 있어 DKR을 활용한 예시들은 보고된 바가 있지만 MOC를 활용한 예시들은 거의 보고된 바가 없다. 게다가, 이 두 가지 개념이 조합되어 천연물 혹은 비천연물의 합성에 활용된 바도 알려져 있지 않아서 새로운 유형의 반응이라고 할 수 있다.

본 전합성은 천연물에 대해 제안된 생합성 경로를 모방하는 전략을 사용하였으며, 입체 센터들을 거의 완벽하게 부분 입체, 거울상 입체 선택적으로 구축하였다. 특히, 매우 높은 수준의 MOC 현상이 양성자성 용매 하에서 관찰되었는데, 이를 이해하기 위한 기전 연구가 수행되었으며, 이를 종합하여 전체적인 반응 기전을 제시하였다.

주요어: Aldol reaction, Biomimetic synthesis, Dynamic kinetic resolution, Memory of chirality, Total synthesis

학번: 2012-31107

국 문 초 록

Part B. 상 전이 촉진제를 이용한 2상 CuAAC 반응

기존의 고전적인 Cu(I) catalyzed azide-alkyne 1,3-dipolar 고리화 첨가 반응 (CuAAC reaction)의 반응 조건은 $CuSO_4 \cdot 5H_2O$와 아스코르브산나트륨의 반응으로부터 *in situ*로 생성된 Cu(I) 촉매와 물과 *t*-BuOH 혼합용매를 사용했다. 하지만 반응에 사용되는 시약인 Cu(I) 촉매 혹은 그 전구체는 일반적으로 물에 높은 용해도를 갖는 반면, 기질인 유기 화합물은 물에 낮은 용해도를 갖는 경우가 많다. 시약과 기질 간 용해성 차이로 인해 고전적인 CuAAC 반응 조건은 활용 가능한 기질의 폭이 넓지 않았고, 이런 단점을 극복하기 위해 다양한 반응 조건들이 개발되어왔다.

본 논문에서는 상 전이 촉진제를 활용한 2상 CuAAC 반응 조건에 대해 보고하고자 한다. 물과 유기 용매로 이루어진 2상 용매 시스템은 시약과 기질의 완전한 용해를 보장한다는 점에서 장점을 갖는다. 수층에서 $CuSO_4 \cdot 5H_2O$와 아스코르브산나트륨의 반응으로부터 *in situ*로 생성된 Cu(I) 촉매는 tris(triazolylmethyl)amine 리간드에 의해서 유기층으로 전이된다. 이 때에 tris(triazolylmethyl)amine 리간드의 적절한 친수성–소수성 균형이 Cu(I)의 전이에 중요하다는 것을 ICP-MS 분석을 통해 제안했다. 유기층

으로 전이된 Cu(I)는 반응 기질과 만나 CuAAC 반응을 일으키며, 다양한 azide, alkyne 기질들이 본 반응 조건에 적합하였다. 특히 일반적인 CuAAC 반응 조건에 적합하지 않았던 free amino 작용기를 갖고 있는 기질, 매우 큰 소수성을 나타내는 기질도 본 CuAAC 반응 조건 하에 효율적으로 반응이 진행되었다.

주요어: Click chemistry, Ligand effect, Phase transfer agent, Solvent effect, Synthetic method

학번: 2012-31107